

ALMA MATER STUDIORUM – UNIVERSITÀ DI BOLOGNA

DOTTORATO DI RICERCA IN
SCIENZE BIOMEDICHE E NEUROMOTORIE

Ciclo XXXVI

Settore Concorsuale: 05/D1

Settore Scientifico Disciplinare: BIO/09

**ROLE OF NEUROINFLAMMATION IN THE PATHOPHYSIOLOGY
OF CDKL5 DEFICIENCY DISORDER**

Presentata da: Nicola Mottolese

Coordinatore Dottorato

Prof.ssa Matilde Yung Follo

Supervisore

Prof.ssa Stefania Trazzi

Co-Supervisore

Prof.ssa Elisabetta Ciani

Esame finale anno 2024

TABLE OF CONTENTS

ABSTRACT	5
1. INTRODUCTION	7
1.1 CDKL5 DEFICIENCY DISORDER	7
1.1.1 HISTORY OF THE DISEASE	7
1.1.2 CLINICAL FEATURES	11
1.2 CYCLIN-DEPENDENT KINASE-LIKE 5 (CDKL5)	15
1.2.1 CDKL5 GENE	15
1.2.2 CDKL5 TRANSCRIPT ISOFORMS	16
1.2.3 CDKL5 PROTEIN STRUCTURE	16
1.2.4 PATHOLOGICAL MUTATIONS	18
1.2.5 CDKL5 EXPRESSION PROFILE	19
1.2.6 CDKL5 SUBSTRATES AND FUNCTIONS	21
1.3 MOUSE MODELS OF CDD	27
1.4 NEUROINFLAMMATION	33
1.4.1 MICROGLIA: ORIGIN, SIGNATURE, AND FUNCTIONS	34
1.4.2 MICROGLIA AND PATHOLOGICAL CONDITIONS	38
1.4.3 LUTEOLIN	41
AIM OF THE STUDY	46
2. MATERIALS AND METHODS	48
2.1 COLONY	48
2.2 TREATMENTS	48
2.2.1 TATk-GFP-CDKL5 PROTEIN TREATMENT	49
2.2.2 LUTEOLIN TREATMENT	49
2.2.3 STATTIC TREATMENT	49
2.2.4 ACETAMINOPHEN TREATMENT	50
2.2.5 NMDA TREATMENT	50
2.2.6 BRDU TREATMENT	50
2.3 HISTOLOGICAL AND IMMUNOHISTOCHEMISTRY PROCEDURES	51
2.3.1 IMMUNOFLUORESCENCE STAINING	51
2.3.2 DCX IMMUNOHISTOCHEMISTRY	52
2.3.3 GOLGI STAINING	53
2.4 IMAGE ACQUISITION AND MEASUREMENTS	53

2.4.1	CELL DENSITY	53
2.4.2	MORPHOMETRIC MICROGLIAL CELL ANALYSIS	54
2.4.3	MEASUREMENT OF THE DENDRITIC TREE	54
2.4.4	DENDRITIC SPINE NUMBER AND MORPHOLOGY	55
2.4.5	QUANTIFICATION OF PSD-95 IMMUNOREACTIVE PUNCTA	55
2.5	MICROGLIA ISOLATION	55
2.6	RNA ISOLATION AND RT-QPCR	56
2.7	WESTERN BLOTTING	57
2.8	BEHAVIORAL ASSAYS	58
2.8.1	HIND-LIMB CLASPING	59
2.8.2	OPEN FIELD TEST	59
2.8.3	PASSIVE AVOIDANCE TEST	59
2.9	STATISTICAL ANALYSIS	60
3.	RESULTS	61
<hr/>		
3.1	INCREASED MICROGLIAL ACTIVATION IN THE BRAIN OF <i>CDKL5</i> KO MICE	61
3.2	NON-CELL AUTONOMOUS MICROGLIAL ACTIVATION IN THE ABSENCE OF <i>CDKL5</i>	63
3.3	TREATMENT WITH LUTEOLIN INHIBITS MICROGLIAL OVERACTIVATION IN <i>CDKL5</i> +/- MICE	65
3.4	INHIBITION OF MICROGLIAL OVERACTIVATION RESTORES SURVIVAL OF CA1 HIPPOCAMPAL NEURONS IN <i>CDKL5</i> +/- MICE	69
3.5	ASSESSMENT OF MICROGLIAL ACTIVATION IN DIFFERENT LIFE STAGES OF <i>CDKL5</i> +/- MICE	70
3.6	LUTEOLIN TREATMENT RESTORES NEURON SURVIVAL IN MIDDLE-AGED <i>CDKL5</i> +/- MICE	72
3.7	TREATMENT WITH LUTEOLIN PREVENTS NMDA-INDUCED SEIZURE PERSISTENCE AND EXCITOTOXICITY IN THE HIPPOCAMPUS OF <i>CDKL5</i> +/- MICE	73
3.8	TREATMENT WITH LUTEOLIN RESTORES SURVIVAL OF NEWBORN CELLS IN THE DENTATE GYRUS OF <i>CDKL5</i> +/- MICE	77
3.9	TREATMENT WITH LUTEOLIN INCREASES HIPPOCAMPAL NEUROGENESIS IN <i>CDKL5</i> +/- MICE	78
3.10	TREATMENT WITH LUTEOLIN IMPROVES MATURATION OF NEWBORN CELLS IN THE DENTATE GYRUS OF <i>CDKL5</i> +/- MICE	81
3.11	TREATMENT WITH LUTEOLIN IMPROVES THE DENDRITIC ARCHITECTURE IN HIPPOCAMPAL AND CORTICAL NEURONS OF <i>CDKL5</i> +/- MICE	82
3.12	TREATMENT WITH LUTEOLIN IMPROVES SPINE MATURATION IN THE BRAIN OF <i>CDKL5</i> +/- MICE	86
3.13	TREATMENT WITH LUTEOLIN TRANSIENTLY BOOSTS BDNF/TRKB SIGNALING PATHWAYS IN THE CORTEX OF <i>CDKL5</i> +/- MICE	88
3.14	TREATMENT WITH LUTEOLIN AMELIORATES BEHAVIORAL DEFICITS IN <i>CDKL5</i> +/- MICE	90

4. DISCUSSION	93
5. CONCLUSION	101
6. BIBLIOGRAPHY	103

ABSTRACT

Cyclin-dependent kinase-like 5 (CDKL5) deficiency disorder (CDD), a rare and severe neurodevelopmental disease caused by mutations in the X-linked *CDKL5* gene, is characterized by early-onset epilepsy, intellectual disability, and autistic features. To date, little is known about the etiology of CDD and no therapies are available. Neuroinflammatory processes are known to contribute to neuronal dysfunction and death. When overactivated in response to neuronal damage and genetic or environmental factors, microglia – the brain macrophages – cause widespread damage to neighboring neurons by producing neurotoxic factors and pro-inflammatory molecules. Importantly, overactivated microglia have been described in several neurodegenerative and neurodevelopmental disorders, suggesting that active neuroinflammation may account for the compromised neuronal survival and/or brain development observed in these pathologies. Recent evidence shows a subclinical chronic inflammatory status in plasma from CDD patients. However, to date, it is unknown whether a similar inflammatory status is present in the brain of CDD patients and, if so, whether it plays a causative or exacerbating role in the pathophysiology of CDD.

Here, we show evidence of a chronic microglia overactivation status in the brain of *Cdkl5* KO mice, characterized by alterations in microglial cell number/morphology and increased pro-inflammatory gene expression. We found that the neuroinflammatory process is already present in the postnatal period in *Cdkl5* KO mice and worsens during aging. Remarkably, by restoring microglia alterations, treatment with luteolin, a natural anti-inflammatory flavonoid, promotes neuronal survival in the brain of *Cdkl5* KO mice since it counteracts hippocampal neuron cell death and protects neurons from NMDA-induced excitotoxic damage. In addition, through the restoration of microglia alterations, luteolin treatment also increases hippocampal neurogenesis and restores dendritic spine maturation and dendritic arborization of hippocampal and cortical pyramidal neurons in *Cdkl5*

KO mice, leading to improved behavioral performance. These findings highlight new insights into the CDD pathophysiology and provide the first evidence that therapeutic approaches aimed at counteracting neuroinflammation could be beneficial in CDD.

1. INTRODUCTION

1.1 CDKL5 Deficiency Disorder

CDKL5 deficiency disorder (CDD, OMIM *300672) is a rare and severe X-linked neurodevelopmental disease caused by mutations in the *cyclin-dependent kinase-like 5* gene (CDKL5, OMIM *300203) (Tao et al., 2004; Weaving et al., 2004).

The *CDKL5* gene, located on the X chromosome (Xp22.13), encodes a serine/threonine kinase which is involved in regulating neuronal migration, axon outgrowth, dendritic morphogenesis, and synapse formation in early postnatal life, and in maintaining synaptic function in the adult brain (Sun and Wang, 2023).

The primary symptoms of CDD include early-onset epilepsy (mostly drug-refractory), generalized hypotonia, developmental intellectual and motor disabilities, and cortical visual impairment. In addition, several accompanying symptoms have been reported: autistic features, sleep disturbances, breathing abnormalities, and gastrointestinal disorders (Fehr et al., 2013; Jakimiec et al., 2020; Leonard et al., 2022; Olson et al., 2019).

CDD is one of the most common genetic causes of epilepsy in early childhood with an estimated incidence between 1 in 40,000-60,000 live births and a female-to-male ratio of 4:1 (López-Rivera et al., 2020; Olson et al., 2021a; Symonds et al., 2019). Life expectancy varies depending on the severity of symptoms and is currently unknown due to underdiagnosis in adults. However, the oldest patients reported so far are in their 40s (Van Bergen et al., 2022).

1.1.1 History of the disease

The *CDKL5* gene was first identified in 1998 during a transcriptional mapping project of the human X chromosome (Katayama et al., 2020; Montini et al., 1998).

The first correlation between *CDKL5* and human diseases was described in 2003, when Kalscheuer and colleagues suggested the involvement of this gene mutation in the pathogenesis of X-linked infantile spasms (ISSX) based on the analysis of two cases of female patients with infantile spasms and profound mental retardation (Jakimiec et al., 2020; Kalscheuer et al., 2003).

Later, Weaving in 2004 (Weaving et al., 2004) and Scala in 2005 (Scala et al., 2005) showed the occurrence of mutations in the *CDKL5* gene in patients previously diagnosed with the early seizure variant of Rett syndrome, suggesting an important regulatory role of this gene in neuronal function (Jakimiec et al., 2020).

Rett Syndrome (RTT, OMIM *312750) is a neurodevelopmental disorder first reported in the 1960s and is estimated to affect 1 in 10,000-15,000 live female births (Katayama et al., 2020). Individuals with RTT usually develop normally for the first 6-18 months of life, but then they start to lose their abilities, including language and motor skills (Hagberg, 2002). Rett syndrome is also characterized by a broad spectrum of clinical manifestations: in the classic form, patients show repetitive hand movements, breathing irregularities, seizures, scoliosis, and gastrointestinal problems (Chahrour and Zoghbi, 2007). Mutations in the X-linked gene encoding *methyl-CpG-binding protein 2* (MECP2) have been found in 90-95% of these patients (Amir et al., 1999).

However, in addition to classic RTT, "atypical" forms have been described: the early seizure variant or Hanefeld variant, and the congenital variant or Rolando variant (Hadzsiev et al., 2011; Vidal et al., 2019). Among these atypical forms, mutations in *MECP2* have been found in only 50-70% of cases, suggesting the involvement of other genes in the onset of RTT, including *forkhead box G1* (FOXP1) and *CDKL5* (Ariani et al., 2008; Weaving et al., 2004).

In 2010, Neul and colleagues suggested diagnostic criteria for patients with classic and atypical RTT (Fig. 1). Specifically, the authors identified 4 main criteria for both classic and atypical RTT, exclusion criteria for classic RTT, and supportive criteria for atypical RTT.

Furthermore, the authors specified some clinical features to differentiate the early seizure variant – as the disorder caused by CDKL5 deficiency was initially defined – from other atypical forms of RTT (Artuso et al., 2010; Neul et al., 2010).

<p>RTT Diagnostic Criteria</p> <p>Consider diagnosis when postnatal deceleration of head growth observed.</p> <p>Required for typical or classic RTT</p> <ol style="list-style-type: none">1. A period of regression followed by recovery or stabilization*2. All main criteria and all exclusion criteria3. Supportive criteria are not required, although often present in typical RTT <p>Required for atypical or variant RTT</p> <ol style="list-style-type: none">1. A period of regression followed by recovery or stabilization*2. At least 2 out of the 4 main criteria3. 5 out of 11 supportive criteria <p>Main Criteria</p> <ol style="list-style-type: none">1. Partial or complete loss of acquired purposeful hand skills.2. Partial or complete loss of acquired spoken language**3. Gait abnormalities: Impaired (dyspraxic) or absence of ability.4. Stereotypic hand movements such as hand wringing/squeezing, clapping/tapping, mouthing and washing/rubbing automatisms <p>Exclusion Criteria for typical RTT</p> <ol style="list-style-type: none">1. Brain injury secondary to trauma (peri- or postnatally), neurometabolic disease, or severe infection that causes neurological problems2. Grossly abnormal psychomotor development in first 6 months of life <p>Supportive Criteria for atypical RTT</p> <ol style="list-style-type: none">1. Breathing disturbances when awake2. Bruxism when awake3. Impaired sleep pattern4. Abnormal muscle tone5. Peripheral vasomotor disturbances6. Scoliosis/kyphosis7. Growth retardation8. Small cold hands and feet9. Inappropriate laughing/screaming spells10. Diminished response to pain11. Intense eye communication - "eye pointing"
--

Figure 1. Diagnostic criteria for RTT [adapted from (Neul et al., 2010)].

In 2013, the increasing number of patients with mutations in the *CDKL5* gene, together with the growing knowledge about the disorder caused by CDKL5 deficiency, led Fehr and colleagues to reevaluate the previous diagnostic criteria. In a study conducted on 77 females and 9 males with pathogenic mutations in the *CDKL5* gene, it was observed that no males and less than 25% of females met the clinical criteria established for early seizure variant of RTT. As a result, the authors

proposed a new set of diagnostic criteria useful in identifying patients with mutations in *CDKL5* (Fig. 2) (Fehr et al., 2013).

Clinical features suggesting a diagnosis of the <i>CDKL5</i> disorder	
Extreme like (a)	Seizures within the first year of life (90% by 3 months) Global developmental delay Severely impaired gross motor function
Very likely (b)	Sleep disturbances Abnormal muscle tone Bruxism Gastrointestinal issues
Likely (c)	Subtle dysmorphic features including three or more of the following: broad/prominent forehead; large 'deep-set' eyes; full lips; tapered fingers; and anteverted nares in males Hand stereotypies Laughing and screaming spells Cold hands or feet Breathing disturbances Peripheral vasomotor disturbances
Unlikely (d)	Independent walking Microcephaly Major congenital malformations

(a) Observed in >90% of cases in the current study.
 (b) Observed in 80–90% of cases in the current study.
 (c) Observed more variably in 40–80% of cases in the current study.
 (d) Observed in <10% of cases in the current study.

Figure 2. Clinical features suggesting a diagnosis of the *CDKL5* disorder [adapted from (Fehr et al., 2013)].

Furthermore, the authors highlighted that although the disorders share some clinical features, the disease associated with *CDKL5* mutation differs from Rett syndrome in the absence of regression after a period of normal development and therefore should be considered as a separate disorder (Fehr et al., 2013).

Nowadays, *CDKL5* deficiency disorder has been distinguished from Rett syndrome and is considered as an independent clinical entity with a specific *International Classification of Diseases, Tenth Revision, Clinical Modification* code (G40.42) (Hong et al., 2022).

1.1.2 *Clinical features*

The most prominent and presenting feature of CDD is the early onset of seizures (Bahi-Buisson et al., 2008a; Fehr et al., 2016a; Leonard et al., 2022). Epilepsy in CDD has been described in three stages (Fig. 3), starting with generalized tonic or tonic-clonic seizures in infancy, with a variable pharmacological response (Bahi-Buisson et al., 2008a; Demarest et al., 2019; Hong et al., 2022). The median age of seizures onset is 6 weeks with 90% onset by 3 months (Fehr et al., 2013; Fehr et al., 2016a). During the first stage, some patients experience a transient period of seizure freedom, known as the honeymoon period. Defined as seizure freedom lasting at least 1 month, the honeymoon period has an average duration of 4-6 months and typically occurs within the first 2 years of life, although some patients may have seizure-free periods later in childhood or adolescence. In the second stage, there is a relapse of previous seizures and onset of epileptic spasms. Finally, in the third stage, spasms may continue or evolve to other seizure types, and most patients continue to have generalized or mixed focal and generalized seizures (Bahi-Buisson et al., 2008a; Hong et al., 2022). Other common types of seizures include generalized tonic, generalized tonic-clonic, generalized myoclonic, and focal seizures, and less commonly clonic, and atonic seizures (Demarest et al., 2019; Kobayashi et al., 2021). Regarding the frequency of epileptic seizures, less than 10% of children with CDD have several episodes per month, about 12% have several episodes per week, and up to 80% have seizures every day. It is important to note that recent studies have reported the presence of a small proportion of patients (1.74%) who do not experience epileptic seizures (Aznar-Laín et al., 2023; Jakimiec et al., 2020). Moreover, the highly refractory nature of epilepsy in CDD puts many patients at high risk for Sudden Unexpected Death in Epilepsy (SUDEP) (Harden et al., 2017; Jakimiec et al., 2020).

Stage I	Stage II	Stage III
Infantile onset motor seizures, variably pharmaco-responsive	Epileptic Encephalopathy with spasms	Refractory Epilepsy, generalized or mixed
Honeymoon period		
Onset: 1 – 10 weeks (median onset: 4 weeks – 2 months)	Onset: 6 – 36 months (median onset: 11 months)	Onset: 2 – 11 years (median onset: 7 years)
Common Seizure Types <ul style="list-style-type: none"> • Generalized tonic • Generalized tonic-clonic • Asymmetric or focal motor • Epileptic spasms • Sequential seizures (e.g. hypermotor-tonic-spasm) 	Common Seizure Types <ul style="list-style-type: none"> • Epileptic spasms • Relapse of previous seizure types • Sequential seizures (e.g. hypermotor-tonic-spasm) 	Common Seizure Types <ul style="list-style-type: none"> • Epileptic spasms • Generalized tonic • Generalized tonic-clonic • Generalized myoclonic • Less common: focal motor, clonic, atonic, absence, sequential seizures (e.g. hypermotor-tonic-spasm)
*Honeymoon period Onset: 2 months – 11 years (median onset: 2 years) Duration: 2.5 months – 6 years (median duration: 6 months)		

Figure 3. Three stages of epilepsy in CDKL5 deficiency disorder [adapted from (Hong et al., 2022)].

Most children with CDD have moderate to severe intellectual disability and show delays in reaching developmental milestones (Fig. 4), such as sitting, grasping, and walking (Fehr et al., 2016b). The analysis of the achievement of developmental milestones by patients with CDD shows that males are mostly affected. Almost 66% of girls can sit without support, 25% can stand, 21% can get up from a sitting position, 23% can walk without assistance until the age of 5, and 13% can run at any developmental stage. In contrast, only 35% of boys can sit unsupported, 11% can stand, and only 5.5% can walk independently. About 50% of girls and 10% of boys reach the ability to grasp (Amin et al., 2017; Fehr et al., 2016b; Kobayashi et al., 2021).

Communication skills are also extremely impaired in CDD patients (Fig. 4) (Fehr et al., 2016b; Jakimiec et al., 2020; Olson et al., 2019). Gestures, facial expressions, and vocalizations are the most common modes of communication. The use of non-verbal communication devices, such as switches and eye gaze-based technology communication, is often limited by cortical visual impairment, but can be used by some individuals with CDD (Fehr et al., 2016b).

Cortical visual disturbances are common and occur in 80% of individuals with CDD (Fig. 4) (Brock et al., 2021; Demarest et al., 2019; Olson et al., 2021b). They present clinically as lack of fixation and lack of following objects with the eyes. In 40.6% of patients, avoidance of eye contact is observed, which is also interpreted as one of the autistic features. Less commonly reported symptoms include rotational or horizontal nystagmus (Jakimiec et al., 2020).

Generalized hypotonia affects all patients, although it appears to be more severe in males (Jakimiec et al., 2020; Olson et al., 2019). Scoliosis is its most common orthopedic complication, occurring in 20% of patients (Fig. 4). The probability of developing scoliosis before the age of 10 is 68.5% (Mangatt et al., 2016).

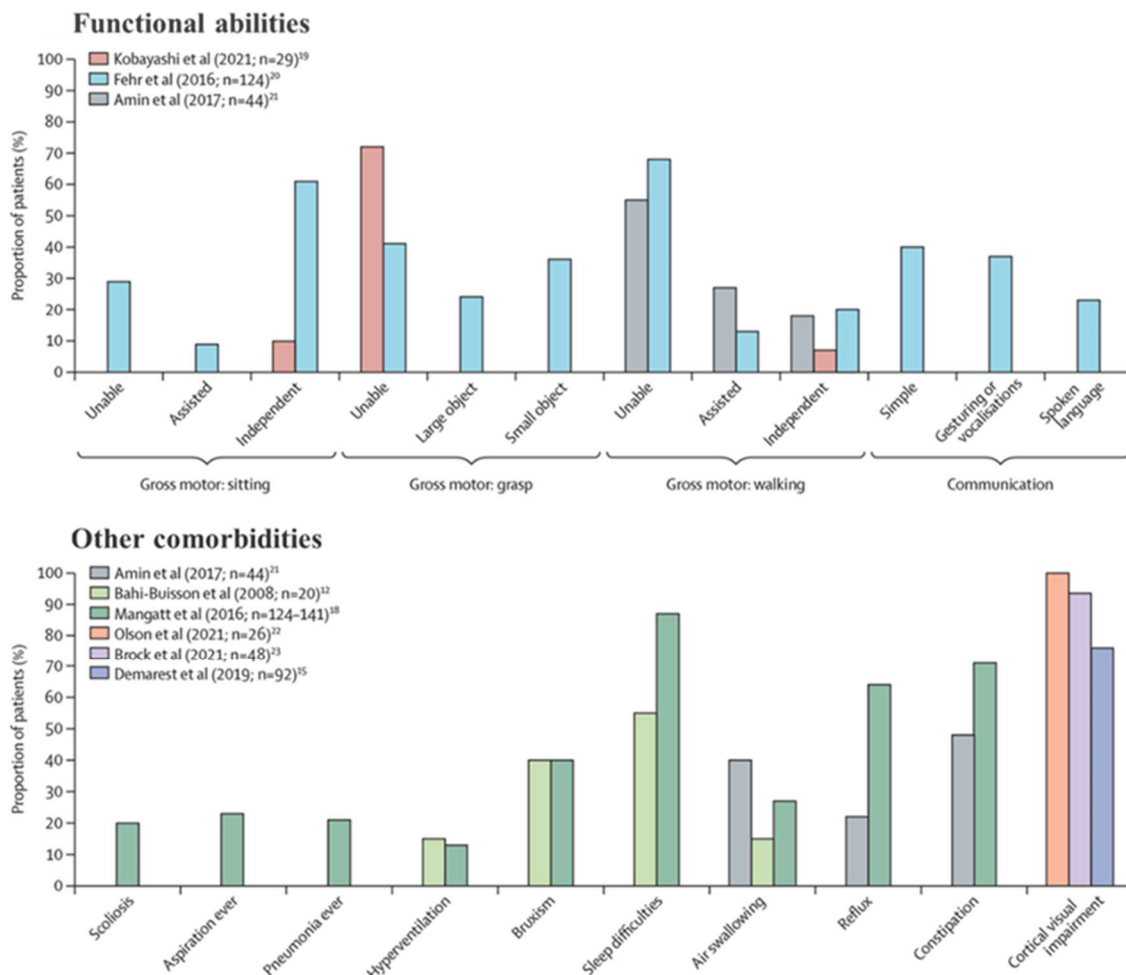


Figure 4. Distribution of CDKL5 deficiency disorder characteristics [adapted from (Leonard et al., 2022)].

Children with CDD may also exhibit autistic-like traits, including social deficits (difficulty in understanding social cues, making eye contact, and engaging in reciprocal social interactions), repetitive behaviors (hand flapping, spinning, or lining up objects), and sensory issues (many children may be overly sensitive or under-sensitive to sensory input, such as touch, sound, or light) (Bahi-Buisson et al., 2008b).

Other comorbidities include gastrointestinal symptoms (constipation, reflux, or air swallowing), sleep difficulties, respiratory disorders (apnea or hyperventilation), and bruxism (Fig. 4). Less commonly reported symptoms include cardiac arrhythmias, apraxia, and tetraplegia (Bahi-Buisson et al., 2008b; Mangatt et al., 2016).

CDD is characterized by a significant phenotypic heterogeneity. The symptoms of patients range from mild forms, with independent walking and pharmacologically-controlled epilepsy, to severe forms with epileptic seizures unresponsive to drug therapy, microcephaly, profound mental and psychomotor retardation, generalized hypotonia, and cortico-visual impairments (Jakimiec et al., 2020). Generally, females exhibit milder forms compared to males. This could be due, at least in part, to the phenomenon of X chromosome inactivation (XCI). According to this phenomenon, in the early stages of female embryonic development, one of the two X chromosomes is randomly and permanently inactivated in somatic cells (Lyon, 1961). This ensures that females, like males, have only one active copy of the X chromosome in each cell of the body. This implies that in heterozygous females with CDD, some somatic cells have an active X chromosome carrying the mutation in *CDKL5*, while others have an active X chromosome carrying a wild-type copy of the gene. This would explain why heterozygous females present milder symptoms compared to hemizygous males, who have a mutated copy of the gene in all somatic cells. However, a clinical study conducted by the International Foundation for *CDKL5* Research Centers of Excellence (COE) highlighted the existence of male patients with a mild phenotype, suggesting the presence of other factors that influence the phenotypic heterogeneity of the disease (Olson et al., 2019). Heterogeneity could

also be influenced by the wide mutational spectrum of *CDKL5*: some mutations have been associated with mild forms, while others have been associated with severe forms (Bahi-Buisson et al., 2008b; Fehr et al., 2016a). However, some studies have shown that the severity of symptoms can also vary among individuals with the same genetic mutation. For example, in a study conducted in 2004 by Weaving and colleagues, it was found that two twins, both carriers of a *CDKL5* mutation, exhibited different phenotypes: one had symptoms overlapping with those of Rett syndrome, while the other had an autistic disorder with mild intellectual disability (Weaving et al., 2004). The fact that genetically identical twins have different clinical features implies that epigenetic and/or environmental factors may also influence the phenotype of CDD.

1.2 Cyclin-Dependent Kinase-Like 5 (CDKL5)

1.2.1 *CDKL5* gene

The human *CDKL5* gene is located on the short arm of the X-chromosome at position 22 (Xp22) and is approximately 240 Kb long (Fig. 5) (Montini et al., 1998).

It is composed of 27 exons: the first 6 exons (1, 1a, 1b, 1c, 1d, 1e) constitute the 5' untranslated region (5'UTR) and contain alternative transcription start sites (TSS); the coding sequence is contained between exons 2-19; the last exons (19-22) constitute the 3' untranslated region (3'UTR) (Hector et al., 2016).

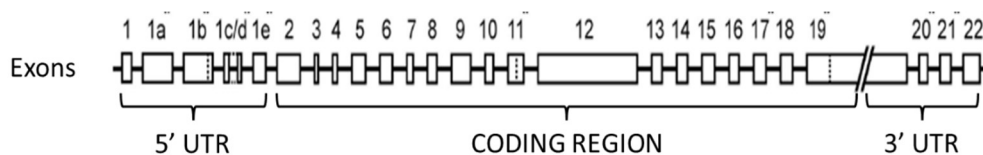


Figure 5. Schematic representation of the human *CDKL5* gene [adapted from (Hector et al., 2016)].

1.2.2 CDKL5 transcript isoforms

The human *CDKL5* gene undergoes alternative splicing¹, resulting in the generation of 5 different transcript isoforms (Fig. 6).

The *hCDKL5_1* transcript (107 kDa, 960 aa) is the predominant isoform in the central nervous system. The transcripts *hCDKL5_2*, *hCDKL5_3*, and *hCDKL5_4* are similar to *hCDKL5_1* but differ from it due to the addition of exon 17, truncation of exon 11, and a combination of both events, respectively (Hector et al., 2016). The *hCDKL5_5* transcript (115 kDa, 1030 aa) is the only isoform that includes exons 20-22 and is particularly expressed in the testes (Hector et al., 2016).

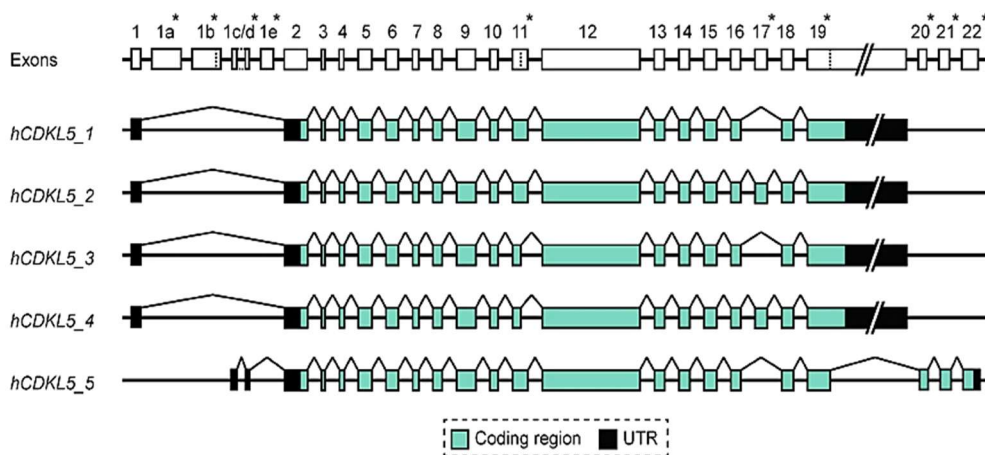


Figure 6. Schematic representation of the human *CDKL5* transcript isoforms. Lines linking exons indicate splicing events. Asterisks next to exon numbers indicate where differences have been found between different transcript isoforms [adapted from (Hector et al., 2016)].

1.2.3 CDKL5 protein structure

CDKL5 is a serine/threonine protein kinase belonging to the CMGC family, which includes cyclin-dependent kinases (CDKs), mitogen-activated protein kinases (MAPKs), glycogen synthase kinases (GSKs), and CDK-like kinases (CDKLs) (Montini et al., 1998).

¹ Alternative splicing is a well-known mechanism in molecular biology where different combinations of exons are included or excluded from the final messenger RNA (mRNA) transcript, resulting in multiple isoforms or variants of a gene (Gilbert, W., 1978. Why genes in pieces? Nature. 271, 501.

The protein is characterized by an N-terminal domain (aa 13-297), highly conserved and homologous to other members of the CDKLs family, and a C-terminal domain spanning over 600 aa (Fig. 7) (Bertani et al., 2006).

The N-terminal domain includes the ATP-binding region (aa 19-43), the serine/threonine kinase active site (aa 131-143), and a Thr-Xaa-Tyr (TEY; aa 169-171) motif, whose dual phosphorylation is required for activation of extracellular signal-regulated kinases (ERKs). Furthermore, through auto-phosphorylation of TEY motif, CDKL5 can self-regulate kinase activity (Bertani et al., 2006; Lin et al., 2005).

The C-terminal domain contains two nuclear localization signals (NLS1 and NLS2; aa 312-315 and 784-789, respectively) and a nuclear export signal (NES, aa 836-845). Therefore, this domain controls the nuclear-cytoplasmic translocation of the protein (Bertani et al., 2006; Lin et al., 2005). In addition, the C-terminal domain has a crucial role in regulating catalytic activity and may facilitate protein binding or target specificity (Canning et al., 2018).

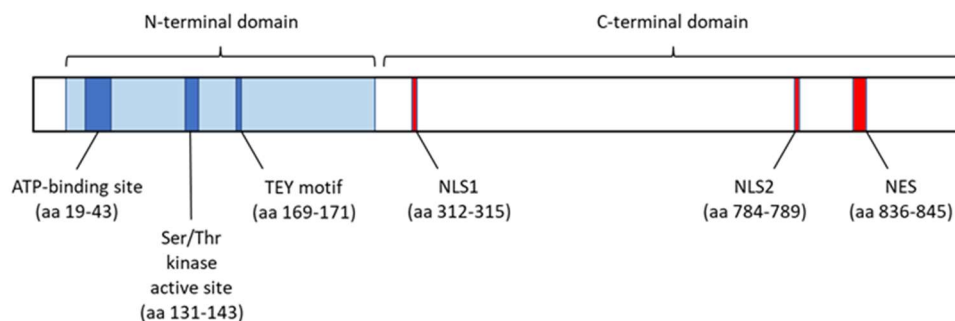


Figure 7. Schematic representation of the human CDKL5 protein [adapted from (Kilstrup-Nielsen et al., 2012)].

The specificity of CDKL5 kinase activity is primarily determined by the consensus sequence of amino acid residues flanking the phosphorylation site of the target protein. Most of the CDKL5 substrates have the following consensus sequence: Arg-Pro-X-Ser/Thr-Ala/Pro/Gly/Ser (Baltussen et al., 2018; Kameshita et al., 2008; Khanam et al., 2021; Trazzi et al., 2016). However, there are some substrates that do not possess this sequence (Kim et al., 2020;

Ricciardi et al., 2012), suggesting that further studies are needed to better understand the molecular basis governing the interaction between CDKL5 and its substrates.

1.2.4 Pathological mutations

To date, more than 265 pathogenic variants within the *CDKL5* gene have been identified, including missense mutations, nonsense mutations, frameshift mutations, and deletions (Fig. 8) (Jakimiec et al., 2020; Kilstrup-Nielsen et al., 2012; MacKay et al., 2021).

About 50% of these variants consist of point mutations. Among them, missense mutations are the most common (38%) and mainly occur in the N-terminal domain, while frameshift mutations and nonsense mutations – which lead to premature formation of stop codon and protein truncation – can occur in both the N-terminal and C-terminal domains (Kilstrup-Nielsen et al., 2012). Specifically, mutations affecting the N-terminal domain can occur within the ATP-binding site or the catalytic site. In the first case, the mutation hinders CDKL5 from properly binding ATP, while in the second case, the mutation prevents the protein from binding its substrate. However, in both cases, the mutation impairs the normal functioning of CDKL5 and its kinase activity (Bahi-Buisson et al., 2012; Hector et al., 2017). Mutations primarily found in the C-terminal domain of CDKL5 include frameshift mutations and nonsense mutations, which lead to increased catalytic activity and nuclear retention of CDKL5 (Bertani et al., 2006; Rusconi et al., 2008). Many studies have shown that patients with mutations within the catalytic site or frameshift mutations located at the end of the C-terminal domain exhibit severe motor impairment, refractory epilepsy, or microcephaly (Russo et al., 2009). Milder forms have been observed in patients with mutations within the ATP-binding site or nonsense mutations in the C-terminal domain. In these patients, better hand use and the ability to walk without assistance have been reported (Bahi-Buisson et al., 2012; Olson et al., 2019). In addition to point mutations, cases of *CDKL5* deletion (several or all exons) have also

been reported. However, the clinical presentation of patients with deletions is not significantly different from that of patients with point mutations (Bahi-Buisson et al., 2010; Bartnik et al., 2011).

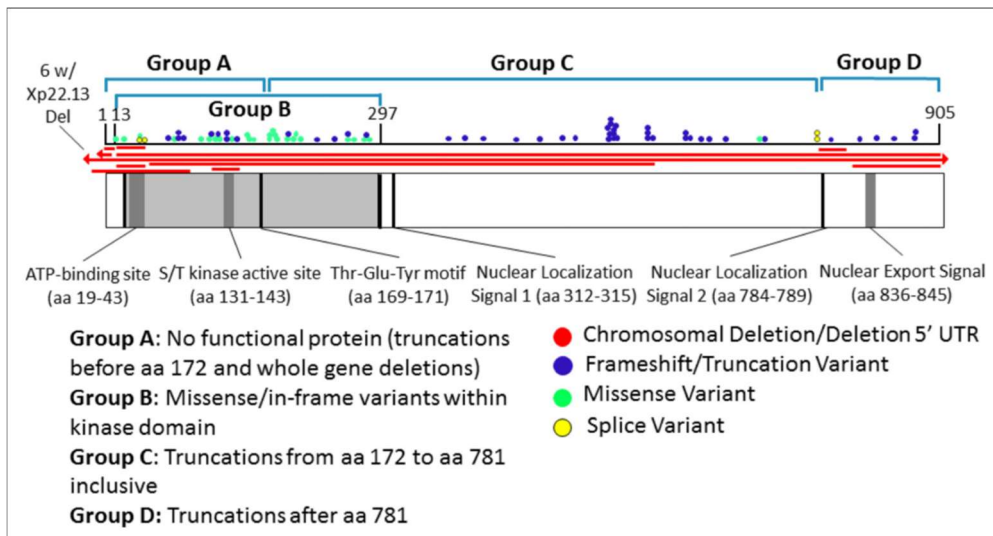


Figure 8. Pathological *CDKL5* mutations. *CDKL5* variants are classified into 4 groups, based on their expected functional consequences [adapted from (Olson et al., 2019)].

Almost all cases of CDD result from *de novo* mutations in the *CDKL5* gene, which occur during the formation of germ cells or in the early stages of embryonic development. In these patients, the mutation is not inherited from parents (Weaving et al., 2004). However, cases of family history of *CDKL5* mutations have also been reported (Allou et al., 2017). This is probably the effect of germinal mosaicism in one of the parents, which results in the transmission of the mutated gene to the offspring.

1.2.5 *CDKL5* expression profile

Expression studies have shown a heterogeneous tissue distribution of *CDKL5* (Hector et al., 2016). The protein is predominantly present in the brain; however, it has also been detected in several peripheral tissues. These include heart, liver, kidney, lung, skeletal muscle, testis, uterus, and gastrointestinal tract (Williamson et al., 2012).

A thorough analysis of *Cdkl5* expression in the adult mouse brain showed that the protein is particularly abundant in the superficial cortical layers of the forebrain (Fig. 9A) (Rusconi et al., 2008). Specifically, high levels of *Cdkl5* transcripts have been detected in the motor, cingulate, piriform and entorhinal cortex, suggesting a CDKL5 involvement in the physiology of these brain regions, which are implicated in higher-order functions such as language and information processing (Kilstrup-Nielsen et al., 2012). *Cdkl5* is also present in the hippocampus, a brain area that regulates long-term learning and memory (Fig. 9A). Specifically, high levels of *Cdkl5* transcripts have been found in all the *Cornu Ammonis* (CA) fields, while low levels have been detected in the dentate gyrus (DG) (Kilstrup-Nielsen et al., 2012). In addition, high levels of *Cdkl5* transcripts have also been found in other brain regions such as the thalamus, striatum, and olfactory bulb, while in the cerebellum and hypothalamus, the transcript levels are very low (Fig. 9A) (Kilstrup-Nielsen et al., 2012).

The expression of *Cdkl5* is very low during embryonic stages of development. Upon birth, the expression is remarkably upregulated, reaching a peak level within the first two weeks of life, and then maintains a relatively high level throughout adulthood (Fig. 9B) (Rusconi et al., 2008).

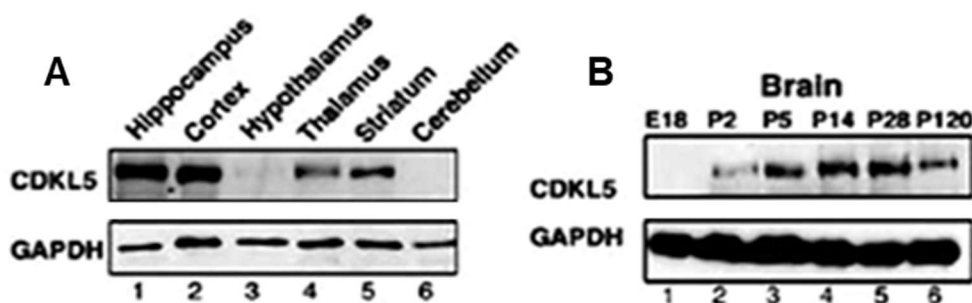


Figure 9. Spatial (A) and temporal (B) expression patterns of *Cdkl5* in the mouse brain [adapted from (Rusconi et al., 2008)].

At the cellular level, *Cdkl5* is highly expressed in both glutamatergic and GABAergic neurons, while it is weakly expressed in glial cells (Rusconi et al., 2008).

The intracellular location of CDKL5 within neurons changes throughout development (Rusconi et al., 2008). During embryonic stages of development, Cdkl5 is mainly localized in the cytoplasm, while starting from early postnatal stages – when Cdkl5 expression is induced together with neuronal maturation – the protein progressively translocates into the nucleus.

Cdkl5 has also been detected in excitatory postsynaptic structures, where it regulates the maturation and growth of dendritic spines and controls excitatory synaptic function (Pizzo et al., 2020; Ricciardi et al., 2012).

1.2.6 CDKL5 substrates and functions

CDKL5 plays an important role in brain development and function through interaction or association with other proteins (Fig. 10) (Hector et al., 2016; Zhu and Xiong, 2019). Some of the most important functions of the protein are summarized below.

- **Neuronal maturation and morphology**

In the early stages of development, CDKL5 is crucial for neuronal morphogenesis. Within the growth cone of developing neurites, CDKL5 interacts with Shootin1 (Nawaz et al., 2016), a brain-specific protein that acts as a regulator of axon formation during the process of neuronal polarization (Toriyama et al., 2006). Once neuronal polarity is established, CDKL5 participates in regulating dendritic arborization through the BDNF/Rac1 signaling pathway. It has been found that brain-derived neurotrophic factor (BDNF) can phosphorylate and activate CDKL5, which in turn activates Rac1, a Rho GTPase involved in cytoskeletal dynamics (Chen et al., 2010). The BDNF/Rac1 signaling pathway activates F-actin, leading to cytoskeletal remodeling in developing neurons and consequent dendritic growth (Zhu and Xiong, 2019).

In 2017, Barbiero and colleagues provided further evidence of CDKL5 involvement in regulating neuronal cytoskeletal dynamics. The authors showed that the loss of CDKL5 negatively regulates the formation of the IQGAP-Rac1-CLIP170 complex – required for microtubule stability and growth – resulting in the alteration of proper cellular morphology (Barbiero et al., 2017a).

Another way in which CDKL5 regulates cytoskeletal dynamics during dendritic arborization is through interaction with EB2 (microtubule-associated protein EB family member 2) and MAP1S (microtubule-associated protein 1S). Phosphorylation of EB2 and MAP1S by CDKL5 causes their dissociation from microtubules (MTs), which promotes the formation of microtubule loops at dendritic tips, required for microtubule stabilization or growth. The absence of CDKL5 leads to increased binding of EB2 and MAP1S to MTs, which results in decreased microtubule dynamics, affecting dendritic branching and leading to impaired neuronal development (Baltussen et al., 2018).

In addition to EB2 and MAP1S, recent studies have shown that CDKL5 can also interact with other microtubule-binding proteins such as ARHGEF2 (Rho-Rac guanine nucleotide exchange factor 2) and DLG5 (discs large MAGUK scaffold protein 5) (Baltussen et al., 2018; Muñoz et al., 2018). These proteins are involved in maintaining cellular polarity, cell adhesion, proliferation and transmission of extracellular signals to the cytoskeleton and membrane (Joo and Olson, 2021; Kwan et al., 2016). Disruption of these processes has been well-characterized in CDKL5-deficient cells (Barbiero et al., 2017a; Nawaz et al., 2016).

Finally, it has been found that CDKL5 can interact with centrosomal protein 131 (CEP131) (Muñoz et al., 2018), which is a component of centriolar satellites that are involved in the regulation of a complex network for primary cilia and flagella formation (Graser et al., 2007). Phosphorylation of CEP131 by CDKL5 plays a key role in controlling centriolar satellites status and regulating critical centrosomal functions in response to cellular stress (Villumsen et al., 2013). Recent studies have identified elongated cilia in *Cdkl5* knockout (KO) rat hippocampal

neurons, and slender cilia in *Cdkl5* KO mouse brains (Di Nardo et al., 2022). However, although patients with CDD do not show a classical ciliopathy, primary cilia play a critical role in the developing brain (Park et al., 2019), and their dysfunction can have an impact on the CDD phenotype (Van Bergen et al., 2022).

- **Dendritic spine structure and synaptic activity**

Synapses are highly specialized structures that allow communication between two neurons. They consist of a presynaptic structure, the axon terminal, which is part of the neuron that sends the information, and a post-synaptic structure located on the receiving neuron. Synapses can have excitatory or inhibitory properties, as they either stimulate or inhibit the activity of the receiving neuron, respectively (Martini et al., 2012). In the cerebral cortex, approximately 90% of the axon terminals of excitatory neurons form synapses on dendritic spines, specialized protrusions that emerge from dendrites (Chapleau et al., 2012). During dendritic spine maturation and synapse formation, CDKL5 binds to the palmitoylated form of PSD-95 (post-synaptic density protein 95), an essential scaffold protein involved in synaptic transmission, signal transduction, and cell adhesion (Zhu et al., 2013). Here, CDKL5 also interacts with NGL-1 (netrin-G ligand-1), an adhesion molecule involved in synaptic formation and homeostasis. Specifically, CDKL5 phosphorylates NGL-1, which in turn binds to PSD-95, forming a complex that stabilizes the dendritic spine structure (Ricciardi et al., 2012). Based on these findings, Della Sala and colleagues suggested that CDKL5 is involved in the stabilization of dendritic spines rather than their formation. The authors also found that the absence of CDKL5 leads to the generation of an increased number of immature spines, resulting in compromised signal transmission (Della Sala et al., 2016).

CDKL5 is also involved in maintaining synaptic function. This role has been confirmed by the identification of a direct interaction between CDKL5 and amphiphysin 1 (AMPH1), a brain-specific protein that

plays an important role in neuronal transmission. It has been found that CDKL5 phosphorylates AMPH1, inhibiting its ability to bind endophilin, which is involved in clathrin-mediated endocytosis. Since endocytosis is crucial for synaptic vesicle recycling, the absence of CDKL5 may impair neuronal activity at the synapse (Sekiguchi et al., 2013).

- **Neuronal proliferation and survival, differentiation, and cell cycle control**

In a study conducted on neuroblastoma cells, Valli and colleagues showed that CDKL5 can inhibit proliferation by promoting cell cycle exit and subsequently induce neuronal differentiation (Valli et al., 2012).

Considering the homology of CDKL5 with MAPKs and CDKs, well-known regulators of cell cycle progression, Fuchs and colleagues further investigated the involvement of the protein in proliferation (Fuchs et al., 2014). The study revealed an increased proliferation rate of neural precursor cells in the hippocampus of adult *Cdkl5* KO mice, suggesting a negative role of CDKL5 on cell proliferation. In addition, the authors also found an increased apoptosis of granule cell precursors, indicating a reduced survival rate of newly formed cells in *Cdkl5* KO mice (Fuchs et al., 2014). These defects have been primarily associated with impairment of the Akt/GSK3 β signaling pathway, which is involved in regulating several events of brain development. Specifically, the loss of CDKL5 leads to decreased phosphorylation and consequent activation of GSK3 β . Considering that GSK3 β exerts a negative control on the survival of newborn neurons (Luo, 2012), these data suggest that the loss of CDKL5 may impair survival and maturation of neurons by disrupting the Akt/GSK3 β signaling pathway (Fuchs et al., 2014).

Furthermore, several studies have shown that the loss of CDKL5 can also alter the Akt/mTOR/rpS6 signaling pathway, which is involved in cell proliferation (Amendola et al., 2014; Wang et al., 2012).

The involvement of CDKL5 in cell cycle control has been further confirmed by a study conducted on proliferating cells, which found that the kinase is able to control cytokinesis and the proper formation of the mitotic spindle (Barbiero et al., 2017b).

- **Nuclear activity**

CDKL5 is involved in the regulation of important nuclear processes through its interaction with many epigenetic and transcriptional factors (Van Bergen et al., 2022; Wang et al., 2012).

Since mutations in the *MECP2* and *CDKL5* genes lead to similar genetic disorders, the correlation between the two has been further investigated. MECP2 is a transcription factor that can specifically bind to methylated DNA (Fuks et al., 2003; Nan et al., 1998). It has been found that CDKL5 phosphorylates MECP2 *in vitro* (Bertani et al., 2006; Mari et al., 2005), suggesting that CDD and RTT may share common molecular pathways. This would partially explain the similar clinical features between the two disorders (Bergo et al., 2015; Mari et al., 2005).

In a study conducted by Kameshita and colleagues, it has been shown that CDKL5 can bind and phosphorylate the N-terminal region of DNA methyltransferase 1 (DNMT1), an enzyme involved in DNA methylation. The study highlighted, for the first time, a possible involvement of CDKL5 in epigenetic mechanisms (Kameshita et al., 2008).

Furthermore, Trazzi and colleagues showed that CDKL5 can phosphorylate histone deacetylase 4 (HDAC4), promoting its cytoplasmic retention in neurons. In contrast, in the absence of CDKL5, HDAC4 translocates into the nucleus and induces histone deacetylation, initiating a cascade of events that contribute to the manifestation of neurodevelopmental defects in *Cdkl5* KO mice (Trazzi et al., 2016).

Finally, in a study conducted by Fuchs and colleagues, it has been found that CDKL5 can interact with SMAD3 (Fuchs et al., 2019), a

transcription factor that plays a crucial role in neuronal function through transforming growth factor (TGF)- β signaling pathway (Yu et al., 2014). Direct phosphorylation of SMAD3 protein by CDKL5 promotes SMAD3 stability. Conversely, reduced SMAD3 levels – as observed by the authors in the cortex and hippocampus of *Cdkl5* KO mice – impairs neuronal survival and maturation (Fuchs et al., 2019).

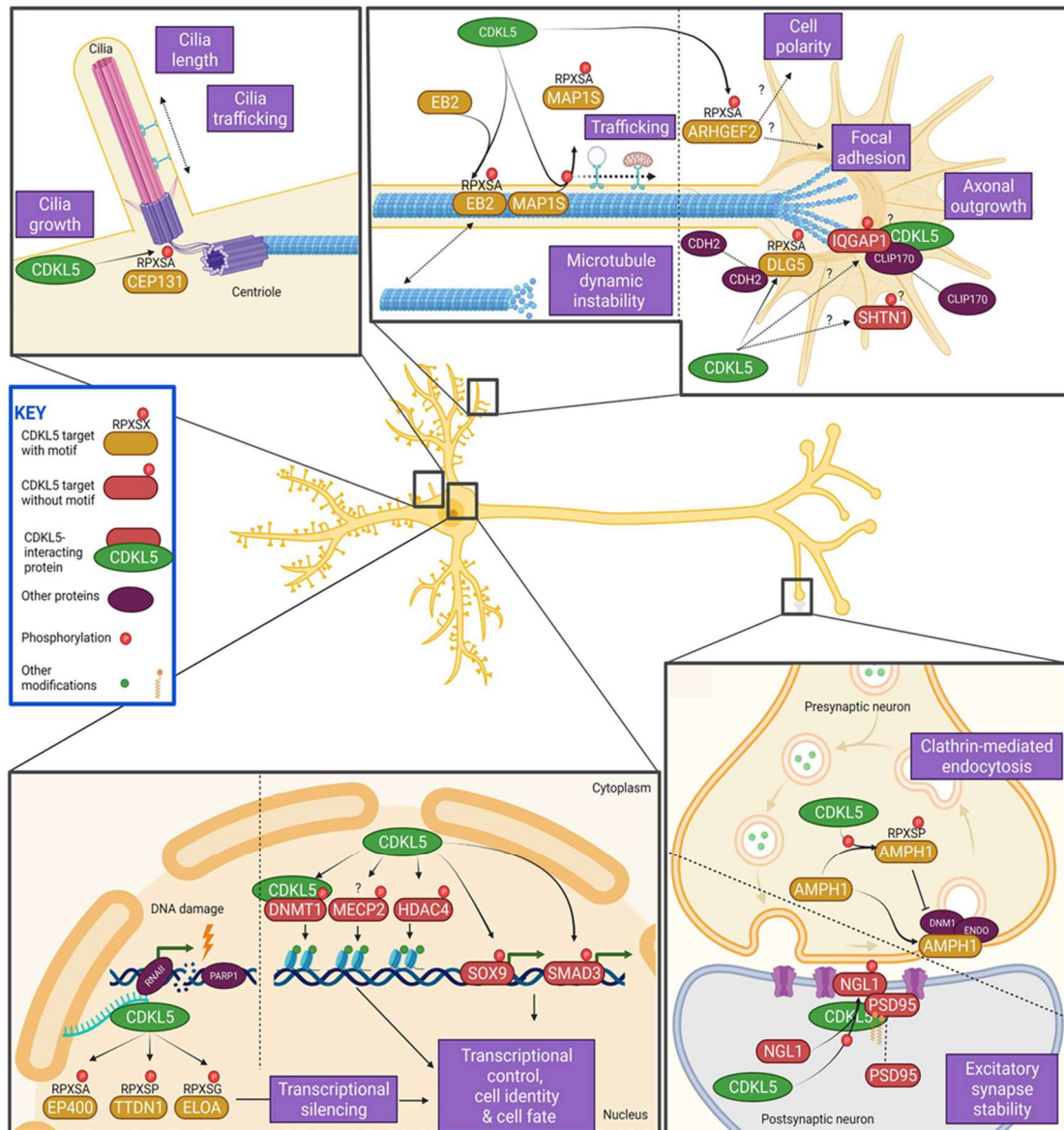


Figure 10. Known CDKL5 targets and affected processes in neurons [adapted from (Van Bergen et al., 2022)].

- **DNA damage-sensing**

Recently, it has been suggested that CDKL5 may also play a key role in recognizing DNA damage in neuronal cells. In 2020, Loi and

colleagues, found that human neuroblastoma cells with a CDKL5 deletion are hypersensitive to DNA damage-induced stress and show increased DNA damage-associated markers (i.e., γ H2Ax, RAD50, and PARP1), reduced cell viability, and impaired neuronal maturation (Loi et al., 2020). Later, Gennaccaro and colleagues found increased levels of DNA repair proteins in the brain of *Cdkl5* KO mice, suggesting that *Cdkl5* deletion accelerates neuronal aging or death through irreparable DNA damage (Gennaccaro et al., 2021a).

Finally, Khanam and colleagues showed that DNA damage induces CDKL5 re-localization to sites of double-stranded DNA breaks (DSB). Here, CDKL5 phosphorylates the proteins ELOA (Elongin A), TTDN1 (Trichothiodystrophy non-photosensitive 1), and EP400 (E1a binding protein P400), leading to transcriptional silencing in the region of the DSB (Khanam et al., 2021).

1.3 Mouse models of CDD

The mouse *Cdkl5* gene consists of 23 exons and produces 5 different transcript isoforms as a result of alternative splicing (Fig. 11). The isoforms predominantly expressed in the brain, *mCdkl5_1* and *mCdkl5_2*, are orthologous to their human counterparts (*hCDKL5_1* and *hCDKL5_2*). In contrast, the other three transcripts, *mCdkl5_6*, *mCdkl5_7*, and *mCdkl5_8*, do not show full orthology to human isoforms (Hector et al., 2016).

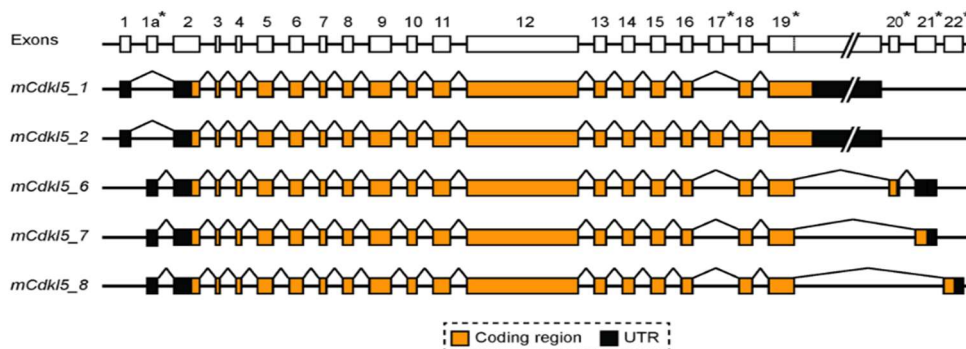


Figure 11. Schematic representation of the mouse *Cdkl5* transcript isoforms. Lines linking exons indicate splicing events. Asterisks next to exon numbers indicate where differences have been found between different transcript isoforms [adapted from (Hector et al., 2016)].

Since the majority of the *CDKL5* coding region is orthologous and well-conserved between human and mouse (Fig. 12), the latter is considered a good model to study the molecular mechanisms underlying the development of CDD and to test potential therapeutic approaches (Hector et al., 2016).

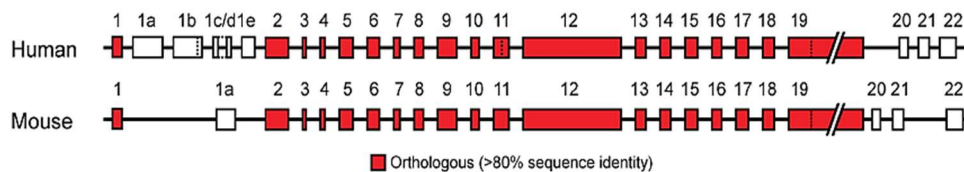


Figure 12. Comparison of human *CDKL5* and mouse *Cdkl5* gene structures [adapted from (Hector et al., 2016)].

Independently, several laboratories have generated both constitutive and conditional *Cdkl5* knockout mice using the site-specific recombinase technology.

The first *Cdkl5* KO mouse was generated in 2012 by deletion of exon 6 (Wang et al., 2012). The authors found several behavioral alterations in these animals, including hyperactivity, motor deficits, auditory impairments, reduced anxiety, and impaired learning and memory. The presence of these deficits showed, for the first time, that the loss of *Cdkl5* in mice causes a phenotype that recapitulates several clinical features observed in CDD patients. Subsequent studies have identified reduced nociception (La Montanara et al., 2020) and further behavioral alterations in these animals, including reduced social interactions, stereotyped movements, and communication deficits, highlighting the presence of autism-like features in this mouse model (Gao et al., 2020; Jhang et al., 2017).

In 2014, Amendola and colleagues developed an additional *Cdkl5* KO mouse by deletion of exon 4 (Amendola et al., 2014). Similar to the model developed by Wang and colleagues (Wang et al., 2012), this *Cdkl5* KO mouse shows several behavioral alterations, including hind-limb clasping, motor deficits, and impaired learning and memory. Several studies have identified additional alterations in this mouse model, such as visual impairments (Mazziotti et al., 2017; Pizzo et al., 2016; Pizzo et al., 2020), respiratory abnormalities (Lo Martire et al.,

2017), increased susceptibility to excitotoxic stress (Amendola et al., 2014; Fuchs et al., 2019), mitochondrial dysfunctions (Carli et al., 2021), compromised arousal modulation (Viglione et al., 2022), and cardiac abnormalities (Loi et al., 2023). Furthermore, a recent study has shown impaired neonatal reflexes in *Cdkl5* KO pups lacking exon 4, demonstrating the presence of early behavioral defects during postnatal development (Tassinari et al., 2023).

It is important to note that, in addition to behavioral deficits, several neuroanatomical abnormalities have been well-characterized in both adult and juvenile *Cdkl5* KO mice lacking exon 4.

Several studies have reported a severe impairment of dendritic arborization in these animals, including reduced total dendritic length and decreased number of branches (Amendola et al., 2014; Fuchs et al., 2015; Fuchs et al., 2014; Tassinari et al., 2023).

Furthermore, *Cdkl5* KO mice with exon 4 deletion show changes in the organization and stability of dendritic spines, as well as in the density of PSD-95 and mGluR5 dendritic clusters in several brain structures, including the somatosensory and visual cortex, and the hippocampus (Della Sala et al., 2016; Fuchs et al., 2015; Gurgone et al., 2023; Pizzo et al., 2016; Tassinari et al., 2023).

In addition, long-term potentiation (LTP) and the frequency of miniature excitatory postsynaptic currents, an indicator of the level of excitatory synaptic transmission, are impaired in *Cdkl5* KO mice lacking exon 4 (Della Sala et al., 2016; Ren et al., 2019). Gennaccaro and colleagues found a higher number of GABAergic terminals in the cortex of *Cdkl5* KO mice compared to wild-type mice, suggesting that increased inhibitory transmission may contribute to the impairment of LTP (Gennaccaro et al., 2021b). Interestingly, the recent finding that CDKL5 is involved in sensory-induced plasticity of both excitatory and inhibitory synapses in the barrel cortex (Pizzo et al., 2020) indicates that CDKL5 deficiency alters both excitation and inhibition, suggesting that the transmission of sensory inputs to the cortex may be less efficient in CDD patients. Finally, it has been found that *Cdkl5* KO mice lacking exon 4 are characterized by an increased rate of apoptotic cell

death in the hippocampus, indicating that the absence of *Cdkl5* increases neuronal vulnerability (Fuchs et al., 2014; Gennaccaro et al., 2021a; Loi et al., 2020).

In 2017, Okuda and colleagues generated a *Cdkl5* KO mouse lacking exon 2 (Okuda et al., 2017). In these animals, the administration of N-methyl-D-aspartate (NMDA) acid can induce severe generalized tonic-clonic seizures, highlighting an abnormal response mediated by the NMDA receptor (NMDAR). The analysis of hippocampal regions revealed an increase in postsynaptic localisation of GluN2B (glutamate ionotropic receptor NMDA type subunit 2B) in the excitatory synapses of these mice. The accumulation of GluN2B is associated with the increased susceptibility to epileptic seizures in the *Cdkl5* KO mice, suggesting the involvement of CDKL5 in controlling the postsynaptic localization of these receptors (Okuda et al., 2017). In a subsequent study, the authors reported several behavioral deficits in this mouse model, including reduced social interactions, motor coordination disorders, and impairment in both acquisition and long-term retention of spatial reference memory (Okuda et al., 2018).

In addition to the previously mentioned *Cdkl5* knock-out mice, a knock-in mouse model has also been developed: the *Cdkl5^{R59X}* mouse (Tang et al., 2019). The *Cdkl5^{R59X}* knock-in mouse carries a nonsense mutation at arginine 59 of the *Cdkl5* gene, mimicking the same mutation found in CDD patients who experience severe epilepsy. These animals exhibit behavioral alterations observed in other murine models of CDD, including social deficits and impairments in memory and learning. Additionally, *Cdkl5^{R59X}* mice show a decreased latency to seizure following pentylenetetrazol (PTZ) administration (Yennawar et al., 2019).

Importantly, in addition to constitutive *Cdkl5* KO mice, several conditional *Cdkl5* KO mice have been developed. In these mouse models, the expression of *Cdkl5* is silenced in specific cell populations. In 2014, Amendola and colleagues, using the transgenes *Emx1::Cre* and *Dlx 5/6::Cre*, silenced the expression of *Cdkl5* within glutamatergic and GABAergic neurons, respectively (Amendola et al., 2014). The

authors demonstrated that distinct phenotypes can be mapped to different neuronal populations in the forebrain. Specifically, hind-limb clasping and reduced head-tracking response were present only in *Emx1*-conditional *Cdkl5* KO (*Emx1*-cKO) mice, while reduced locomotion was characteristic of *Dlx5/6*-conditional *Cdkl5* KO (*Dlx5/6*-cKO) mice (Amendola et al., 2014). Recently, using *Emx1*-cKO mice, Lupori and colleagues have demonstrated that selective cortical deletion of CDKL5 from excitatory cells is sufficient to produce abnormalities in visual cortical responses, demonstrating that the normal functioning of cortical circuits is dependent on CDKL5 (Lupori et al., 2019).

The *Nex*-cKO mouse is a conditional knock-out model in which *Cdkl5* has been removed from the glutamatergic neurons of the forebrain, specifically those in the cortex and hippocampus (Tang et al., 2017). It is important to note that *Nex*-cKO mice do not exhibit alterations in activity, anxiety, or social behavior. However, they show deficits in hippocampal-dependent learning and memory, suggesting that CDKL5 in glutamatergic neurons of the hippocampus plays a key role in learning and memory mechanisms (Tang et al., 2017).

Furthermore, two conditional knock-out models of CDD were generated to study the effects of *Cdkl5* loss-of-function in CaMKII α -positive excitatory neurons and GAD65-positive inhibitory neurons (Schroeder et al., 2019). Behavioral studies were not conducted in these mice; however, it was found that the loss of *Cdkl5* in these neuronal populations differentially dysregulate components of the mTOR signaling (Schroeder et al., 2019), a pathway involved in the regulation of gene expression, protein synthesis, and neuronal growth (Lipton and Sahin, 2014).

Finally, Terzic and colleagues temporally manipulated the endogenous *Cdkl5* expression through the development of a special conditional KO mouse model (Terzic et al., 2021a). The authors showed that post-developmental loss of *Cdkl5* in adult mice leads to behavioral deficits similar to those observed in germline KO mice, indicating an indispensable role for CDKL5 also in adulthood.

Importantly, the authors observed that the restoration of *Cdkl5* ameliorated CDD-related behavioral impairments of these mice, demonstrating the potential for disease reversal in CDD (Terzic et al., 2021a).

Overall, the mouse models described above recapitulate many of the clinical features observed in CDD patients, including learning and memory impairments, autistic-like behaviors, and motor deficits; and exhibit dysmorphic neuronal architecture, disrupted signaling pathways, and compromised neuronal connectivity. However, the major symptom of CDKL5 deficiency is epilepsy. Although for many years it was believed that mouse models of CDD did not show epilepsy, except after administration of a convulsant agent (Amendola et al., 2014; Fuchs et al., 2019; Okuda et al., 2017; Yennawar et al., 2019), spontaneous seizures have recently been reported in these animals.

In a study conducted by Mulcahey and colleagues, recurrent spontaneous seizures were reported, for the first time, in aged heterozygous female *Cdkl5* mice (Mulcahey et al., 2020). Epileptic spasms were the major spontaneous seizure type, characterized by sudden-onset body spasm typically associated with generalized slow-wave activity on the EEG (Mulcahey et al., 2020).

In a further study conducted on aged heterozygous female *Cdkl5* mice by Terzic and colleagues, the occurrence of overt, myoclonic and tonic-clonic behavioral seizure-like events was reported (Terzic et al., 2021b). However, these events were not observed in hemizygous male and homozygous female mice, suggesting that X-linked cellular mosaicism is a driving factor underlying these seizure-like events (Terzic et al., 2021b).

The results of these studies have highlighted the importance of heterozygous female *Cdkl5* mice, whose neuroanatomical and behavioral deficits have been well-characterized (Fuchs et al., 2018), in understanding the mechanisms underlying epileptogenesis in CDD. Finally, Wang and colleagues, through the development of a specific conditional KO model, demonstrated that the absence of *Cdkl5* in

glutamatergic neurons of the forebrain, but not in GABAergic neurons, leads to recurrent spontaneous epileptic seizures in hemizygous male mice between 2 and 7 months of age (Wang et al., 2021). This model (Wang et al., 2021) represents a new tool to elucidate the pathogenic mechanism of epilepsy in CDD and introduces an experimental platform to develop therapies against CDD-related seizures.

1.4 Neuroinflammation

Neuroinflammation is the natural response of the body to injuries, infections, or harmful stimuli that occur within the central nervous system (CNS) and involves different immune cells and molecules (Kaur et al., 2020; Kwon and Koh, 2020). The inflammatory response within the CNS can be induced by endogenous (e.g., genetic mutations and protein aggregation) or environmental (e.g., infections, trauma, drugs) factors (Kwon and Koh, 2020). Upon exposure to these stimuli, the immune cells of the CNS – microglia and astrocytes – release pro-inflammatory molecules, such as cytokines, chemokines, and reactive oxygen species (Muzio et al., 2021). Although this is a crucial defense mechanism, chronic or excessive neuroinflammation can have harmful effects on the nervous system. In fact, prolonged activation of immune cells and the release of inflammatory molecules can damage neurons, compromise neuronal communication, and disrupt homeostasis within the CNS, leading to the onset of neurological diseases (Javanmehr et al., 2022; Kaur et al., 2020; Kwon and Koh, 2020).

Recently, neuroinflammation has received special attention in research due to its involvement in several CNS diseases, including neurodegenerative and neurodevelopmental disorders. Specifically, a growing number of studies have shown that therapies targeting microglia can be a valid strategy to counteract the progression of these diseases (Subramaniam and Federoff, 2017; Wes et al., 2016).

1.4.1 *Microglia: origin, signature, and functions*

Microglia are the primary immune cells of the central nervous system. These cells represent the first line of defense against harmful insults in the brain (Javanmehr et al., 2022; Kofler and Wiley, 2011).

Microglia constitute 5% of the cells within the human brain parenchyma and are more abundant in the white matter compared to the gray matter (Martini et al., 2012; Mittelbronn et al., 2001). It is important to note that during an infection or injury, this percentage increases significantly (Witcher et al., 2021).

Unlike all other cells in the nervous system, which originate from the ectodermal embryonic germ layer, microglia derive from the mesodermal germ layer (Martini et al., 2012). Specifically, microglia derive from myeloid progenitor cells of the yolk sac expressing the transcription factor RUNX1 and the receptor tyrosine kinase c-Kit, also known as CD117 (Kierdorf et al., 2013). During embryonic development, these cells migrate through the bloodstream to the developing CNS, where they settle and differentiate (Ginhoux et al., 2010; Gomez Perdiguero et al., 2015).

Transcriptomic analyses have revealed that in the adult brain, microglia express a wide range of markers, including the triggering receptor expressed on myeloid cells 2b (TREM2b), chemokine receptor 1 (CX3CR1), CD11b, CD45, and allograft inflammatory factor-1 (AIF-1, also known as IBA-1) (Javanmehr et al., 2022). The latter is an actin-binding protein, and is a well-established marker for the identification of microglia in immunohistochemical analyses since it is highly expressed in these cells under both physiological and pathological conditions (Ito et al., 1998).

In their “resting” state – in the absence of injuries and/or pathogens in the CNS – microglia exhibit a ramified phenotype, with a typically round cell body and a multitude of highly dynamic, thin cytoplasmic processes that actively detect potential alterations in the brain microenvironment, contributing to the maintenance of its homeostasis (Salter and Stevens, 2017). However, the morphology of microglial

cells can differ depending on the region of the CNS under consideration (Arcuri et al., 2017). For instance, in the white matter, microglia have an elongated soma; in the gray matter, they have a typically round soma; while in circumventricular and perivascular regions, microglia have a more compact cell body with shorter cytoplasmic processes (Sominsky et al., 2018).

The main function of microglial cells is to engulf and eliminate – through phagocytosis – pathogens, damaged cells, or debris potentially present in the brain microenvironment (Illes et al., 2021; Kofler and Wiley, 2011). When microglia detect danger signals, that can disrupt CNS homeostasis, they undergo "activation". During this process, microglia increase proliferative activity, retract their cytoplasmic processes, and enlarge their cell body, transitioning from a quiescent ramified form (resting state) to an amoeboid form (reactive state) (Davis et al., 2017; Streit, 2000). These morphological changes promote the rapid migration to the injured site, where microglia exert their phagocytic activity (Stence et al., 2001).

There are two distinct phenotypes of activated microglia depending on the detected stimuli and pathological events: the M1 (pro-inflammatory) phenotype and the M2 (anti-inflammatory) phenotype (Fig. 14) (Cherry et al., 2014; Luo and Chen, 2012).

Pro-inflammatory triggers derived from pathogens (e.g., lipopolysaccharide [LPS]) or in response to neuronal damage induce resting microglia to express the M1 phenotype, leading to the release of pro-inflammatory factors such as interleukin (IL)-1 α , IL-1 β , IL-6, IL-12, tumor necrosis factor (TNF)- α , and nitric oxide (NO) (Du et al., 2017; Orihuela et al., 2016). These mediators can generate an inflammatory state, which in turn promotes the clearance of pathogens and/or cellular debris from the brain microenvironment. However, if this condition persists for a long time, it can have a harmful impact on the CNS. In fact, if microglia are chronically activated in the M1 phenotype, they continuously release pro-inflammatory cytokines that disrupt the structure and activity of neurons (Hickman et al., 2018). Furthermore, in response to the injury, neurons release soluble factors

(e.g., μ -calpain, MMP3, α -synuclein, neuromelanin) that maintain microglia in a reactive state, stimulating the continuous release of pro-inflammatory cytokines. This self-perpetuating cycle of neurotoxicity is known as reactive microgliosis, and partially explains the involvement of microglia in the pathogenesis and/or exacerbation of CNS disorders characterized by chronic neuroinflammation (Fig. 13) (Lull and Block, 2010).

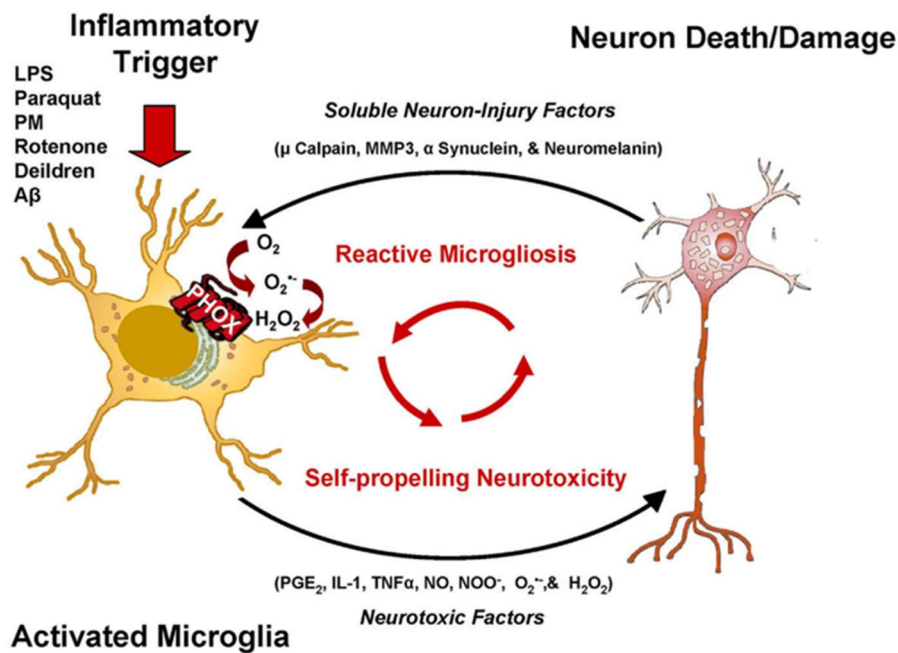


Figure 13. Reactive microgliosis drives chronic neuron damage [adapted from (Lull and Block, 2010)].

On the other hand, the M2 phenotype, induced by anti-inflammatory cytokines such as IL-4 and IL-10, suppresses inflammation, promotes extracellular matrix remodeling, and supports neuronal survival through the release of protective/trophic factors such as BDNF, TGF- β , CX3CL13, and insulin-like growth factor (IGF)-1 (Kwon and Koh, 2020). The M2 phenotype can be further categorized into M2a, M2b, and M2c phenotypes (Wendimu and Hooks, 2022).

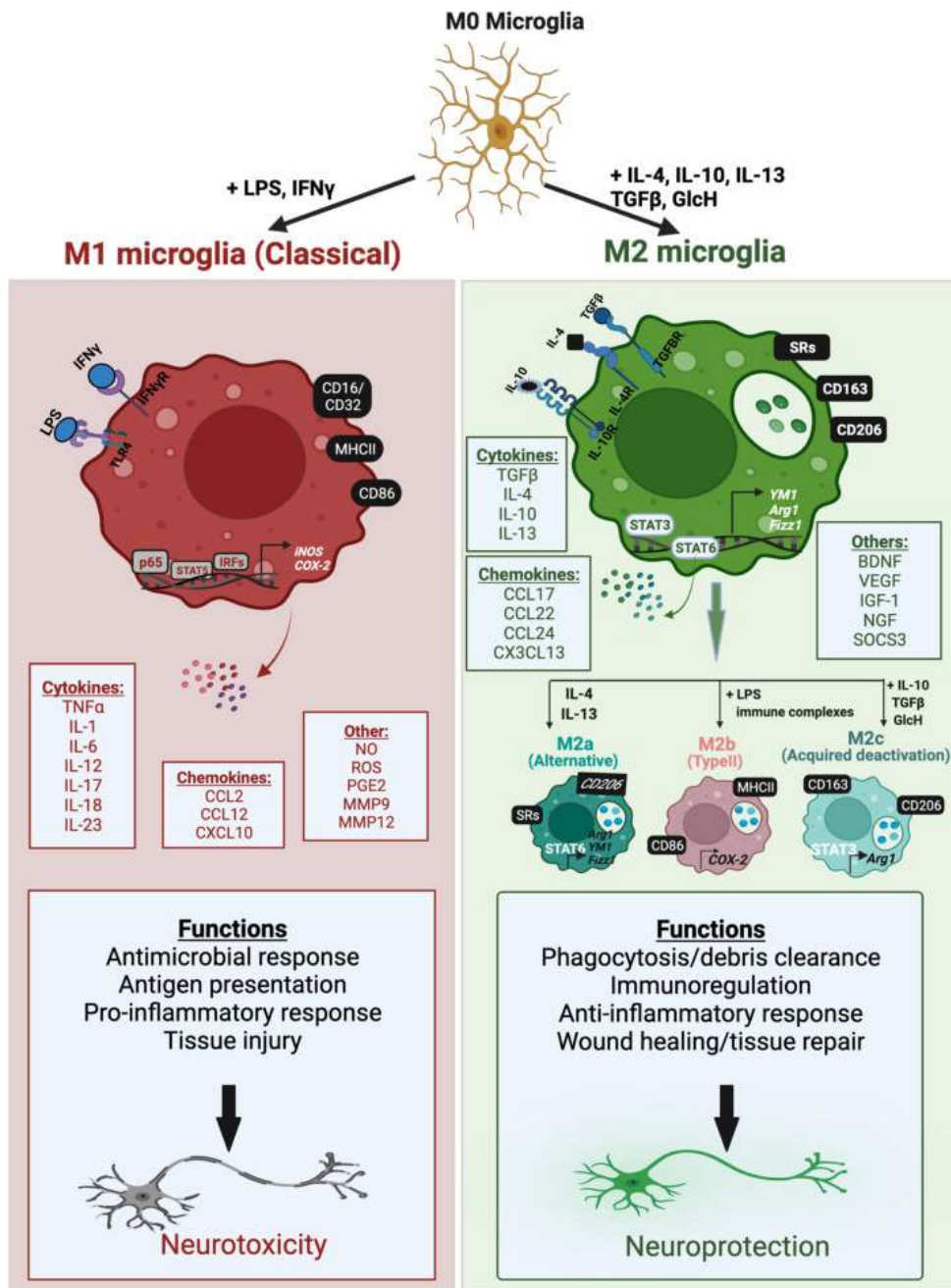


Figure 14. Microglial activation phenotypes and functions [adapted from (Wendimu and Hooks, 2022)].

However, it is important to note that recent research has suggested that the traditional categorization of microglial activation into M1 and M2 states may not fully capture the complexity of microglial phenotypes (Javanmehr et al., 2022). While the M1 and M2 classification has been widely used to describe pro-inflammatory and anti-inflammatory states, it is becoming increasingly clear that

microglia exhibit a broader range of transcriptional states beyond this binary classification (Ochocka and Kaminska, 2021).

In addition to their immune function, microglial cells play important roles in development, neuronal connectivity, and synaptic plasticity (Salter and Beggs, 2014; Tremblay et al., 2011).

During CNS development, microglia can engulf and clear neurons that die as a result of programmed cell death, a process that eliminates excess neurons generated as part of normal development and ongoing neurogenesis in the brain (Brown and Neher, 2014; Marín-Teva et al., 2011).

Furthermore, during development, microglia sculpt immature neuronal circuits by eliminating synaptic structures (i.e., axons and dendritic spines) in a process known as synaptic pruning (Paolicelli et al., 2011; Schafer et al., 2012). This process plays a crucial role in CNS development as it allows neural circuits to reach their final configuration (Paolicelli et al., 2011). Alterations in synaptic pruning have been implicated in the onset of neurodevelopmental disorders such as autism and schizophrenia (Boksa, 2012; Kim et al., 2017).

Finally, microglia can also monitor neuronal activity and synaptic function through the expression of various receptors for cytokines, chemokines, and both excitatory and inhibitory neurotransmitters (Wake et al., 2013).

1.4.2 Microglia and pathological conditions

Since microglia play an important role in the development and homeostasis of the CNS, alterations in the functionality of these cells are involved in the onset of a wide range of CNS diseases, such as neurodegenerative and neurodevelopmental disorders (Boksa, 2012; Essa et al., 2013; Kim et al., 2017; Maezawa and Jin, 2010; Salter and Stevens, 2017; Zhang et al., 2021a).

Growing evidence suggests that during aging, microglia undergo morphological and functional changes, such as reduced branching, increased cell body size, decreased migration to the injured site, and

increased release of pro-inflammatory cytokines (e.g., IL-1 β , TNF- α , IL-6) (Miller and Streit, 2007; Njie et al., 2012). These age-related microglial dysfunctions, combined with a chronic stress environment, brain trauma, or genetic predisposing factors, can contribute to the progressive onset of Alzheimer's disease (AD) and other neurodegenerative diseases, including Parkinson's disease (PD), amyotrophic lateral sclerosis (ALS), and frontotemporal dementia (FTD) (von Bernhardi et al., 2015; Wong, 2013).

Moreover, experimental evidence has demonstrated that microglia are impaired in autism spectrum disorders (ASD), a group of neurodevelopmental disorders characterized by severe deficits in communication and social interaction (Salter and Stevens, 2017). Specifically, post-mortem studies conducted in patients with ASD have identified abnormalities in the density and morphology of microglial cells (Morgan et al., 2010; Tetreault et al., 2012; Vargas et al., 2005). In addition, further analyses performed in these patients have also found increased expression of specific microglial genes (e.g., genes encoding pro-inflammatory cytokines) (Gupta et al., 2014; Suzuki et al., 2013; Voineagu et al., 2011), and impaired synaptic pruning (Hutsler and Zhang, 2010).

Furthermore, it has been demonstrated that microglia also play an important role in RTT (Derecki et al., 2012; Maezawa and Jin, 2010; Schafer et al., 2016). Recently, it has been demonstrated that the aberrant response of microglia to insults originating from neurons or other cells (e.g., astrocytes) contributes to the neuronal and circuit dysfunction observed in the *Mecp2*-null mouse brain, mouse model of RTT (Schafer et al., 2016). Additionally, in a study conducted on *Mecp2*-null mice, Maezawa and Jin found that microglia can release high levels of glutamate in the brain of these animals, compromising neuronal functionality and suggesting that neuroinflammation may influence the onset and progression of RTT (Maezawa and Jin, 2010). It is important to note that glutamate is an amino acid that can have excitotoxic effects on neurons (Zhou and Danbolt, 2014). In fact, high levels of glutamate in the brain microenvironment cause structural and

functional alterations in neurons, which in turn lead to their death. The excitotoxic effect of glutamate is mediated by its binding to the NMDA receptor. Upon glutamate binding, NMDAR activates a signaling pathway that inhibits mitochondrial respiratory chain complex IV activity and induces a rapid drop in intracellular adenosine triphosphate (ATP) levels. Cellular energy loss impairs dendritic and axonal transport and leads to neuronal death (Takeuchi, 2010). Therefore, it is believed that chronic activation of microglia and the subsequent release of glutamate may lead to an increased susceptibility to excitotoxic stress in neurons (Takeuchi, 2010). Finally, experimental and clinical evidence strongly supports the involvement of microglia in the pathophysiology of human epilepsy (Fig. 15) (Aronica et al., 2017; Rana and Musto, 2018; Villasana-Salazar and Vezzani, 2023; Zhao et al., 2018).

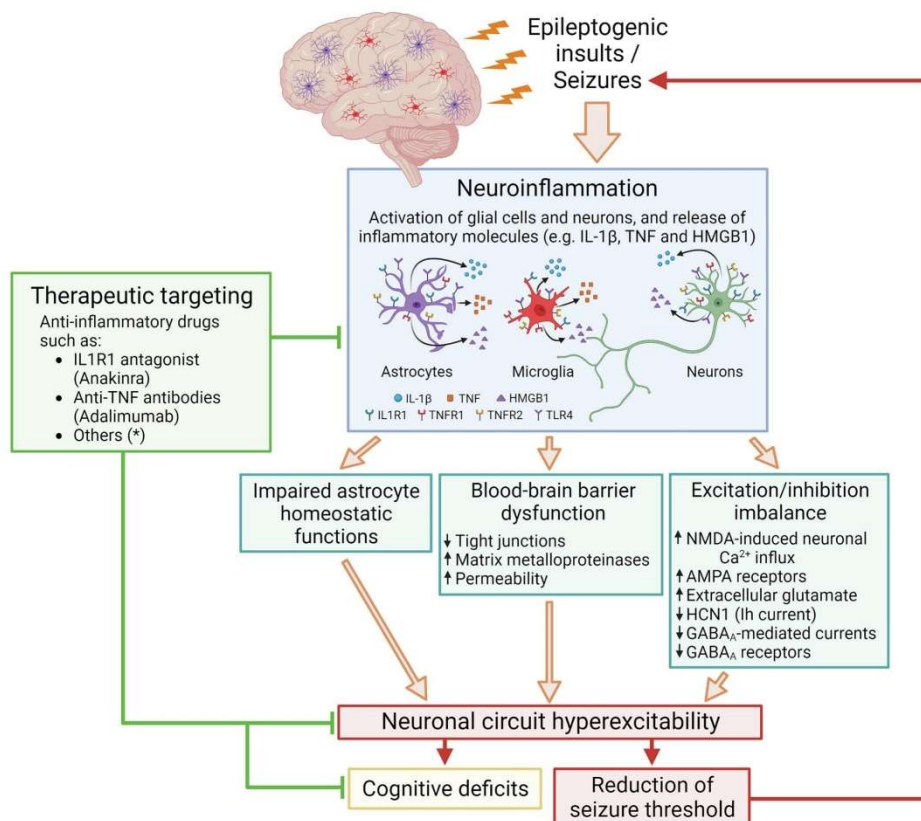


Figure 15. Cascade of events induced by neuroinflammation and resulting in altered neuronal excitability [adapted from (Villasana-Salazar and Vezzani, 2023)].

Epileptic seizures were recently induced in rats after intraventricular injection with an activated microglia-conditioned medium, suggesting that activation of microglia may also be an important process for the onset of epilepsy (Zhao et al., 2018). Finally, proof-of-concept studies, which have validated several therapeutic approaches targeting inflammatory mechanisms in preclinical models, have indicated that these may represent new avenues for the development of drugs against epilepsy (Aronica et al., 2017; Villasana-Salazar and Vezzani, 2023).

The modulation of microglial activation has received significant attention as a potential therapeutic approach for several neurological diseases (Liu et al., 2019; Sucksdorff et al., 2019; Zhang et al., 2021a). In addition to conventional pharmacological approaches targeting microglial activation (e.g., nonsteroidal anti-inflammatory drugs, immunomodulators), in recent years, the use of alternative strategies has been increasingly prominent (Yousefizadeh et al., 2022). In this context, it is important to note the growing use of phytochemicals. Phytochemicals are biologically active compounds found in plants. Over the years, these naturally occurring compounds have shown efficacy against human diseases. Specifically, various classes of phytochemical substances have been characterized, and their anti-inflammatory mechanisms have been elucidated in several neurological disorders (Kaur et al., 2020). To date, luteolin stands out as one of the most commonly used phytochemicals to modulate microglial activation.

1.4.3 Luteolin

Several studies have shown that the consumption of plant-based foods reduces the risk of developing several diseases (Pandey and Rizvi, 2009). This is partly attributed to the abundant presence of phytochemicals, including flavonoids, in these foods. Flavonoids are plant-derived polyphenolic compounds known for their antioxidant, anti-inflammatory, anticancer, neuroprotective, and cardioprotective

properties. To date, more than 8,000 flavonoids have been identified, classified into 6 subgroups: chalcones, flavones, flavonols, flavanols, anthocyanins, and isoflavones (Nabavi et al., 2015).

Luteolin (3',4',5,7-tetrahydroxyflavone) is a flavonoid belonging to the flavone subgroup. It can be extracted from various plant sources, including carrot, pepper, celery, peppermint, thyme, rosemary, olive, pomegranate, artichoke, turnip, and oregano, where the concentration of luteolin is the highest (1,028.75mg/100g) (Muruganathan et al., 2022).

Structurally, luteolin (molecular formula $C_{15}H_{10}O_6$) has a classic flavone 15C skeleton structure, also known as C6-C3-C6, consisting in two benzene rings and one oxygen-containing ring which presents a C2-C3 double bond. As a tetrahydroxy flavone, luteolin possesses 4 hydroxy groups located at positions 3', 4', 5, and 7 (Fig. 16) (Taheri et al., 2021).

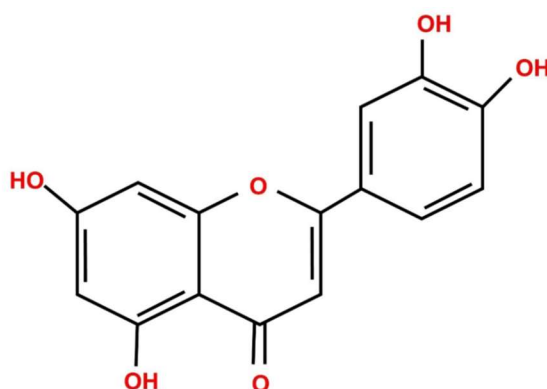


Figure 16. Chemical structure of luteolin [adapted from (Muruganathan et al., 2022)].

This structure allows the molecule to exert multiple pharmacological effects. It has been demonstrated that luteolin possesses antioxidant, anti-inflammatory, antitumor, antimicrobial, and antiallergic properties (Ashaari et al., 2018; Aziz et al., 2018; Muruganathan et al., 2022).

In vitro and *in vivo* studies have shown that luteolin effectively counteracts the process of inflammation by inhibiting the release of pro-inflammatory cytokines (e.g., IL-1 β , IL-2, IL-6, TNF- α) and stimulating the release of anti-inflammatory cytokines (e.g., IL-10, IL-4) by immune cells (Aziz et al., 2018). Moreover, it has been

demonstrated that luteolin can cross the blood-brain barrier and modulate the activity of microglial cells (Sawmiller et al., 2014). In addition, *in vitro* and *in vivo* studies have shown that luteolin is able to inhibit activated microglia and promote the release of BDNF, a neurotrophin essential for neuronal survival (Yoo et al., 2013; Zhen et al., 2016)). Based on these findings, it is believed that luteolin may have a neuroprotective effect.

Luteolin exerts its anti-inflammatory action by regulating the activity of transcription factors NF- κ B (nuclear factor kappa-light-chain-enhancer of activated B cells), AP-1 (activator protein 1), and STAT3 in immune cells (Fig. 17) (Aziz et al., 2018; Muruganathan et al., 2022).

Specifically, luteolin promotes the inactivation of NF- κ B by inhibiting the degradation of its inhibitor (I κ B); blocks the nuclear translocation of AP-1; and suppresses the phosphorylation of STAT3, thereby blocking its activity. Overall, these effects alter the transcription of genes involved in the inflammatory process, inhibiting the expression of pro-inflammatory mediators, and promoting the expression of anti-inflammatory mediators (Aziz et al., 2018).

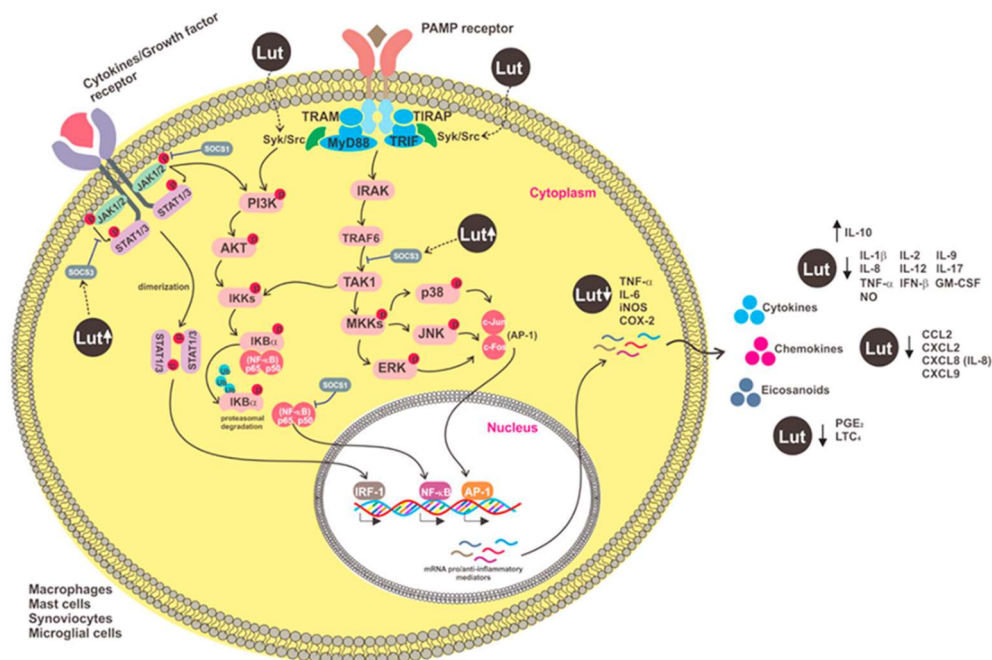


Figure 17. Mechanism of action of luteolin [adapted from (Aziz et al., 2018)].

Due to its anti-inflammatory and neuroprotective properties, the role of luteolin in the treatment of CNS diseases characterized by neuroinflammatory processes has been investigated.

Experimental evidence has shown that pre-treatment with luteolin significantly reduces the frequency of pentylenetetrazol (PTZ)-induced tonic-clonic seizures in mouse models of epilepsy (Birman et al., 2012; Shaikh et al., 2013; Tambe et al., 2017; Zhen et al., 2016).

Furthermore, several clinical studies have demonstrated the beneficial effects of luteolin in the treatment of autism spectrum disorders (Fig. 18) (Savino et al., 2023).

Study (Author, Year, and Reference)	Study Design	Study Population	Intervention Details (Duration and Dose)	Key Findings
Bertolino et al. 2017	Case report	A 10-year old male child with ASD	12 months 700 mg + 70 mg b.i.d.	<ul style="list-style-type: none"> Improved sociability and motor stereotypies; Reduced enuresis
Taliou et al. 2013	Open-label study	50 children (4–10 years old) (n = 42 boys; n = 8 girls)	26 weeks 200 mg/day	<ul style="list-style-type: none"> Improved adaptive functioning; Ameliorated behavioral difficulties; Transient irritability
Theoharides et al. 2012	Case series	37 children (4–14 years old) (n = 29 boys; n = 8 girls)	4 months 200 mg/day	<ul style="list-style-type: none"> Improved gastrointestinal dysfunction and allergy; Increased eye contact, attention and social interaction; Good tolerability
Tsilioni et al. 2015	Open-label study	40 children (4–10 years old) (n = 34 boys; n = 6 girls)	26 weeks 200 mg/day	<ul style="list-style-type: none"> Decreased IL-6 and TNF; No effect on CRH and NT; Improved sociability, communication daily living skills

Figure 18. Effects of luteolin on ASD in clinical studies [adapted from (Savino et al., 2023)].

An uncontrolled open case series conducted on 37 autistic children (29 males and 8 females, aged 4 to 14 years) showed that treatment with luteolin for 4 months improved gastrointestinal symptoms in approximately 75% of the children, visual contact and attention in 50%, social interactions in 25%, and communication skills in approximately 10% (Theoharides et al., 2012). In a subsequent study involving 50 children (42 males and 8 females, aged 4 to 10 years), it was found that a dietary supplement formulation containing luteolin could provide significant benefits in ASD children both in adaptive functioning and behavioral difficulties (Taliou et al., 2013). Furthermore, an open-label trial on a cohort of 40 ASD children (34 males and 6 females, aged 4

to 10 years) demonstrated that serum levels of IL-6 and TNF- α significantly decreased after a 26-week treatment period with luteolin, compared to normotypic controls (Tsilioni et al., 2015). Finally, Bertolino and colleagues reported that a combined treatment of luteolin and palmitoylethanolamide (PEA) for 12 months improved the clinical picture in a 10-year-old male child, with a reduction in stereotyped behaviors (Bertolino et al., 2017).

These results have demonstrated that treatment with luteolin has no side effects and is also able to ameliorate the symptoms of CNS disorders characterized by neuroinflammatory processes. However, further studies should be performed to increase the bioavailability and absorption of luteolin by different delivery systems, and determine the optimal dose of luteolin in humans to achieve a significant therapeutic effect (Nabavi et al., 2015).

AIM OF THE STUDY

Microglia, the immune cells of the central nervous system (CNS), have recently taken center stage in research as key players in CNS health and disease. Under healthy conditions, microglia contribute to brain homeostasis by eliminating or remodeling synapses, supporting myelin turnover, monitoring neural firing, and actively scavenging the local environment for pathogens or tissue damage (Salter and Stevens, 2017; Sominsky et al., 2018). In response to an immune challenge, pathogen, or injury, microglia undergo "activation". During this process, microglia increase proliferative activity, retract their cytoplasmic processes, enlarge their cell body, and start the expression of pro-inflammatory mediators, such as inducible nitric oxide synthase (iNOS), interleukin (IL)-1 β , and tumor necrosis factor (TNF)- α (Jin et al., 2019; Kozlowski and Weimer, 2012). Recently, dysregulation of microglia function has been found to be involved in several neurodevelopmental and neurodegenerative disorders, suggesting that active neuroinflammation may account for the compromised brain development/neuronal survival observed in these pathologies (Dong et al., 2009; Essa et al., 2013; Salter and Stevens, 2017).

Mutations in the *cyclin-dependent kinase-like 5* gene (CDKL5) cause CDKL5 deficiency disorder (CDD), a severe neurodevelopmental disease characterized by early onset treatment-resistant epilepsy, gross motor impairment, severe intellectual disability, and autistic features (Fehr et al., 2013; Leonard et al., 2022; Olson et al., 2019). No cure or effective treatments are currently available to ameliorate cognitive and behavioral symptoms for CDD.

Mounting evidence suggests that inflammatory processes are involved in the pathophysiology of CDD. Recently, a major cytokine dysregulation that is proportional to clinical severity, inflammatory status, and redox imbalance has been found in the plasma of children affected by CDD (Cortelazzo et al., 2017; Leoncini et al., 2015), suggesting a subclinical chronic inflammatory status in these patients.

However, to date, it is unknown whether a similar inflammatory status is also present in the brain of CDD patients and whether it plays a causative or exacerbating role in the pathophysiology of CDD. In addition, *Cdkl5* knockout (KO) mice – mouse models of CDD – show high susceptibility to excitotoxic stimuli compared to their wild-type counterpart (Fuchs et al., 2019), a feature that suggests the potential involvement of neuroinflammatory processes (Viviani et al., 2014).

Since abnormal immune response during critical windows of development and consequent abnormal production of neuroinflammatory mediators may have an impact on the function and structure of the brain (Di Marco et al., 2016), **the overall goal of this study was to investigate the role of neuroinflammatory processes in the pathophysiology of CDD.**

In particular the specific aims of this project were:

1. to determine whether a chronic inflammatory status is present in the brain of *Cdkl5* KO mice;
2. to evaluate the effect of pharmacological inhibition of microglial activation, through luteolin treatment, on brain development and behavior, as well as on neuronal susceptibility to excitotoxic stress in *Cdkl5* KO mice.

Since these aspects of the pathology have been so far overlooked, studying the role of neuroinflammation in CDD will generate important knowledge, not only to better understand CDD etiology, but also to develop therapeutic approaches that are still missing for CDD.

2. MATERIALS AND METHODS

2.1 Colony

The mice used in this work derived from the *Cdkl5* null strain in the C57BL/6N background developed in (Amendola et al., 2014) and backcrossed in C57BL/6J for three generations. Mice for experiments were produced by crossing *Cdkl5* +/- females with *Cdkl5* +/Y males. Littermate controls were used for all experiments. Animals were genotyped by PCR on genomic DNA using the following primers:

108F: 5'-ACGATAGAAATAGAGGATCAACCC-3';

109R: 5'-CCCAAGTATACCCCTTTCCA-3';

125R: 5'-CTGTGACTAGGGGCTAGAGA-3'.

The day of birth was designed as postnatal day (P) zero and animals with 24 hours of age were considered as 1-day-old animals (P1). After weaning (P21-23), mice were housed three to five per cage and maintained in a temperature- (23°C) and humidity-controlled environment with a standard 12 h light/dark cycle, and provided with standard mouse chow and water *ad libitum*. Animals' day-to-day health and comfort were monitored by the veterinary service. Experiments were performed in accordance with the Italian and European Community law for the use of experimental animals and were approved by Bologna University Bioethical Committee. All possible efforts were made to minimize suffering and the number of animals used. Experiments were carried out on a total of 239 *Cdkl5* KO mice (*Cdkl5* +/Y, n=4; *Cdkl5* -/Y, n=4; *Cdkl5* +/+, n=75; *Cdkl5* +/-, n=156).

2.2 Treatments

All treatments were performed in the animal house at the same hour of the day.

2.2.1 *TATκ-GFP-CDKL5 protein treatment*

Brain sections processed for AIF-1 immunohistochemistry were derived from animals used in (Trazzi et al., 2018). Briefly, 6-month-old wild-type (+/Y) and *Cdkl5* -/Y mice were implanted subcutaneously with a programmable pump (IPRECIO, Primetech, Japan) equipped with a refillable reservoir. The pump was connected to a catheter implanted in the carotid artery. The IPRECIO reservoir (130 µl) was filled with either TATκ-GFP-CDKL5 or TATκ-GFP. A 10-day infusion protocol was programmed as follows: 2 daily (1 in the morning and 1 in the evening) boluses (20 µl each corresponding to 50 ng of protein) were administered at 10 µl/h with a low constant release (0.4 µl/h) during the rest of the day to prevent catheter occlusion. Every 2 or 3 days, mice were briefly anesthetized to refill the IPRECIO reservoir (transdermal injection) with fresh solutions.

2.2.2 *Luteolin treatment*

Mice were intraperitoneally (i.p.) injected with vehicle (2% DMSO in saline) or luteolin (10 mg/kg in saline; Tocris Bioscience, Bristol, UK) daily for 7 or 20 days. The dose of luteolin was chosen based on (Zhou et al., 2019). The day after the last treatment, mice were sacrificed for histological and Western blot analyses.

2.2.3 *Stattic treatment*

Mice were i.p. injected with vehicle (2% DMSO + 30% polyethylene glycol) or Stattic (20 mg/Kg; Sigma-Aldrich, Saint Louis, MO, USA) every other day for 7 days, for a total of four injections. The dose of Stattic was chosen based on (Millot et al., 2020). Animals were sacrificed the day after the last treatment for histological analyses.

2.2.4 *Acetaminophen treatment*

Mice were i.p. injected with vehicle (2% DMSO in saline) or acetaminophen (APAP; 100 mg/kg; Sigma-Aldrich, Saint Louis, MO, USA) daily for 7 days. The dose of APAP was chosen based on (Pinto et al., 2020). Animals were sacrificed the day after the last treatment for histological analyses.

2.2.5 *NMDA treatment*

Mice were subjected to a single intraperitoneal injection of NMDA (60 mg/kg; Sigma-Aldrich, Saint Louis, MO, USA) in 0.1 M phosphate-buffered saline (PBS) after 7 days of luteolin treatment. Animals were sacrificed 24 h or 8 days after NMDA injection for histological analyses. Seizure grades were scored according to (Wu et al., 2005) and recorded during a 1-h observation period. NMDA-induced seizures were scored as follows: 0 – no abnormalities; 1 – exploring, sniffing, and grooming ceased, with mice becoming motionless; 2 – forelimb and/or tail extension, appearance of rigid posture; 3 – myoclonic jerks of the head and neck with brief twitching movements, or repetitive movements with head-bobbing or “wet-dog shakes”; 4 – forelimb clonus and partial rearing, or rearing and falling; 5 – forelimb clonus, continuous rearing, and falling; 6 – tonic-clonic movements with loss of posture tone, often resulting in death.

2.2.6 *BrdU Treatment*

Mice were subjected to a single subcutaneous injection of 5-Bromo-2'-deoxyuridine (BrdU; 150 mg/kg; Sigma-Aldrich, Saint Louis, MO, USA) on the twentieth day of luteolin treatment, and sacrificed the following day.

2.3 Histological and immunohistochemistry procedures

Animals were anesthetized with isoflurane (2% in pure oxygen) and sacrificed through cervical dislocation. Brains were quickly removed and cut along the midline. Left hemispheres were Golgi-stained or quickly frozen and used for Western blot analyses. Right hemispheres were fixed by immersion in 4% paraformaldehyde in 0.1 M phosphate-buffered saline (PBS) for 48 h, kept in 15-20% sucrose for an additional 24 h, frozen with dry ice, and stored at - 80°C. Right hemispheres were then cut with a freezing microtome (Microm GmbH, Walldorf, Germany) into 30- μ m-thick coronal sections, which were serially collected in 96-well plates containing a solution composed of 30% glycerol, 30% ethylene glycol, 0.02% sodium azide in 0.1 M PBS, and then processed for immunohistochemistry procedures, as described below.

2.3.1 Immunofluorescence staining

One out of every eight free-floating sections from the hippocampal formation was incubated overnight at 4°C with one of the following primary antibodies: rabbit polyclonal anti-AIF-1 antibody (1:300; Thermo Fisher Scientific, Waltham, MA, USA), mouse monoclonal anti-NeuN antibody (1:250; Merck Millipore, Burlington, MA, USA), rabbit polyclonal anti-GFAP antibody (1:400; Abcam, Cambridge, UK), mouse monoclonal anti-GAD67 antibody (1:500; Merck Millipore, Burlington, MA, USA), rabbit monoclonal anti-Ki-67 antibody (1:200; Thermo Fisher Scientific, Waltham, MA, USA), rabbit polyclonal anti-DCX antibody (1:300; Thermo Fisher Scientific, Waltham, MA, USA), and rabbit polyclonal anti-PSD-95 antibody (1:200; Abcam, Cambridge, UK). The following day, the sections were incubated for 2 h at room temperature with a Cy3-conjugated anti-rabbit IgG secondary antibody (1:200; Jackson ImmunoResearch Laboratories, West Grove, PA, USA) for AIF-1, GFAP, Ki-67, DCX, and PSD-95 immunohistochemistry, and with a Cy3-conjugated anti-mouse IgG

secondary antibody (1:200; Jackson ImmunoResearch Laboratories, West Grove, PA, USA) for GAD67 and NeuN immunohistochemistry. Nuclei were counterstained with Hoechst 33342 (Sigma-Aldrich, Saint Louis, MO, USA).

For cleaved caspase-3 immunofluorescence, one out of every six free-floating sections from the hippocampal formation was incubated overnight at 4°C with a rabbit polyclonal anti-cleaved caspase-3 antibody (1:200; Cell Signaling Technology, Danvers, MA, USA). The following day, the sections were incubated for 2 h at room temperature with an HRP-conjugated anti-rabbit IgG secondary antibody (1:200; Jackson ImmunoResearch Laboratories, West Grove, PA, USA). Detection was performed using the TSA[®] Cyanine 3 Plus Fluorescence Kit (Perkin Elmer, Waltham, MA, USA), and nuclei were counterstained with Hoechst 33342 (Sigma-Aldrich, Saint Louis, MO, USA).

For BrdU immunofluorescence, one out of every eight free-floating sections from the hippocampal formation was denatured in 2 N HCl for 30 min at 37°C, and then incubated overnight at 4°C with a rat monoclonal anti-BrdU antibody (1:200; Abcam, Cambridge, UK). The following day, the sections were incubated for 2 h at room temperature with a Cy3-conjugated anti-rat IgG secondary antibody (1:200; Jackson ImmunoResearch, WestGrove, PE, USA). Nuclei were counterstained with Hoechst 33342 (Sigma-Aldrich, Saint Louis, MO, USA).

2.3.2 *DCX immunohistochemistry*

One out of every six free-floating sections from the hippocampal formation was incubated overnight at 4°C with a goat polyclonal anti-DCX antibody (1:100; Santa Cruz Biotechnology, Dallas, TX, USA). The following day, the sections were incubated with a biotinylated anti-goat IgG secondary antibody (1:200, Vector BioLabs, Malver, PA, USA) for 2 h and then for 1 h with the VECTASTAIN[®] ABC kit (Vector

BioLabs, Malver, PA, USA). Detection was performed using Vector® DAB Substrate kit (Vector BioLabs, Malver, PA, USA).

2.3.3 Golgi staining

Left hemispheres were Golgi-stained using the FD Rapid Golgi Stain™ Kit (FD NeuroTechnologies, Columbia, MD, USA). Briefly, hemispheres were immersed in the impregnation solution containing mercuric chloride, potassium dichromate, and potassium chromate, and stored at room temperature in the dark for 3 weeks. Hemispheres were then cut with a cryostat (Histo-Line Laboratories, Pantigliate, Italy) into 100-µm-thick coronal sections, which were directly mounted onto Superfrost® Plus Microscope Slides (Thermo Fisher Scientific, Waltham, MA, USA) and air-dried at room temperature for 1 day. After drying, sections were rinsed with distilled water, stained in the developing solution of FD Rapid Golgi Stain™ Kit (FD NeuroTechnologies, Columbia, MD, USA), and coverslipped with DPX mounting medium (Sigma-Aldrich, Saint Louis, MO, USA).

2.4 Image acquisition and measurements

Fluorescence images were taken with an Eclipse TE 2000-S microscope equipped with a DS-Qi2 digital SLR camera (Nikon Instruments, Tokyo, Japan). A light microscope (Leica Microsystems, Wetzlar, Germany) equipped with motorized stage, focus control system, and color digital camera (Coolsnap-Pro; Media Cybernetics, Rockville, MD, USA) were used for bright field images. Measurements were carried out using the Image-Pro Plus software (Media Cybernetics, Rockville, MD, USA).

2.4.1 Cell density

The number of AIF-1-positive cells in the hippocampus and somatosensory cortex was manually counted using the point tool of

the Image-Pro Plus software (Media Cybernetics, Rockville, MD, USA), and cell density was established as AIF-1-positive cells/mm³. The density of Hoechst-positive nuclei in the CA1 field and in the dentate gyrus of the hippocampus were manually counted and expressed as cells/mm³. The density of NeuN-, Cleaved caspase-3-, GAD67-, and GFAP-positive cells in the CA1 field of the hippocampus were manually counted and expressed as cells/mm³. Ki-67-, BrdU-, and DCX-positive cells were counted in the subgranular and granular zone of the dentate gyrus of the hippocampus and expressed as number of cells/mm.

2.4.2 Morphometric microglial cell analysis

Starting from 20x magnification images of AIF-1-stained hippocampal and cortical slices, microglial cell body size was manually drawn using the measurement function of the Image-Pro Plus software (Media Cybernetics, Rockville, MD, USA) and expressed in μm^2 . The roundness index of each microglial cell was calculated as reported in (Davis et al., 2017) with the following equation: $\text{roundness} = 4A/\pi M^2$, where A is the area and M is the length of the major axis of each microglial cell's soma. Approximately 120 microglial cells were analyzed from each sample.

2.4.3 Measurement of the Dendritic Tree

Dendritic trees of newborn DCX-positive granule neurons (15-20 per animal) and Golgi-stained pyramidal neurons (apical and basal dendrites) from hippocampal CA1 field and layers II/III of the somatosensory cortex were traced using custom-designed software for dendritic reconstruction (Immagini Computer, Milan, Italy), interfaced with the Image-Pro Plus software (Media Cybernetics, Rockville, MD, USA). The dendritic tree was traced live, at a final magnification of 500x, by focusing on the depth of the section. The operator starts with branches that emerge from the cell soma and after

drawing the first parent branch, proceeds with all the daughter branches of the next order in a centrifugal direction. At the end of tracing, the software reconstructs the number and length of individual branches, the mean length of branches of each order, and the total dendritic length.

2.4.4 Dendritic Spine Number and Morphology

In Golgi-stained sections, dendritic spines of hippocampal and cortical pyramidal neurons were visualized with a 100x oil immersion objective lens. Based on their morphology, dendritic spines can be divided into two different categories that reflect their state of maturation: immature spines and mature spines. The number of spines belonging to the two different groups (immature spines: filopodium-like, thin- and stubby-shaped; mature spines: mushroom- and cup-shaped) was counted and expressed as a percentage. About 200-250 spines from 25 to 30 dendrites, derived from 10 to 20 neurons, were analyzed per condition.

2.4.5 Quantification of PSD-95 Immunoreactive Puncta

Images from the hippocampal CA1 field were acquired using a LEICA TCS SL confocal microscope (Leica Microsystems, Wetzlar, Germany; objective 63, NA 1.32; zoom factor = 8). Three to four sections per animal were analyzed. In each section, three images of the region of interest were captured, and the number of PSD-95 immunoreactive puncta was evaluated and expressed per μm^2 .

2.5 Microglia isolation

Microglial cells were isolated following the protocol published in (Slepko and Levi, 1996). Briefly, wild-type (+/+) and *Cdk15* +/- mice were anesthetized with isoflurane (2% in pure oxygen) and transcardially perfused with 0.1 M phosphate-buffered saline (PBS). Brains were transferred to ice-cold PBS (without Ca^{2+} and Mg^{2+} , with

NaHCO₃, 0.75 g/l, Hepes buffer 10 mM, pH 7.4), freed of meninges, minced in serum-free Dulbecco Modified Eagle Medium (DMEM) containing 0.25% trypsin and 0.02% EDTA, and incubated at 37°C for 60 min. Enzymatic digestion was blocked by adding DMEM supplemented with 10% heat-inactivated Fetal Bovine Serum (FBS). After centrifugation (2000 rpm at 4°C for 5 min), samples were incubated with a DNase solution (serum-free DMEM containing 40 µg/ml DNase Type I) for 15 min at 37°C. Samples were then centrifuged, transferred to ice-cold DMEM, and sieved through a nylon mesh 40-µm pore size (Corning Cell Strainer; Corning Incorporated, Corning, NY, USA). DMEM (21.4 ml) with sieved tissue derived from 2 mouse brains was mixed with 8.6 ml of cold isotonic Percoll® (GE Healthcare, Chicago, IL, USA) in PBS and centrifuged (2000 rpm at 4°C for 20 min). Pellet was washed in PBS and finally resuspended in 1 ml of TRI reagent® (Sigma-Aldrich, Saint Louis, MO, USA) and stored at -80°C or processed for RNA extraction. For Western blotting analyses, protein extracts were prepared from microglial cells purified from 4 to 6 mouse brains.

2.6 RNA isolation and RT-qPCR

Microglial RNA isolation was performed using the Direct-zol RNA MiniPrep kit (Zymo Research, Irvine, CA, USA), and cDNA synthesis was achieved with 1 µg of total RNA using iScript™ Advanced cDNA Synthesis Kit (Bio-Rad, Hercules, CA, USA) according to the manufacturer's instructions. Real-time PCR was performed using SsoAdvanced Universal SYBR Green Supermix (Bio-Rad, Hercules, CA, USA) in an iQ5 Real-Time PCR Detection System (Bio-Rad, Hercules, CA, USA). We used primer pairs (Table 1) that gave an efficiency close to 100%. GAPDH (glyceraldehyde 3-phosphate dehydrogenase) was used as reference gene for normalization in the qPCR. Each biological replicate was run in three technical replicates. Relative quantification was performed using the $\Delta\Delta C_t$ method.

Gene		Primer sequence (5'-3')
<i>IL-1β</i>	<i>Forward</i>	TGCCACCTTTTGACAGTGATG
	<i>Reverse</i>	TGATGTGCTGCTGCGAGATT
<i>IL-6</i>	<i>Forward</i>	CTCTGCAAGAGACTTCCATCCA
	<i>Reverse</i>	GACAGGTCTGTTGGGAGTGG
<i>TNF-α</i>	<i>Forward</i>	TAGCCACGTCGTAGCAAAC
	<i>Reverse</i>	GCAGCCTTGTCCCTTGAAGA
<i>CX3CR1</i>	<i>Forward</i>	TGCTTGCACATTGGGGAGACTGGA
	<i>Reverse</i>	AGGGAACGCTAAAGTCCTGGCTGA
<i>AIF-1</i>	<i>Forward</i>	GTCCTTGAAGCGAATGCTGG
	<i>Reverse</i>	CATTCTCAAGATGGCAGATC
<i>mCdk15</i>	<i>Forward</i>	TGCAGACACAAGGAAACACATGA
	<i>Reverse</i>	TTTCCTGCTTGAGAGTGCGAA
<i>CD11b</i>	<i>Forward</i>	CCTTGTTCTCTTTGATGCAG
	<i>Reverse</i>	GTGATGACAACACTAGGATCTT
<i>NeuN</i>	<i>Forward</i>	ACACACACACTCCATACTGAGG
	<i>Reverse</i>	GCTCTGGGCTCTCTGTTTGC

Table 1. List of primers used for quantitative RT-PCR.

2.7 Western blotting

For the preparation of total cell extracts, tissue samples were homogenized in RIPA buffer (50 mM Tris-HCl, pH 7.4, 150 mM NaCl, 1% Triton-X100, 0.5% sodium deoxycholate, 0.1% SDS) supplemented with 1 mM PMSF and 1% protease and phosphatase inhibitor cocktail (Sigma-Aldrich, Saint Louis, MO, USA). Protein concentration was determined using the Bradford method (Bradford, 1976). Equivalent amounts (50 μ g) of protein were subjected to electrophoresis on a 4-12% Mini-PROTEAN® TGX™ Gel (Bio-Rad, Hercules, CA, USA) and transferred to a Hybond ECL nitrocellulose

membrane (GE Healthcare, Chicago, IL, USA). The following primary antibodies were used: rabbit polyclonal anti-CDKL5 (1:500; Sigma-Aldrich, Saint Louis, MO, USA), rabbit polyclonal anti-phospho-STAT3 (Tyr705; 1:1000; Cell Signaling Technology, Danvers, MA, USA), rabbit polyclonal anti-STAT3 (1:1000; Sigma-Aldrich, Saint Louis, MO, USA), rabbit polyclonal anti-AIF-1 antibody (1:1000; Thermo Fisher Scientific, Waltham, MA, USA), rabbit polyclonal anti-BDNF (1:500; Santa Cruz Biotechnology, Dallas, TX, USA), rabbit polyclonal anti-phospho-TrkB (Ser816; 1:500; Merck Millipore, Burlington, MA, USA), rabbit polyclonal anti-TrkB (1:500; Santa Cruz Biotechnology, Dallas, TX, USA), rabbit polyclonal anti-phospho-Erk1/2 (Thr202/Tyr204; 1:1000; Cell Signaling Technology, Danvers, MA, USA), rabbit polyclonal anti-Erk1/2 (1:1000; Cell Signaling Technology, Danvers, MA, USA), rabbit polyclonal anti-phospho-Akt (Ser473; 1:1000; Cell Signaling Technology, Danvers, MA, USA), rabbit polyclonal anti-Akt (1:1000; Cell Signaling Technology, Danvers, MA, USA), and rabbit polyclonal anti-GAPDH (1:5000; Sigma-Aldrich, Saint Louis, MO, USA). An HRP-conjugated goat anti-rabbit IgG secondary antibody (1:5000; Jackson ImmunoResearch Laboratories, West Grove, PA, USA) was used. Densitometric analysis of digitized Western blot images was performed using Chemidoc™ XRS+ Imaging System and the Image Lab™ Software (Bio-Rad, Hercules, CA, USA). This software automatically highlights any saturated pixels of Western blot images in red. Images acquired with exposure times that generated protein signals out of a linear range were not considered for quantification.

2.8 Behavioral assays

All behavioral studies and analyses were performed blinded to genotype and treatment. Mice were allowed to habituate to the testing room for at least 1 h before the test, and testing was performed at the same time of day. A total of 57 animals separated into 2 independent test cohorts were used for the behavioral studies. A first test cohort

consisted of 30 animals (vehicle-treated *Cdk15* +/+ n=10; vehicle-treated *Cdk15* +/- n=10; luteolin-treated *Cdk15* +/- n=10). A second test cohort consisted of 27 animals (vehicle-treated *Cdk15* +/+ n=11; vehicle-treated *Cdk15* +/- n=8; luteolin-treated *Cdk15* +/- n=8). Starting from the eighth day of luteolin treatment, the animals were behaviorally tested with a sequence of tests arranged to minimize the effect of one test influencing the subsequent evaluation of the next, and mice were allowed to recover for 3-6 days between different tests.

2.8.1 Hind-Limb Clasping

Animals were suspended by their tail for 2 min and hind-limb clasping time was assessed independently by two operators from video recordings. A clasping event is defined by the retraction of hind-limbs into the body and toward the midline.

2.8.2 Open Field Test

To assess locomotion, the animals were placed in the center of a square arena (50 x 50 cm) and their behavior was monitored for 15 min using a video camera placed above the center of the arena. Distinct features of locomotor activity, including total distance travelled, average locomotion velocity, and the time spent in the center, were scored using EthoVision 15XT software (Noldus, Wageningen, The Netherlands). The average locomotion velocity was calculated as the ratio between distance travelled and time. The number of stereotypical jumps (repetitive beam breaks < 1 s) was manually counted by a trained observer. Test chambers were cleaned with 70% ethanol between test subjects.

2.8.3 Passive Avoidance Test

For the passive avoidance task, the equipment consisted of a tilting-floor box (47 x 18 x 26 cm) divided into 2 compartments (lit and dark)

by a sliding door, and a control unit that incorporated a shocker (Ugo Basile, Gemonio, Italy). Upon entering the dark compartment, mice received a brief mild foot shock (0.4 mA for 3 s) and were removed from the chamber after a 15-s delay. After a 24-h retention period, mice were returned to the illuminated compartment, and the latency to re-enter the dark chamber was measured, up to 360 s. The chambers were cleaned with 70% ethanol between testing of one subject and another.

2.9 Statistical analysis

Statistical analysis was performed with GraphPad Prism (version 7). Values are expressed as means \pm standard error (SEM). The significance of results was obtained using two-tailed unpaired t-test and one way or two-way ANOVA followed by Fisher's LSD post hoc test, as specified in the figure legends. A probability level of $p < 0.05$ was considered statistically significant. The confidence level was taken as 95%.

3. RESULTS

3.1 Increased microglial activation in the brain of *Cdk15* KO mice

To investigate whether inflammatory processes could be involved in the pathophysiology of CDD, we counted the number and analyzed the morphology of microglia (AIF-1-positive cells) in the hippocampus and cortex of male (-/Y) and female (+/-) *Cdk15* KO mice and wild-type (+/Y, +/+) littermates. We found an increase in the number of microglial cells in both the analyzed brain regions of -/Y and +/- *Cdk15* KO mice in comparison with their +/Y and +/+ counterparts (Fig. 19A-C).

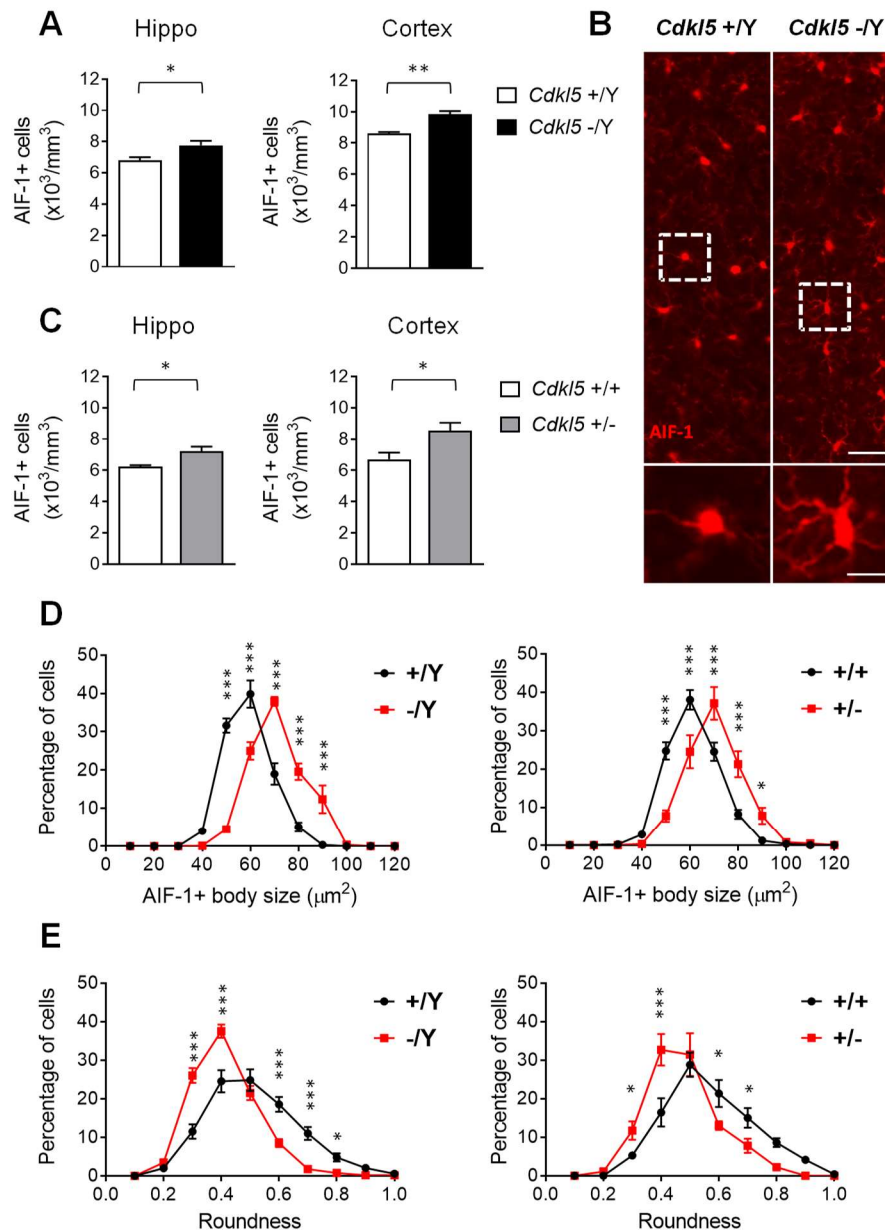


Figure 19. Increased microglial activation in the brain of *Cdkl5* KO mice. A,C: Number of AIF-1-positive cells in hippocampal (Hippo) and somatosensory cortex (Cortex) sections from 3-month-old *Cdkl5* male (+/Y n=4, -/Y n=4; A), and female (+/+ n=5, +/- n=6; C) mice. **B:** Representative fluorescence images of cortical sections processed for AIF-1 immunohistochemistry of a wild-type (+/Y) and a *Cdkl5* -/Y mouse. The dotted boxes in the upper panels indicate microglial cells shown in magnification in lower panels. High magnification (scale bar = 10 μ m) and low magnification (scale bar = 30 μ m). **D:** Distribution analysis of cell body size of AIF-1-positive cells in the somatosensory cortex of 3-month-old *Cdkl5* male (+/Y n=4, -/Y n=4; on the left), and female (+/+ n=4, +/- n=6; on the right) mice, showing a shift to larger cell body size in the absence of *Cdkl5*. **E:** Distribution analysis of AIF-1-positive cells circularity (roundness) in the somatosensory cortex of *Cdkl5* mice as in D. In *Cdkl5* KO mice, microglial cells are more irregularly shaped (lower roundness index) showing a left-shifted distribution compared to that of wild-type mice. Values in A and C are represented as means \pm SEM. * $p < 0.05$, ** $p < 0.01$ (two-tailed Student's t-test). Values in D and E are represented as means \pm SEM. * $p < 0.05$, *** $p < 0.001$ (Fisher's LSD test after two-way ANOVA).

Moreover, microglial cells in *Cdkl5* KO mice presented an enlarged body size (Fig. 19D) and reduced roundness of the cell body (Fig. 19E) compared to wild-type counterparts (Fig. 19B,D,E). Together, these data indicate that in the absence of *Cdkl5*, microglia adopted a bigger, more irregular soma shape, typical of a state of activation (Torres-Platas et al., 2014).

Importantly, replacement of CDKL5 protein through a systemic injection of a TAT κ -GFP-CDKL5 fusion protein (Trazzi et al., 2018) reversed microglial activation in *Cdkl5* KO mice. We found a lower number of microglial cells (Fig. 20A,C) with a smaller body size (Fig. 20B,C) in the hippocampus and cortex of TAT κ -GFP-CDKL5-treated *Cdkl5* -/Y mice compared to *Cdkl5* -/Y mice treated with a TAT κ -GFP control protein, indicating the reversibility of the inflammatory phenotype due to the absence of *Cdkl5*.

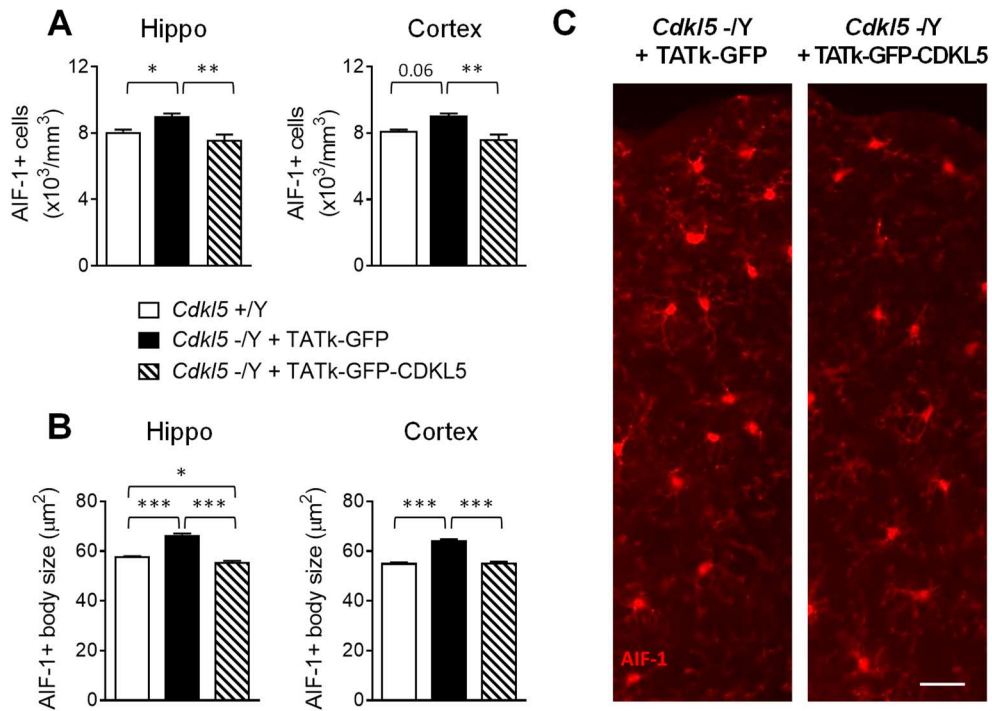


Figure 20. Effect of TATκ-GFP-CDKL5 administration on microglial activation in *Cdkl5* KO mice. **A:** Number of AIF-1-positive cells in hippocampal (Hippo) and somatosensory cortex (Cortex) sections from 6-month-old wild-type mice (+/Y n=2) and *Cdkl5*^{-/-} mice treated with TATκ-GFP (n= 5) or TATκ-GFP-CDKL5 (n= 5) protein as described in (Trazzi et al., 2018). **B:** Mean cell body size of AIF-1-positive cells in the hippocampus and somatosensory cortex of *Cdkl5* KO mice as in A. Values are represented as means \pm SEM. * p<0.05, ** p<0.01, *** p<0.001 (Fisher's LSD after one-way ANOVA). **C:** Examples of cortical sections processed for AIF-1 immunostaining of a *Cdkl5*^{-/-} mouse treated with TATκ-GFP or TATκ-GFP-CDKL5 as in A. Scale bar = 30 μm .

3.2 Non-cell autonomous microglial activation in the absence of *Cdkl5*

In order to investigate whether microglial activation in *Cdkl5* KO mice is a cell-autonomous effect, we first evaluated *Cdkl5* expression levels in purified microglial cells. Isolation of highly enriched microglial cells was confirmed by the high levels of microglia specific markers (AIF-1 and CD11b) and low levels of the neuronal marker (NeuN) in microglia extracts in comparison with cortical extracts from wild-type mice (Fig. 21A). Regarding *Cdkl5* expression, real time and western blot analyses showed very low *Cdkl5* mRNA levels (Fig. 21B) and

undetectable protein levels (Fig. 21C) in microglial cells compared to cortical extracts of wild-type mice, suggesting that Cdk15 function is of minor relevance in these cells. Next, we evaluated microglial activation in *Emx1*-cKO mice, which carry *Cdk15* deletion only in excitatory neurons of the forebrain, but not in microglial cells (Amendola et al., 2014; Lupori et al., 2019). Similarly to *Cdk15* KO mice, *Emx1*-cKO mice showed increased number and body size of microglial cells in the hippocampus (Fig. 21D), suggesting a non-cell autonomous microglial overactivation in the absence of Cdk15, probably caused by neuronal alterations. In addition, we found that *Emx1*-cKO mice, similarly to *Cdk15* KO mice (Gennaccaro et al., 2021a), showed a decreased number of NeuN-positive cells in the hippocampal CA1 field (Fig. 21E), suggesting that neuronal loss could underlie microglial overactivation in *Emx1*-cKO mice.

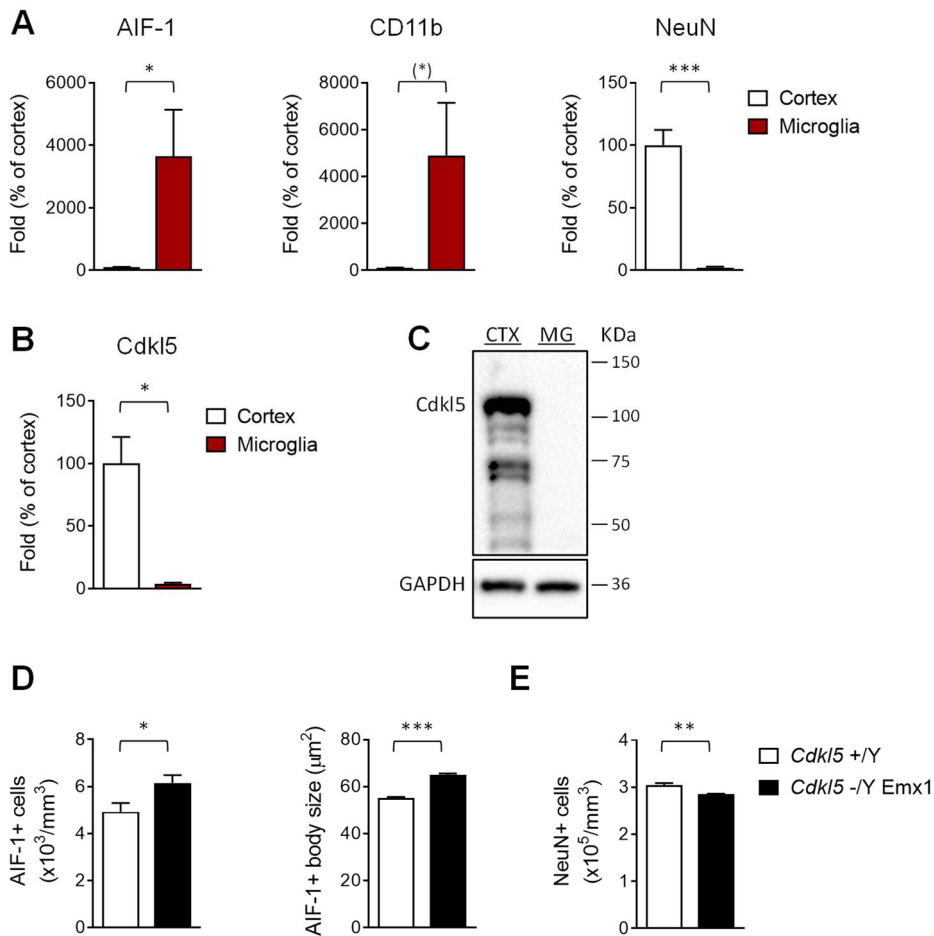


Figure 21. Non-cell autonomous microglial activation in the absence of Cdk15. **A:** Real-time qPCR analysis of AIF-1, CD11b, and NeuN gene expression in the cortex of 3-month-old wild-type mice (+/+ n=6) and microglial cells purified

from 3-month-old wild-type mice (+/+ n=6). Data are given as a percentage of wild-type (+/+) mice cortical expression. **B:** Expression of *Cdkl5* mRNA in cortex of 3-month-old wild-type mice (+/+ n=3) and microglial cells purified from 3-month-old wild-type mice (+/+ n=3). Data are given as a percentage of *Cdkl5* cortical expression. **C:** Example of immunoblot showing *Cdkl5* and GAPDH levels in extracts from somatosensory cortex (CTX) of a wild-type (+/+) mouse and from microglial cells (MG) purified from wild-type mice (+/+ n=4). **D:** Number of AIF-1-positive cells (on the left) and mean cell body size of AIF-1-positive cells (on the right) in hippocampal sections of wild-type mice (+/+ n=4) and *Emx1*-cKO mice (-/- *Emx1* n=5). **E:** Quantification of NeuN-positive cells in CA1 field of hippocampal sections of wild-type mice (+/+ n=3) and *Emx1*-cKO mice (-/- *Emx1* n=3). Values are represented as means \pm SEM. (*) $p=0.057$, * $p<0.05$, ** $p<0.01$, *** $p<0.001$ (two-tailed Student's t-test).

3.3 Treatment with luteolin inhibits microglial overactivation in *Cdkl5* +/- mice

Luteolin, a naturally occurring polyphenolic flavonoid, is a potent microglia inhibitor that possesses antioxidant, anti-inflammatory, and neuroprotective effects both *in vitro* and *in vivo* (Ashaari et al., 2018; Aziz et al., 2018). Since the majority of CDD patients are heterozygous females (Bahi-Buisson and Bienvenu, 2012), we tested the efficacy of an *in vivo* treatment with luteolin on microglial overactivation in the heterozygous female mouse model of CDD. 3-month-old heterozygous females *Cdkl5* mice (+/-) were daily injected with vehicle or luteolin (10 mg/Kg, i.p.) for 7 or 20 days. While both short- and long-term treatments with luteolin did not affect microglial cell number in the cortex of *Cdkl5* +/- mice (Fig. 22A,C), a 7-day treatment was sufficient to recover microglial cell body size at the wild-type level in both cortex and hippocampus (Fig. 22B). In brain homogenates of *Cdkl5* +/- mice, we found significantly higher levels of phosphorylated STAT3 (P-STAT3), a key promoter of the pro-inflammatory phenotype in microglial cells (Jin et al., 2019; Przanowski et al., 2014), in comparison with their wild-type counterparts (Fig. 22D-F). A 7-day treatment with luteolin restored P-STAT3 levels to those of wild-type mice (Fig. 22D,F). No differences in total STAT3 levels were observed

in vehicle- or luteolin-treated *Cdk15* +/- mice in comparison with their wild-type counterparts (Fig. 22E,F).

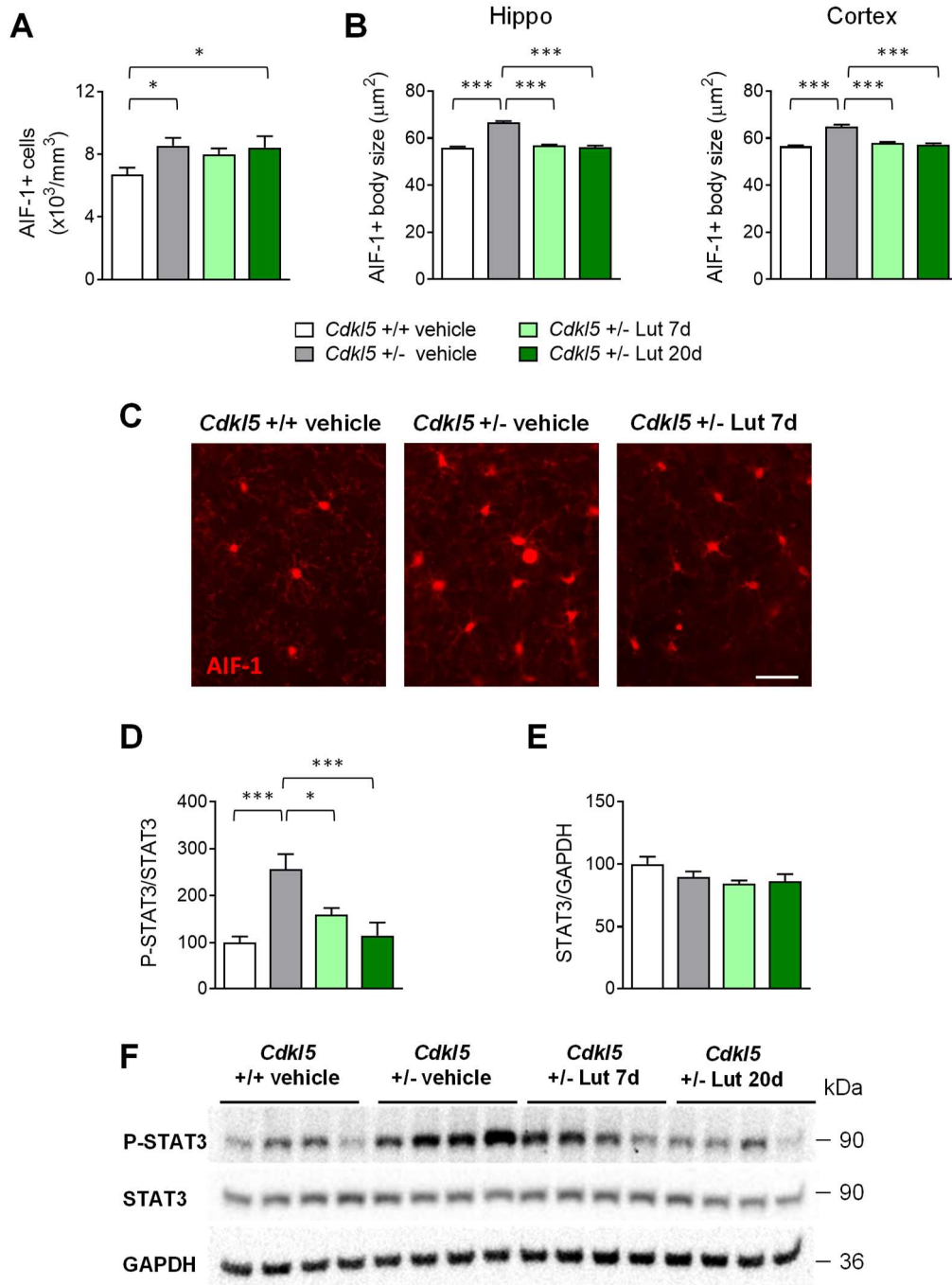


Figure 22. Effects of luteolin treatment on microglial activation in *Cdk15* +/- mice. **A:** Number of AIF-1-positive cells in somatosensory cortex from 3-month-old vehicle-treated *Cdk15* mice (+/+ n=5, +/- n=6) and *Cdk15* +/- mice daily treated with luteolin intraperitoneal injections (10 mg/Kg) for 7 (Lut 7d, n=4) or 20 (Lut 20d, n=4) days. **B:** Mean cell body size of AIF-1-positive cells in hippocampal (Hippo) and somatosensory cortex (Cortex) sections of *Cdk15* mice as in A. **C:** Representative fluorescence images of cortical sections processed for AIF-1 immunohistochemistry of a vehicle-treated wild-type (+/+) mouse, a vehicle-

treated *Cdkl5* +/- mouse, and a 7-day luteolin-treated *Cdkl5* +/- mouse (Lut 7d). Scale bar = 30 μ m. **D,E**: Western blot analysis of P-STAT3 (Tyr 705), STAT3, and GAPDH levels in somatosensory cortex homogenates from vehicle-treated *Cdkl5* mice (+/+ n=4, +/- n=4) and luteolin-treated *Cdkl5* +/- mice as in A. Histograms show P-STAT3 (Tyr 705) protein levels normalized to corresponding total STAT3 protein levels in D, and STAT3 levels normalized to GAPDH in E. Data are expressed as percentages of wild-type (+/+) mice. **F**: Example of immunoblots from 4 animals of each experimental group. Values are represented as means \pm SEM. * p<0.05, *** p<0.001 (Fisher's LSD test after one-way ANOVA).

To confirm microglial overactivation in the brain of *Cdkl5* +/- mice, we measured the expression of molecules involved in the microglial neuroinflammatory response in purified microglial cells, along with the levels of P-STAT3 and AIF-1. We found increased expression of IL-1 β and IL-6 cytokines, TNF- α , and microglial markers (CX3CR1 and AIF-1) in microglia from *Cdkl5* +/- mice in comparison with wild-types (Fig. 23A,B). Importantly, the increased expression of neuroinflammatory markers was recovered by a 7-day treatment with luteolin (Fig. 23A,B). Similarly to what we observed in cortical extracts (Fig. 22D-F), we found an increase in P-STAT3 levels in microglial cells of *Cdkl5* +/- mice, but higher levels of total STAT3 in comparison with wild-type microglia (Fig. 23C,E). A 7-day treatment with luteolin drastically reduced total STAT3 levels in microglial cells (Fig. 23C,E), and accordingly, the amount of STAT3 in the active form (Fig. 23C,E). Similarly, AIF-1 levels were higher in microglial cells from *Cdkl5* +/- mice and returned to the control value after a 7-day treatment with luteolin (Fig. 23D,E).

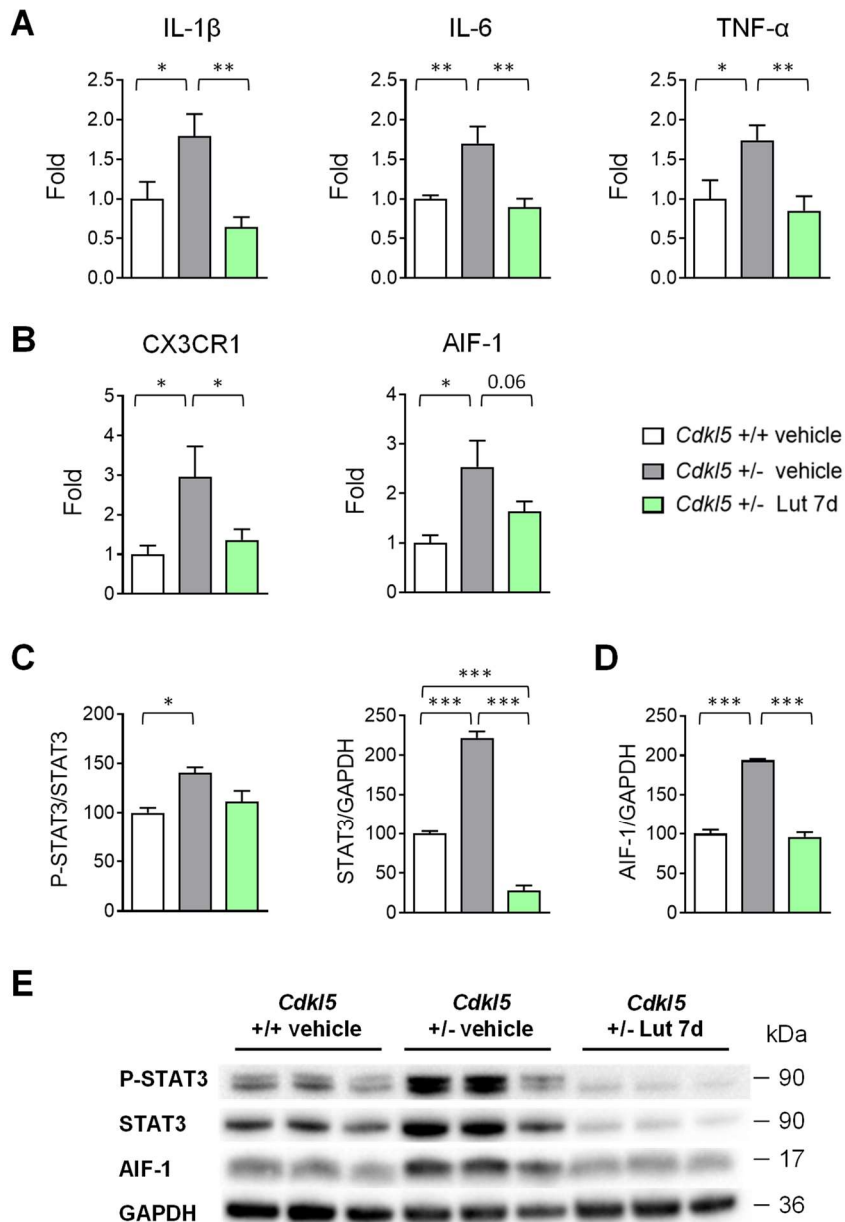


Figure 23. Effects of luteolin treatment on neuroinflammatory gene expression in microglial cells of *Cdkl5* +/- mice. **A:** Real-time qPCR analysis of interleukin 1 β (IL-1 β), interleukin 6 (IL-6), and tumor necrosis factor (TNF)- α gene expression in microglial cells isolated from the brain of 3-month-old vehicle-treated *Cdkl5* mice (+/+ n=6, +/- n=5) and 7-day luteolin-treated *Cdkl5* +/- mice (n=6). **B:** Expression of CX3C motif chemokine receptor 1 (CX3CR1) and allograft inflammatory factor 1 (AIF-1) in microglial cells isolated from the brain of mice as in A. Data are given as fold change in comparison with microglial cells from wild-type (+/+) mice. * p<0.05, ** p<0.01 (Fisher's LSD test after one-way ANOVA). **C,D:** Western blot analysis of P-STAT3 (Tyr 705), STAT3, AIF-1, and GAPDH levels in microglial cells isolated from the brain of 3-month-old vehicle-treated *Cdkl5* mice (+/+ n=4, +/- n=4) and 7-day luteolin-treated *Cdkl5* +/- mice (n=6). Histograms show P-STAT3 protein levels normalized to corresponding total

STAT3 protein levels (C, left panel), STAT3 levels normalized to GAPDH (C, right panel), and AIF-1 levels normalized to GAPDH (D). **E:** Example of immunoblots from the same experimental group as in C. The results in C and D are expressed as percentages of protein levels in wild-type (+/+) microglial cells. Values are represented as means \pm SEM of three technical replicates from the same sample; each sample has been obtained by mixing microglial cells purified from the brain of vehicle-treated *Cdkl5* mice (+/+ n=4, +/- n=4) and 7-day luteolin-treated *Cdkl5* +/- mice (n=6). * p<0.05, *** p<0.001 (Fisher's LSD test after one-way ANOVA).

3.4 Inhibition of microglial overactivation restores survival of CA1 hippocampal neurons in *Cdkl5* +/- mice

To assess the efficacy of luteolin treatment on neuron survival, we evaluated the density of NeuN-positive cells in the CA1 field of the hippocampus of *Cdkl5* +/- mice. Similarly to male *Cdkl5* -/Y mice (Gennaccaro et al., 2021a), female *Cdkl5* +/- mice showed a low number of NeuN-positive pyramidal neurons in the CA1 field compared to wild-type mice (Fig. 24A). We found that a 7-day luteolin treatment restored neuronal number in *Cdkl5* +/- mice (Fig. 24A). To confirm the beneficial effect of microglia inhibition on neuron viability, we treated *Cdkl5* +/- mice with acetaminophen (APAP), a main Cox2 inhibitor that reduces Prostaglandin E2 (PGE2) production and suppresses microglial activation and pro-inflammatory cytokines (Greco et al., 2003; Zhao et al., 2017). A 7-day treatment with APAP (100 mg/Kg, i.p.) restored microglial cell body size and neuron survival in the hippocampus of *Cdkl5* +/- mice (Fig. 24B,C) to levels found in wild-type mice. Furthermore, we assessed the effect of treatment with Stattic, a selective inhibitor of STAT3 activation (Lu et al., 2014; Millot et al., 2020; Yokota et al., 2018). A 7-day *in vivo* inhibition of STAT3 with Stattic (20 mg/Kg, i.p.) recovered microglial cell body size in the hippocampus of *Cdkl5* +/- mice (Fig. 24D). Accordingly, with the inhibition of microglia overactivation, we found a restoration of neuron survival in Stattic-treated *Cdkl5* +/- mice (Fig. 24E). Overall, these results suggest the detrimental role of microglial overactivation on neuronal survival in *Cdkl5* +/- mice.

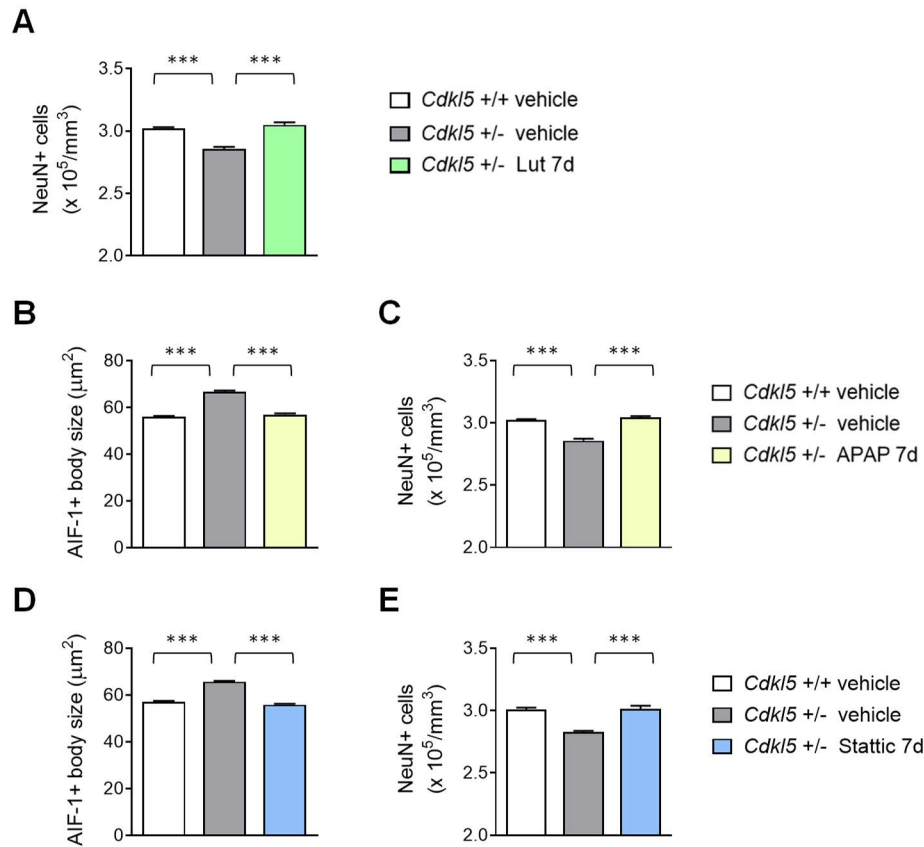


Figure 24. Effect of inhibition of microglial overactivation on hippocampal neuron survival in *Cdk15* +/- mice. **A:** Number of NeuN-positive cells in CA1 field of hippocampal sections from 3-month-old vehicle-treated *Cdk15* mice (+/+ n=3, +/- n=3) and 7-day luteolin-treated *Cdk15* +/- mice (n=4). **B:** Mean cell body size of AIF-1-positive cells in the hippocampus of 3-month-old vehicle-treated *Cdk15* (+/+ n=5, +/- n=6) and *Cdk15* +/- mice injected with acetaminophen (APAP; 100 mg/Kg, i.p.) for 7 consecutive days (n=4). **C:** Number of NeuN-positive cells in CA1 field of hippocampal sections from mice treated as in B. **D:** Mean cell body size of AIF-1-positive cells in the hippocampus of 3-month-old vehicle-treated *Cdk15* mice (+/+ n=4, +/- n=4) and *Cdk15* +/- mice injected with Stattic (20 mg/Kg, i.p.) for 7 consecutive days (n=4). **E:** Number of NeuN-positive cells in CA1 field of hippocampal sections from mice treated as in D. Values are represented as means \pm SEM. *** p<0.001 (Fisher's LSD test after one-way ANOVA).

3.5 Assessment of microglial activation in different life stages of *Cdk15* +/- mice

To assess whether microglia overactivation is already present at an early stage of life and to monitor its evolution with age, we analyzed the status of microglial cells in the brain of *Cdk15* +/- mice at different

developmental stages (young, 20-day-old; adult, 3-month-old; and middle-aged, 11-month-old mice). We found that an increase in microglial cell number and soma size was already present in the cortex and hippocampus of young *Cdk15* +/- mice compared to their wild-type counterparts of the same age (Fig. 25A,B). A significant decrease in the density of microglial cells with age was present in both *Cdk15* +/- and wild-type mice compared to their 20-day-old counterparts (Fig. 25A,B). Surprisingly, while the difference in the number of microglial cells was maintained between *Cdk15* +/- and wild-type mice at 3 months of age, there was no longer a difference in middle-aged mice (Fig. 25A,B). In contrast, increased microglial body size in *Cdk15* +/- mice was present in all three age groups compared to their wild-type counterparts of the same age (Fig. 25A,B). Interestingly, an age-dependent worsening of microglial activation, and, therefore, microglial body size, was observed in both middle-aged *Cdk15* +/- and wild-type mice (Fig. 25A,B).

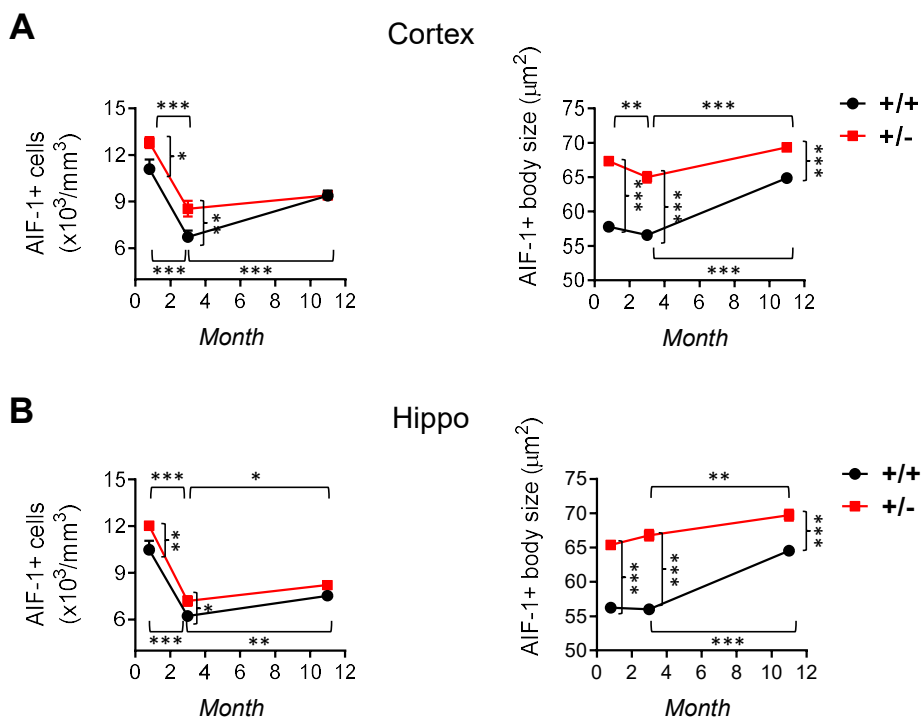


Figure 25. Assessment of microglial activation in different life stages of *Cdk15* +/- mice. **A,B:** Number of AIF-1-positive cells (on the left) and mean cell body size of AIF-1-positive cells (on the right) in somatosensory cortex (Cortex; A) and hippocampal sections (Hippo; B) from young (20-day-old; +/+ n=5, +/- n=6), adult (3-month-old; +/+ n=5, +/- n=6), and middle-aged (11-month-old; +/+ n=4,

+/- n=4) *Cdkl5* mice. Values are represented as means \pm SEM. * $p < 0.05$, ** $p < 0.01$, *** $p < 0.001$ (Fisher's LSD test after two-way ANOVA).

3.6 Luteolin treatment restores neuron survival in middle-aged *Cdkl5* +/- mice

Age-related changes in microglial cells consistent with their activation have been documented in aging (Miller and Streit, 2007; Sheng et al., 1998), and it has been suggested that they contribute to the brain decline in pathological conditions (Spittau, 2017; von Bernhardi et al., 2010). Recent evidence showed an age-dependent decreased hippocampal neuron survival in middle-aged *Cdkl5* KO mice, paralleled by an increased cognitive decline (Gennaccaro et al., 2021a). To explore the possibility that microglial overactivation in middle-aged *Cdkl5* KO mice could underlie the higher neuronal loss, we assessed the efficacy of a 7-day treatment with luteolin in counteracting neuronal loss in 11-month-old *Cdkl5* +/- mice (Fig. 26A). Treatment with luteolin reduced microglial cell body size in the hippocampus of middle-aged *Cdkl5* +/- mice to even lower levels compared to those of wild-type mice of the same age (Fig. 26B). Importantly, the reduced number of Hoechst-positive nuclei (Fig. 26C) and NeuN-positive cells (Fig. 26D), and the increased number of apoptotic cleaved caspase-3-positive cells (Fig. 26E) in middle-aged *Cdkl5* +/- mice were strongly improved by treatment with luteolin for 7 days (Fig. 26C-E).

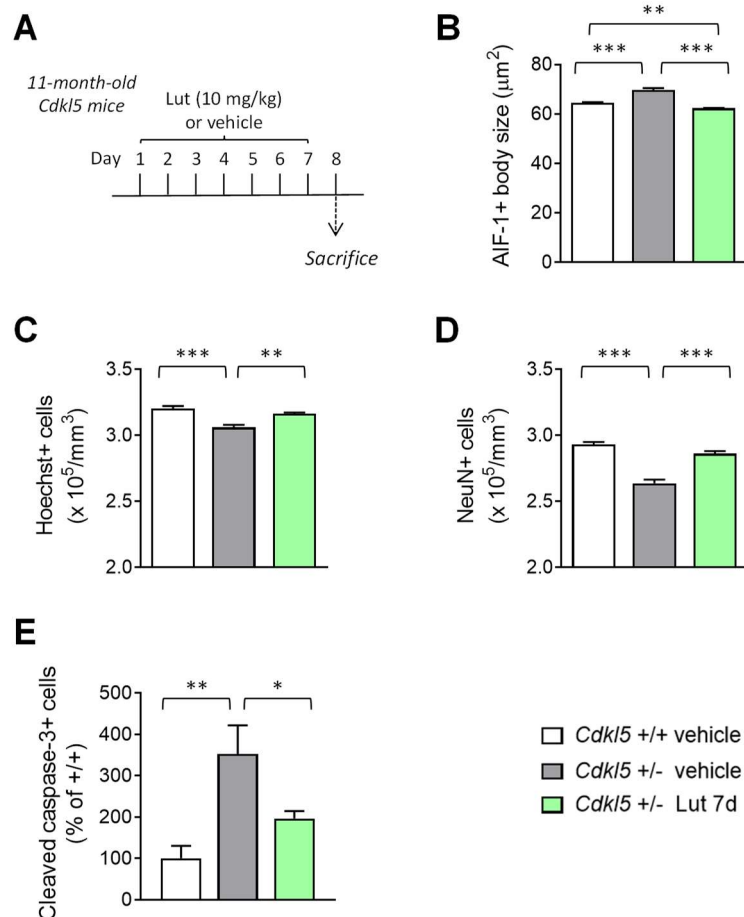


Figure 26. Effect of luteolin treatment in middle-aged *Cdk15* +/- mice. A: Experimental plan. Middle-aged (11-month-old) *Cdk15* mice were treated with vehicle or luteolin for 7 consecutive days. Mice were sacrificed 1 day after the end of treatment. **B:** Mean cell body size of AIF-1-positive cells in the hippocampus of middle-aged (11-month-old) vehicle-treated *Cdk15* mice (+/+ n=4, +/- n=4) and 7-day luteolin-treated *Cdk15* +/- mice (n=4). **C,D:** Number of Hoechst-positive cells (C) and NeuN-positive cells (D) in CA1 field of hippocampal sections from mice treated as in B. **E:** Number of cleaved caspase-3-positive cells in the hippocampus of middle-aged (11-month-old) *Cdk15* mice treated as in A. Data are given as a percentage of wild-type (+/+) mice. Values are represented as means \pm SEM. * p<0.05, ** p<0.01, *** p<0.001 (Fisher's LSD test after one-way ANOVA).

3.7 Treatment with luteolin prevents NMDA-induced seizure persistence and excitotoxicity in the hippocampus of *Cdk15* +/- mice

Increasing evidence supports a link between inflammation and epilepsy (Vezzani, 2014; Vezzani et al., 2023). To investigate whether

microglia overactivation predisposes induced seizure-like events and has a causative role in the increased neuronal susceptibility to excitotoxic stress in *Cdkl5* KO mice (Fuchs et al., 2019; Loi et al., 2020), we pre-treated *Cdkl5* +/- mice for 7 days with luteolin before NMDA (60 mg/kg, i.p.) administration (Fig. 27A). Seizure grades were scored during a 60-min observation period after NMDA injection, and mice were sacrificed 1 day or 8 days afterwards (Fig. 27A). We found that *Cdkl5* +/- mice showed a different trend of seizure persistence (Fig. 27B), but no difference in seizure severity (Fig. 27C), compared to the NMDA-treated wild-type counterparts. We found that, while in wild-type mice the highest scores occur in the first 5-15 min, *Cdkl5* +/- mice showed a persistence in the higher seizure scores up to 30-35 min after NMDA administration. In addition, seizure freedom is achieved more slowly in *Cdkl5* +/- mice in comparison with wild-type mice. Importantly, pre-treatment with luteolin for 7 days shortens seizure persistence in NMDA-treated *Cdkl5* +/- mice (Fig. 27B), suggesting that microglial activation is involved in the susceptibility to prolonged seizures that characterizes *Cdkl5* KO mice. As expected, microglial activation increased in the hippocampus of both *Cdkl5* +/- and *Cdkl5* +/+ mice after NMDA treatment (Fig. 27D). Nevertheless, after NMDA stimulation, the soma volume of microglial cells in *Cdkl5* +/- mice was higher than that of NMDA-treated wild-type mice (Fig. 27D). Importantly, a 7-day pre-treatment with luteolin was able to counteract both basal and NMDA-induced microglial activation in *Cdkl5* +/- mice, bringing microglial soma size back to that of the vehicle-treated wild-type mouse condition (Fig. 27D). Neuronal death was assessed 1 day after NMDA administration using immunohistochemistry for cleaved caspase-3, and 8 days after using Hoechst staining and immunohistochemistry for NeuN. In the CA1 field of the hippocampus, NMDA-treated *Cdkl5* +/- mice showed a higher number of cleaved caspase-3-positive cells (Fig. 27E,F) and a lower number of Hoechst-positive nuclei (Fig. 28A) and NeuN-positive cells (Fig. 28B) in comparison with NMDA-treated wild-type mice, indicating increased cell death in *Cdkl5* +/- mice after the excitotoxic stimulus.

Importantly, pre-treatment with luteolin for 7 days reduced cell death at 1 day after NMDA administration in *Cdk15* +/- mice (Fig. 27E,F), thus preventing neuronal loss in the hippocampal CA1 field (Fig. 28A,B).

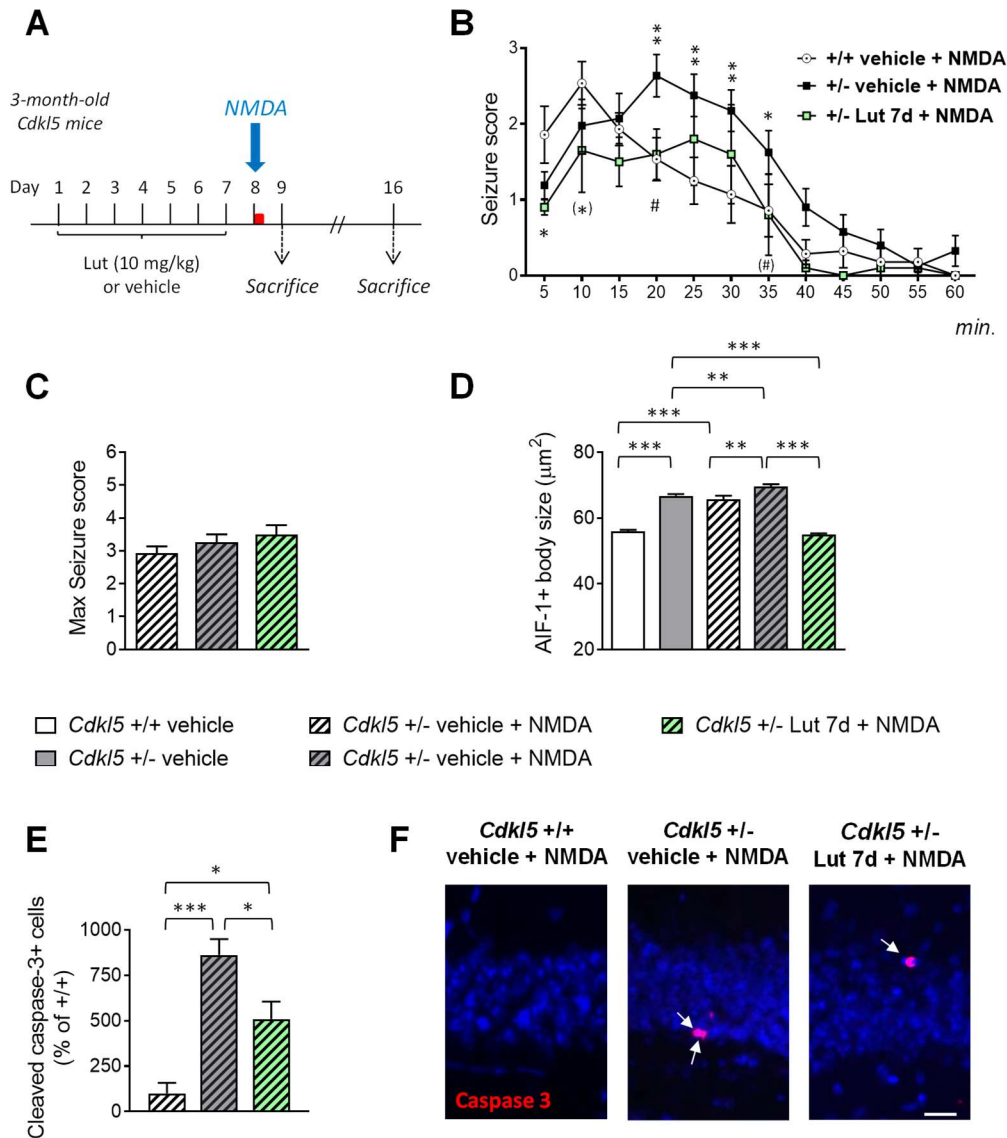


Figure 27. Effect of luteolin treatment on NMDA-induced excitotoxicity in the hippocampus of *Cdk15* +/- mice. **A:** Experimental plan. 3-month-old *Cdk15* mice were treated with a single intraperitoneal injection of NMDA (60 mg/kg) after 7 days of vehicle or luteolin treatment. Seizure grades were scored in a 60-minute observation period after NMDA injection (red square). Animals were sacrificed 1 day or 8 days after NMDA administration. **B:** Graph represents seizure score of 3-month-old *Cdk15* mice (+/+ n=14, +/- n=21) treated with vehicle and a single intraperitoneal injection of NMDA, and *Cdk15* +/- mice (n= 10) pre-treated for 7 days with luteolin before NMDA injection. Values are represented as means \pm SEM. (*) p=0.056, * p<0.05, ** p<0.01, as compared to the NMDA-treated wild-type (+/+) mice; (#) p=0.055, # p<0.05, as compared to the NMDA-treated *Cdk15* +/- mice (Fisher's LSD test after two-way ANOVA). **C:** Histogram shows the mean

of the maximum seizure score in mice treated as in B. **D**: Mean cell body size of AIF-1-positive cells in the hippocampus of 3-month-old *Cdkl5* mice (+/+ n=5, +/- n=6) treated with vehicle only, *Cdkl5* mice (+/+ n=3, +/- n=3) treated with vehicle and NMDA, and *Cdkl5* +/- mice (n=3) pre-treated for 7 days with luteolin before NMDA injection. Mice were sacrificed 8 days after NMDA treatment. **E**: Number of cleaved caspase-3-positive cells in the hippocampus of 3-month-old *Cdkl5* mice (+/+ n=3, +/- n=4) treated with vehicle and NMDA, and *Cdkl5* +/- mice (n=4) pre-treated for 7 days with luteolin before NMDA injection. Mice were sacrificed 24 h after NMDA treatment. Data are given as a percentage of NMDA-treated wild-type (+/+) mice. Values in C, D, and E are represented as means \pm SEM. * $p < 0.05$, ** $p < 0.01$, *** $p < 0.001$ (Fisher's LSD test after one-way ANOVA). **F**: Examples of cleaved caspase-3-positive cells (white arrows) in the hippocampus of mice treated as in E. Scale bar = 20 μm .

As both pyramidal neurons and GAD67-positive interneurons are NeuN-positive (Kiljan et al., 2019), to exclude an effect of the treatments on the number of interneurons, we evaluated the number of GAD67-positive cells in the hippocampus of treated *Cdkl5* +/- mice (Fig. 28C). We found no difference in the number of inhibitory interneurons among vehicle/NMDA-treated *Cdkl5* +/+, vehicle/NMDA-treated *Cdkl5* +/-, and luteolin/NMDA-treated *Cdkl5* +/- mice (Fig. 28C), indicating that NMDA-induced excitotoxicity does not affect inhibitory neuron viability and that pre-treatment with luteolin does not promote their survival. Similarly, we found no differences in the number of GFAP-positive astrocytes (Fig. 28D).

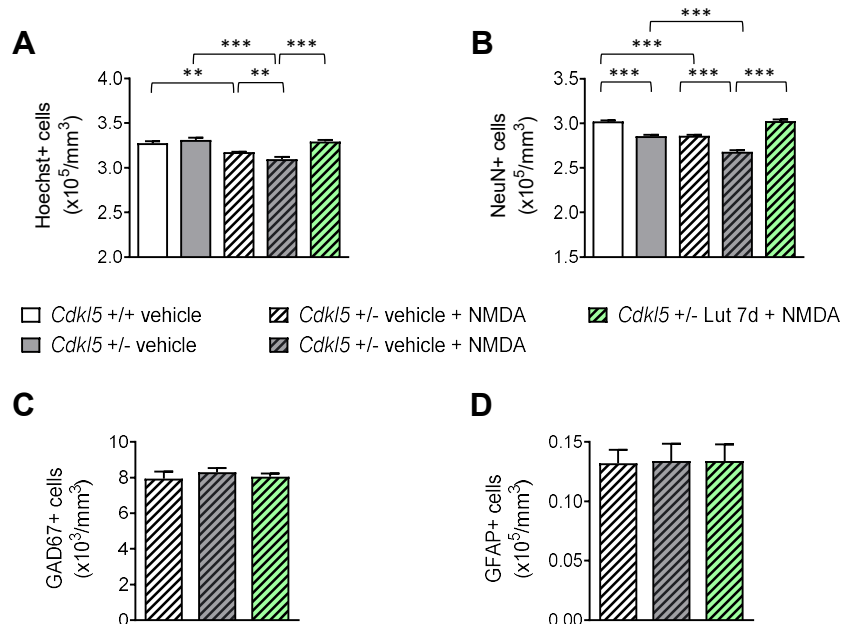


Figure 28. Pro-survival effect of luteolin treatment on NMDA-induced excitotoxicity in the hippocampus of *Cdkl5* +/- mice. A,B: Number of Hoechst-positive cells (A), and NeuN-positive cells (B) in CA1 field of hippocampal sections from 3-month-old *Cdkl5* mice (+/+ n=4, +/- n=5) treated with vehicle only, *Cdkl5* mice (+/+ n=6, +/- n=5) treated with vehicle and NMDA, and *Cdkl5* +/- mice (n=6) pre-treated for 7 days with luteolin before NMDA injection. Mice were sacrificed 8 days after NMDA treatment. **C,D:** Number of GAD67-positive cells (C) and GFAP-positive cells (D) in CA1 field of hippocampal sections from 3-month-old *Cdkl5* mice (+/+ n=4, +/- n=4) treated with vehicle and NMDA, and *Cdkl5* +/- mice (n=4) pre-treated for 7 days with luteolin before NMDA injection. Mice were sacrificed 8 days after NMDA treatment. Values are presented as means \pm SEM. ** $p < 0.01$, *** $p < 0.001$ (Fisher's LSD test after one-way ANOVA).

3.8 Treatment with luteolin restores survival of newborn cells in the dentate gyrus of *Cdkl5* +/- mice

Loss of *Cdkl5* impairs survival and maturation of newborn hippocampal neurons (Fuchs et al., 2015; Fuchs et al., 2014). In order to evaluate the efficacy of an *in vivo* treatment with luteolin on the survival rate of new neurons, we assessed the number of doublecortin (DCX)-positive cells in the dentate gyrus (DG) of vehicle-treated *Cdkl5* +/- and *Cdkl5* +/+ mice and *Cdkl5* +/- mice treated with luteolin for 7 days. We found that treatment with luteolin restored the number of DCX-positive granule neurons in *Cdkl5* +/- mice (Fig. 29A,B). To determine whether increased proliferation rate underlies the positive effect of luteolin on newborn neuronal number, we counted proliferating cells immunostained for Ki-67, an endogenous marker of actively proliferating cells. We found that luteolin-treated *Cdkl5* +/- mice had the same number of Ki-67-labeled cells as vehicle-treated *Cdkl5* +/- and *Cdkl5* +/+ mice (Fig. 29C). This evidence indicates that the higher number of DCX-positive cells in luteolin-treated *Cdkl5* +/- mice is not due to an increase in proliferation rate.

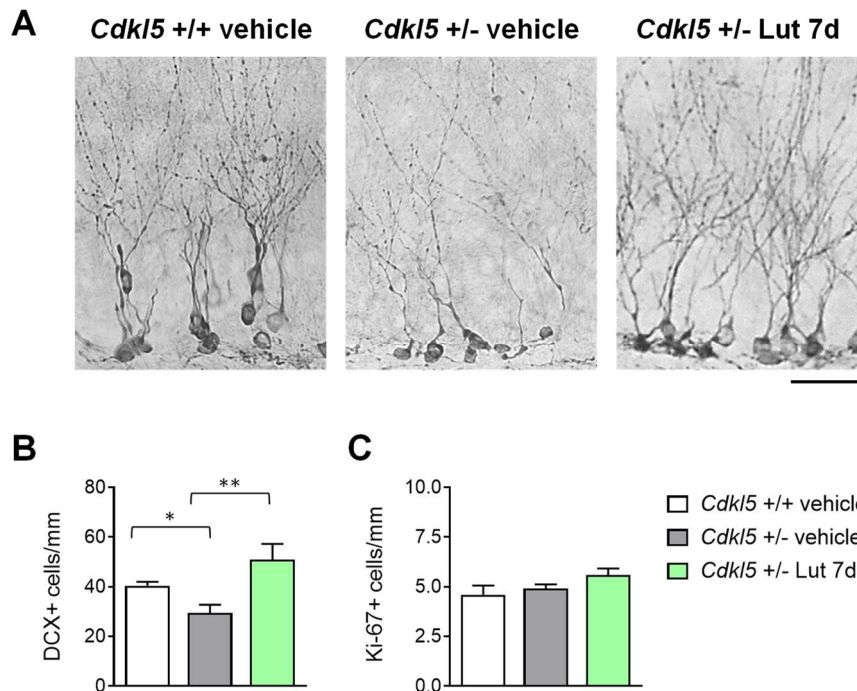


Figure 29. Effect of luteolin treatment on survival of postmitotic granule neurons in *Cdkl5* +/- mice. **A:** Examples of sections processed for DCX immunostaining from the dentate gyrus (DG) of a vehicle-treated wild-type (+/+) mouse, a vehicle-treated *Cdkl5* +/- mouse, and a 7-day luteolin-treated *Cdkl5* +/- mouse. Scale bar = 40 μ m. **B:** Number of DCX-positive cells in the DG of vehicle-treated *Cdkl5* mice (+/+ n=6, +/- n=6) mice, and 7-day luteolin-treated *Cdkl5* +/- mice (n=4). **C:** Number of Ki-67-positive cells in the DG of mice as in B. Values in B and C are represented as means \pm SEM. * p<0.05, ** p<0.01 (Fisher's LSD test after one-way ANOVA).

3.9 Treatment with luteolin increases hippocampal neurogenesis in *Cdkl5* +/- mice

Our evidence that a 7-day treatment with luteolin is able to increase the number of DCX-positive cells in the DG of *Cdkl5* +/- mice, without increasing the proliferation rate, led us to investigate whether prolonged luteolin administration could enhance the pool of proliferating precursors in the hippocampus of *Cdkl5* +/- mice. To this purpose, we evaluated the number of proliferating cells in the subgranular and granular zone of the DG of *Cdkl5* +/- mice subjected to a 20-day treatment with luteolin, whose anti-inflammatory effects were previously confirmed (Fig. 22A,B). We found a higher number of

Ki-67-positive cells in *Cdkl5* +/- mice treated with luteolin for 20 days compared to vehicle-treated *Cdkl5* +/- (Fig. 30A,E), indicating that a long-term luteolin treatment enhances the pool of proliferating precursors. In order to confirm the effect of prolonged luteolin administration on hippocampal cell proliferation, mice were subjected to a single subcutaneous injection of BrdU (150 mg/kg) on the 20th day of luteolin treatment and the number of BrdU-positive cells in the DG was evaluated 24 h after the injection. As expected, we found an increase in the number of BrdU-positive cells in the DG of *Cdkl5* +/- mice treated with luteolin for 20 days, confirming that a long-term luteolin treatment increases the proliferation rate of precursor granule cells of the DG (Fig. 30B,E). In order to assess the effect of prolonged luteolin administration on neuronal survival, the number of DCX-positive newborn granule cells was quantified. After 20 days of luteolin treatment, the number of newborn granule cells in *Cdkl5* +/- mice not only recovered but even significantly increased compared to the number of DCX-positive cells present in wild-type mice (Fig. 30C,E), suggesting that long-term luteolin treatment has more beneficial effects on neurogenesis than short-term treatment. To establish the impact of the increased neurogenesis in 20-day luteolin-treated *Cdkl5* +/- mice on the overall granule cell number, we stereologically evaluated the granule cell density in the DG of vehicle-treated *Cdkl5* +/- and *Cdkl5* +/+ mice and *Cdkl5* +/- mice treated with luteolin for 20 days. Consistent with the higher number of DCX-positive cells in *Cdkl5* +/- mice (Fig. 30C), we observed a higher number of Hoechst-stained nuclei in the granule cell layer of 20-day luteolin-treated *Cdkl5* +/- mice, indicating that prolonged luteolin administration restored cellularity in the DG of *Cdkl5* +/- mice (Fig. 30D).

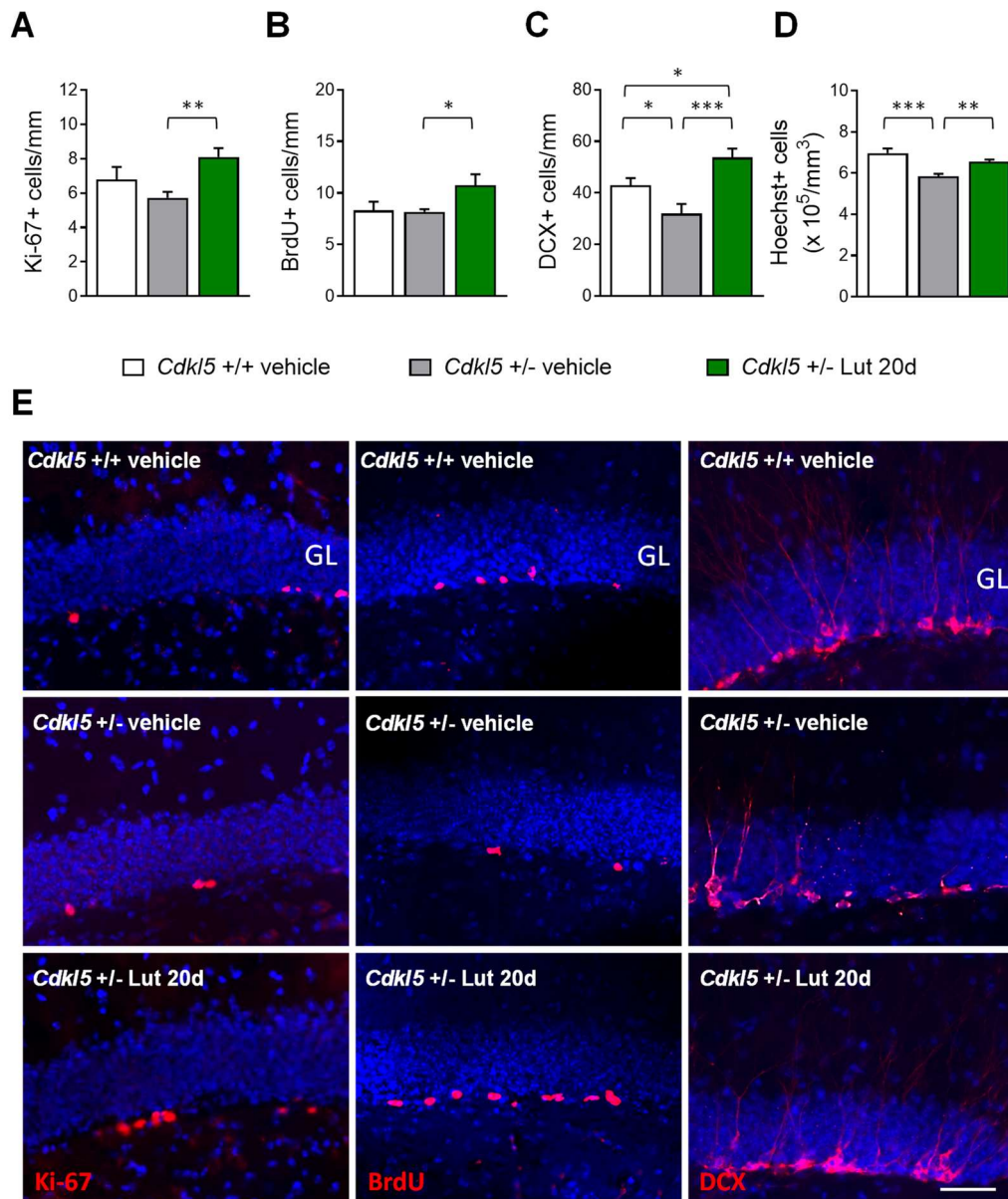


Figure 30. Effect of luteolin treatment on hippocampal neurogenesis in *Cdkl5* +/- mice. **A:** Number of Ki-67-positive cells in the subgranular zone (SGZ) of the dentate gyrus (DG) of vehicle-treated *Cdkl5* mice (+/+ n=8, +/- n=9) and 20-day luteolin-treated *Cdkl5* +/- mice (n= 8). **B:** Number of BrdU-positive cells in the SGZ of vehicle-treated *Cdkl5* mice (+/+ n=4, +/- n=4) and 20-day luteolin-treated *Cdkl5* +/- mice (n=4). **C:** Number of DCX-positive cells in the granular layer (GL) of the DG of vehicle-treated *Cdkl5* mice (+/+ n=7, +/- n=7) and 20-day luteolin treated *Cdkl5* +/- mice (n=7). **D:** Number of Hoechst-positive cells in the GL of the DG of vehicle-treated *Cdkl5* mice (+/+ n=4, +/- n=4) and 20-day luteolin-treated *Cdkl5* +/- mice (n=4). **E:** Examples of sections processed for fluorescent immunostaining for Ki-67 (left), BrdU (middle), and DCX (right) from the DG of an animal from each experimental condition. Scale bar = 50 μm . Values are represented as means \pm SEM. * $p < 0.05$, ** $p < 0.01$, *** $p < 0.001$ (Fisher's LSD test after one-way ANOVA).

3.10 Treatment with luteolin improves maturation of newborn cells in the dentate gyrus of *Cdk15* +/- mice

To establish the effect of inhibition of microglia overactivation on dendritic development of newborn granule cells, we examined the dendritic morphology of DCX-positive cells. We examined the total length of dendritic tree, as well as the number and mean length of dendritic segments. As previously found (Fuchs et al., 2014), loss of *Cdk15* causes dendritic hypotrophy of newborn cells in the dentate gyrus of *Cdk15* +/- mice (Fig. 31A,D).

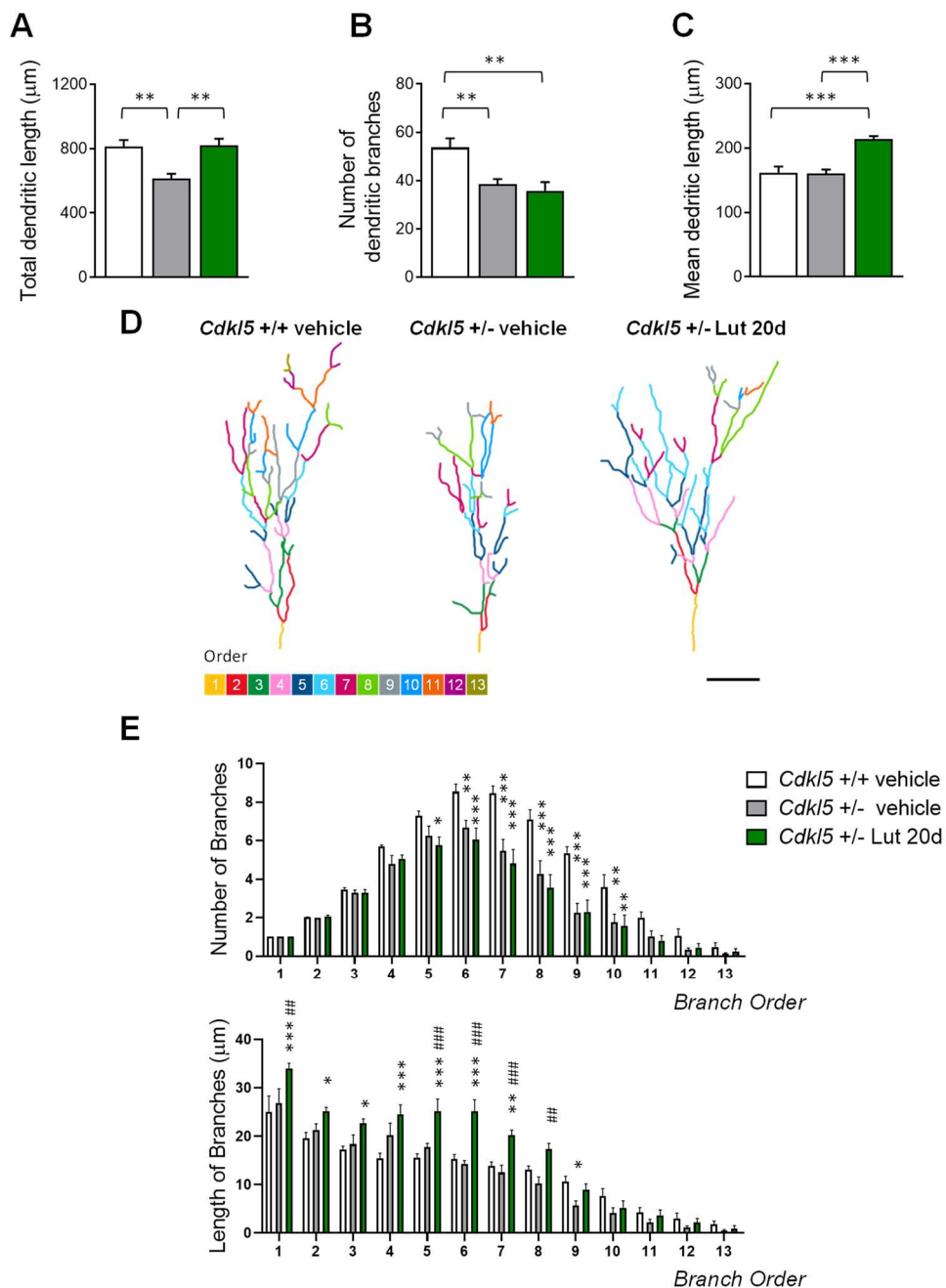


Figure 31. Effect of luteolin treatment on dendritic development of newborn granule cells in the dentate gyrus of *Cdkl5* +/- mice. **A-C:** Total dendritic length (A), mean number of dendritic branches (B) and mean dendritic length (C) of DCX-positive cells in the dentate gyrus (DG) of vehicle-treated *Cdkl5* mice (+/+ n=5, +/- n=5) and 20-day luteolin-treated *Cdkl5* +/- mice (n=6). **D:** Examples of the reconstructed dendritic tree of DCX-positive granule cell of one animal from each experimental condition. Scale bar = 40 μ m. **E:** Quantification of the mean number (upper histogram) and mean length (lower histogram) of branches of different orders in DCX-positive granule cells of *Cdkl5* mice treated as in A. Dendrites were traced in a centrifugal direction. Numbers indicate the different dendritic branch orders. Values are represented as means \pm SEM. * p<0.05, ** p<0.01, *** p<0.001, as compared to the vehicle-treated wild-type (+/+) mice; ## p<0.01; ### p<0.001, as compared to the vehicle-treated *Cdkl5* +/- mice (Fisher's LSD test after one-way ANOVA for data set in A-C, and after two-way ANOVA for data set in E).

This defect was mainly due to a lower number of dendritic branching (Fig. 31B,D). *Cdkl5* +/- mice had fewer branches of the orders higher than 5, while a difference in mean length was present only in branches of order 9 (Fig. 31E). A 20-day luteolin treatment recovered the total dendritic length of newborn granule cells in *Cdkl5* +/- mice to wild-type levels (Fig. 31A,D). The recovery was primarily due to an increase in the mean length of dendrites, which became significantly longer than that of wild-type mice (Fig. 31C,D), especially for the first 7 orders (Fig. 31E). In contrast, treatment did not improve the number of branches of DCX-positive cells in *Cdkl5* +/- mice (Fig. 31B,D).

3.11 Treatment with luteolin improves the dendritic architecture in hippocampal and cortical neurons of *Cdkl5* +/- mice

Previous evidence showed that hippocampal and cortical pyramidal neurons of *Cdkl5* KO mice are characterized by severe dendritic hypotrophy (Amendola et al., 2014; Fuchs et al., 2020; Fuchs et al., 2018; Fuchs et al., 2014; Ren et al., 2019; Tang et al., 2017; Tassinari et al., 2023; Trazzi et al., 2018). In order to establish whether a 20-day treatment with luteolin also ameliorates dendritic arborization defects of neurons already present at birth, we examined the dendritic tree of

Golgi-stained pyramidal neurons in the hippocampus and cortex of *Cdk15* +/- mice (Fig. 32A). Both apical and basal dendrites of pyramidal hippocampal and cortical neurons of *Cdk15* +/- mice had a shorter total length (Fig. 32B,C) and a reduced number of branches (Fig. 32D,E), in comparison with wild-type mice. In *Cdk15* +/- mice treated with luteolin for 20 days, the total dendritic length and number of branches underwent an increase and became similar to those of the wild-type mice (Fig. 32B-E).

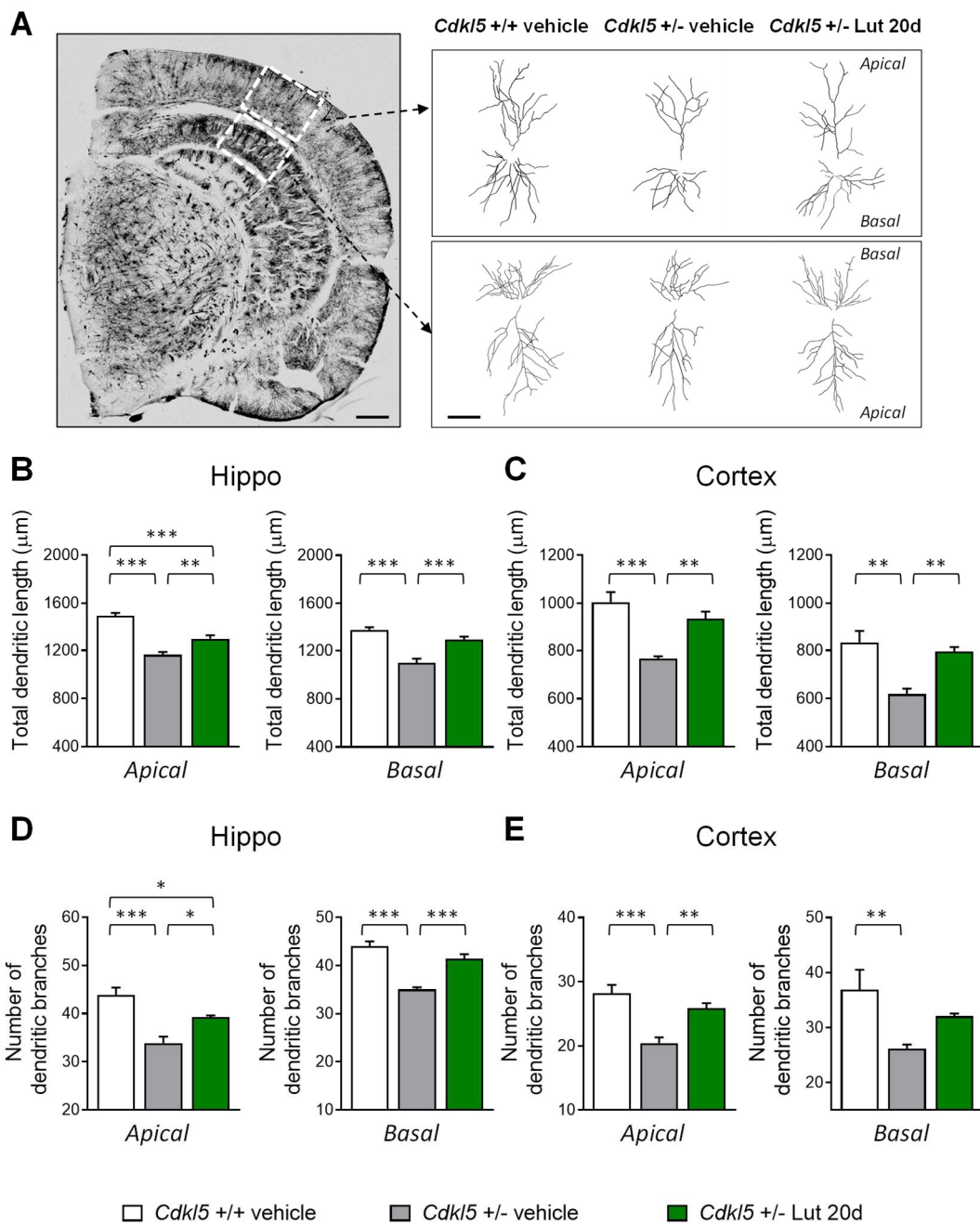


Figure 32. Effect of luteolin treatment on dendritic architecture of hippocampal and cortical neurons in *Cdkl5* +/- mice. **A:** Representative image of a Golgi-stained section (panel on the left; scale bar = 500 μ m), showing the portion of hippocampal and cortical regions where the dendritic arbor of pyramidal neurons was traced (areas enclosed in the dashed square). On the right, examples of the reconstructed apical and basal dendritic tree of Golgi-stained cortical (upper) and CA1 (lower) pyramidal neurons of one animal from each experimental group. Scale bar = 40 μ m. **B,C:** Total dendritic length of apical (on the left) and basal (on the right) dendrites of Golgi-stained pyramidal neurons in the CA1 field of the hippocampus (Hippo; B) and in somatosensory cortex (Cortex; C) of vehicle-treated *Cdkl5* mice (+/+ n=4, +/- n=4) and 20-day luteolin-treated *Cdkl5* +/- mice (n=4). **D,E:** Number of dendritic branches of apical (on the left) and basal (on the right) dendrites of Golgi-stained pyramidal neurons in the CA1 field (Hippo; D) and somatosensory cortex (Cortex; E) of mice as in B. Values are represented as means \pm SEM. * p<0.05, ** p<0.01, *** p<0.001 (Fisher's LSD test after one-way ANOVA).

We next examined the effect of a 20-day luteolin treatment on each dendritic order separately. In hippocampal neurons of *Cdkl5* +/- mice, dendritic hypotrophy was due to a reduced number of branches of an order higher than 3 (Fig. 33A) and, in the basal dendrites, a lack of branches of an order higher than 8 (Fig. 33A, black arrows). In cortical neurons, *Cdkl5* +/- mice had a similar number of branches of orders 1 and 4 for apical dendrites, and orders 1 and 2 for basal dendrites compared to wild-type mice, but fewer branches of subsequent orders (Fig. 33B). Unlike wild-type mice, *Cdkl5* +/- mice lacked branches of orders 10 and 11 for apical dendrites, and orders 7 and 8 for basal dendrites (Fig. 33B, black arrows). In *Cdkl5* +/- mice treated with luteolin for 20 days, the number of branches became similar to that of wild-type mice (Fig. 33A,B).

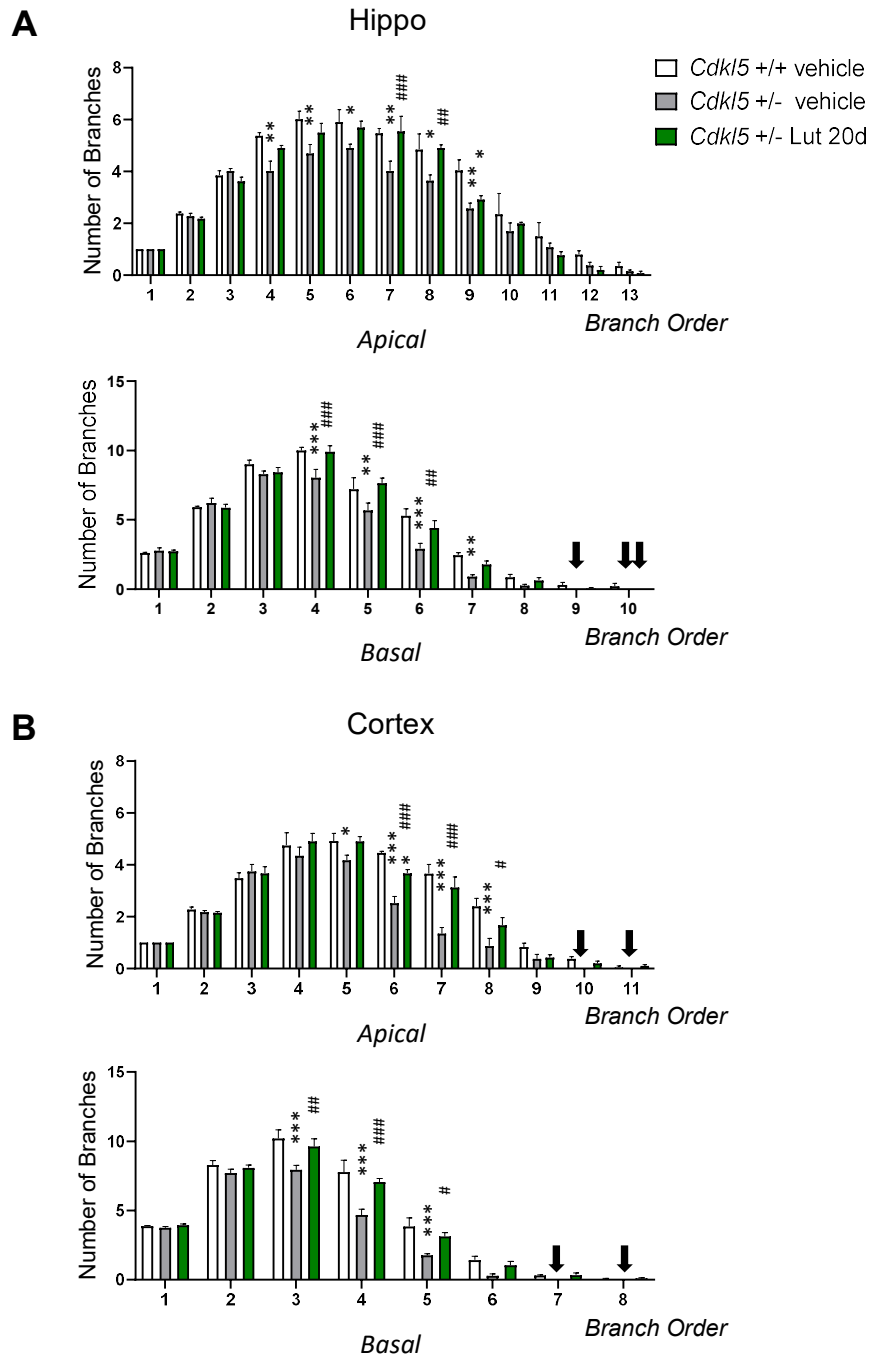


Figure 33. Effect of luteolin treatment on dendritic arborization complexity of hippocampal and cortical neurons in $Cdkl5$ +/- mice. **A,B:** Quantification of the number of branches of different orders of apical dendrites (upper panel) and basal dendrites (lower panel) in Golgi-stained hippocampal (Hippo; A) and cortical (Cortex; B) pyramidal neurons of vehicle-treated $Cdkl5$ mice (+/+ n=4, +/- n=4) and 20-day luteolin-treated $Cdkl5$ +/- mice (n=4). Dendrites were traced in a centrifugal direction. Numbers indicate the different dendritic branch orders. Black arrows indicate the lack of branches of that order. Values are represented as means \pm SEM. * $p < 0.05$, ** $p < 0.01$, *** $p < 0.001$, as compared to the vehicle-treated wild-type (+/+) mice; # $p < 0.05$, ## $p < 0.01$, ### $p < 0.001$, as compared to the vehicle-treated $Cdkl5$ +/- mice (Fisher's LSD test after two-way ANOVA).

3.12 Treatment with luteolin improves spine maturation in the brain of *Cdk15* +/- mice

Alterations in dendritic spine morphology and defects in synaptogenesis have been consistently reported in *Cdk15* KO mice (Amendola et al., 2014; Della Sala et al., 2016; Fuchs et al., 2018; Fuchs et al., 2015; Fuchs et al., 2014; Gurgone et al., 2023; Tassinari et al., 2023; Trazzi et al., 2018; Trazzi et al., 2016). To investigate the effect of luteolin treatment on dendritic spine development, we analyzed the dendritic spine morphology of Golgi-stained hippocampal and cortical pyramidal neurons. Separate counts of different classes of dendritic spines confirmed that pyramidal neurons of both hippocampal CA1 field (Fig. 34A,B) and the somatosensory cortex (Fig. 34C) of *Cdk15* +/- mice had a higher percentage of immature spines (filopodium-like, thin-shaped, and stubby-shaped) and a reduced percentage of mature spines (mushroom and cup shaped), compared to wild-type mice. After 20 days of luteolin treatment, *Cdk15* +/- mice showed a similar percentage of mature and immature spines compared to wild-type mice (Fig. 34A-C), suggesting that a long-term treatment was able to restore dendritic spine maturation. Since a proper dendritic spine morphology is essential for the formation of synaptic contacts, we further evaluated the number of immunoreactive puncta for PSD-95 (post-synaptic density protein 95) in the hippocampus of *Cdk15* +/- mice. *Cdk15* +/- mice displayed a strong reduction in the number of PSD-95-positive puncta compared to wild-type mice (Fig. 34D,E). Importantly, a 20-day luteolin treatment promoted a significant increase in the number of synaptic puncta in *Cdk15* +/- mice (Fig. 34D,E).

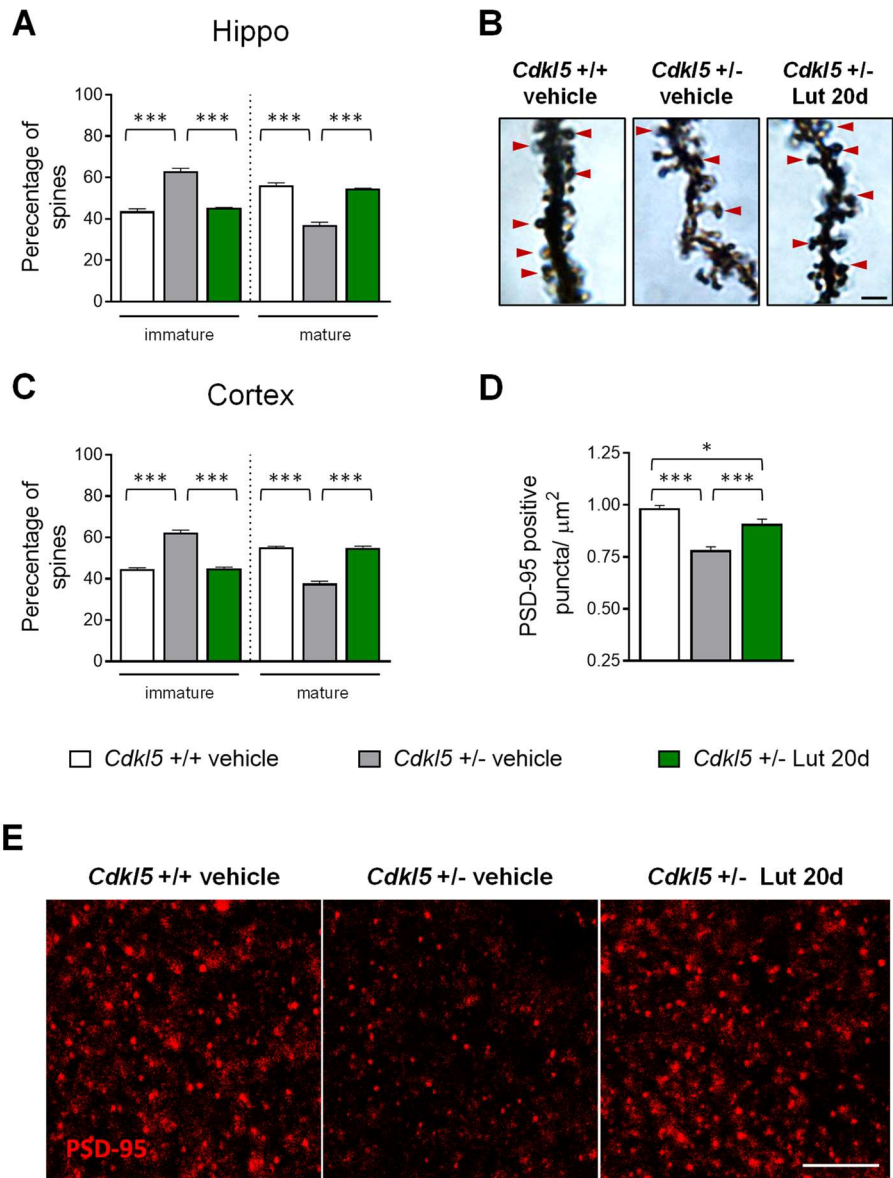


Figure 34. Effect of luteolin treatment on neuronal connectivity in *Cdkl5* +/- mice. **A,C:** Percentage of immature and mature dendritic spines in relation to the total number of protrusions in hippocampal (Hippo; **A**) and cortical (Cortex; **C**) pyramidal neurons of vehicle-treated *Cdkl5* mice (+/+ n=4, +/- n=4) and 20-day luteolin-treated *Cdkl5* +/- mice (n=4). **B:** Examples of Golgi-stained hippocampal pyramidal neurons of one animal from each experimental group; red arrows represent mature spines. Scale bar = 2 μm. **D:** Number of fluorescent puncta per μm², exhibiting PSD-95 immunoreactivity in the CA1 field of the hippocampus of vehicle-treated *Cdkl5* mice (+/+ n=4, +/- n=4) and 20-day luteolin-treated *Cdkl5* +/- mice (n=4). **E:** Representative fluorescence images of PSD-95-immunoreactive puncta in the hippocampus of one animal from each experimental group. Scale bar = 6 μm. Values are represented as means ± SEM. * p<0.05, *** p<0.001 (Fisher's LSD test after two-way ANOVA).

3.13 Treatment with luteolin transiently boosts BDNF/TrkB signaling pathways in the cortex of *Cdk15* +/- mice

BDNF/TrkB signaling activates several intracellular pathways that play an important role in neuronal differentiation, dendritic morphogenesis, neuroprotection and modulation of synaptic interactions, which are critical for cognition and memory (Kowiański et al., 2018). Among these, TrkB phosphorylation leads to phosphatidylinositol 3-kinase (PI3K)/Akt and extracellular signal-regulated kinase (Erk) activation (Cunha et al., 2010). We found that a 7-day luteolin treatment promotes an increase in BDNF levels in the cortex of *Cdk15* +/- mice (Fig. 35A). Surprisingly, we found that luteolin-dependent increased BDNF levels were not maintained after 20 days of treatment (Fig. 35A). To investigate the pathways activated by luteolin-induced BDNF expression and their maintenance over time, we first analyzed the levels of phosphorylated TrkB (P-TrkB) using Western blot in cortical homogenates of *Cdk15* +/- mice. As previously reported in male *Cdk15* -/Y mice (Ren et al., 2019), although no significant differences in BDNF levels were observed (Fig. 35A), a significantly lower level of P-TrkB was present in the *Cdk15* +/- cortex compared to that of wild-type mice (Fig. 35B). Importantly, a 7-day luteolin treatment normalized P-TrkB levels to those of the wild-type condition by increasing BDNF levels (Fig. 35B). As expected, after 20 days of luteolin treatment, the P-TrkB levels were no longer different from those of vehicle-treated *Cdk15* +/- mice (Fig. 35B). We next examined the main downstream effectors of the TrkB pathway. Predictably, we found a significantly increased Erk and Akt phosphorylation in the cortex of 7-day luteolin-treated *Cdk15* +/- mice, in comparison with wild-type mice (Fig. 35C,D), whereas no significant differences between 20-day luteolin-treated and vehicle-treated *Cdk15* +/- mice were observed (Fig. 35C,D).

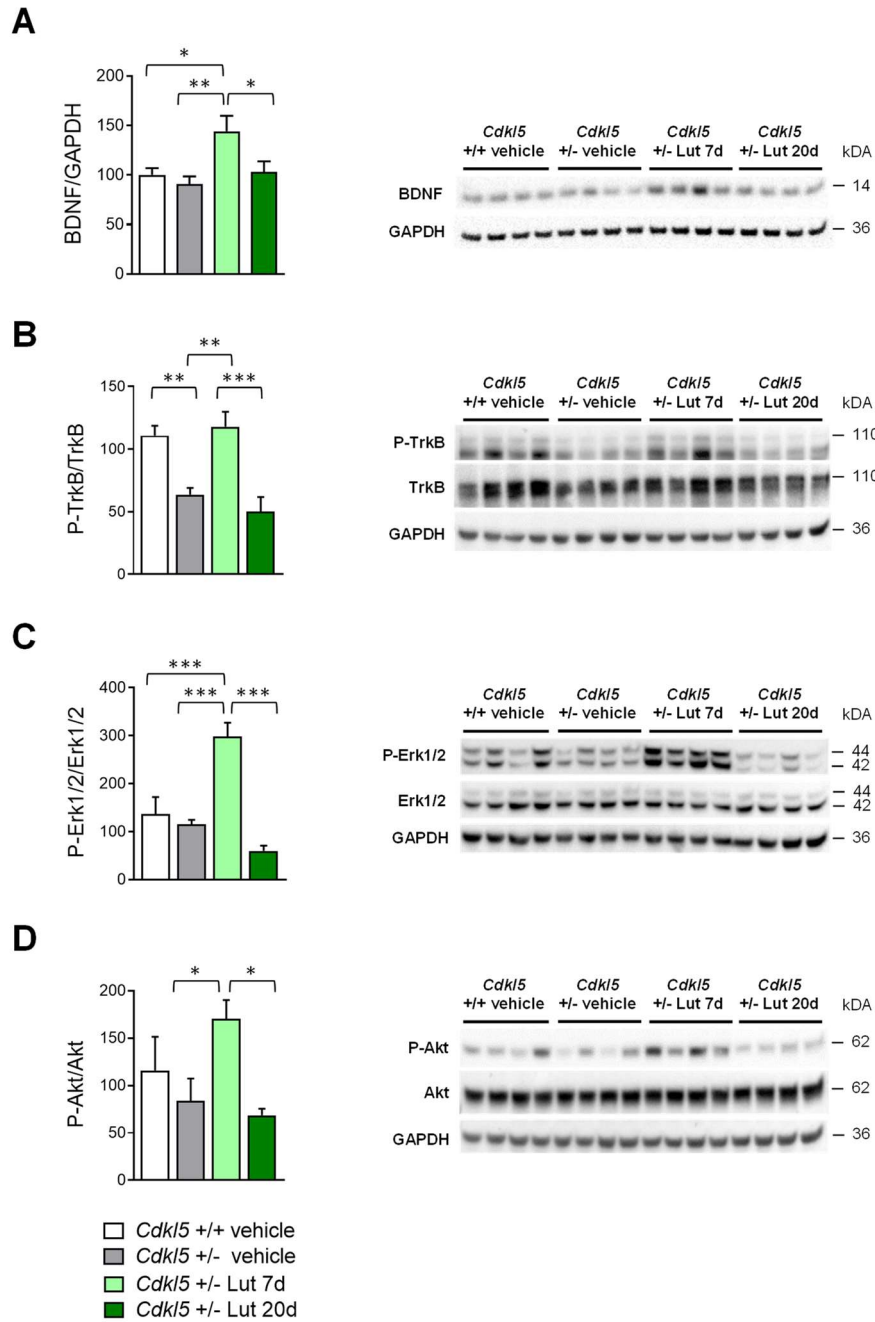


Figure 35. Effect of luteolin treatment on BDNF/TrkB signaling pathway activation in the cortex of *Cdk15* +/- mice. **A:** Western blot analysis of BDNF levels in somatosensory cortex homogenates from vehicle-treated *Cdk15* mice (+/+ n=4, +/- n=4), 7-day luteolin-treated *Cdk15* +/- mice (Lut 7d, n=4) and 20-day luteolin-treated *Cdk15* +/- mice (Lut 20d, n=4). The histogram on the left shows mature BDNF protein levels normalized to GAPDH protein levels. Examples of immunoblot for mature BDNF on the right. **B:** Histogram on the left shows protein levels of phosphorylated TrkB normalized to the respective total form in cortex homogenates from mice treated as in A. Examples of immunoblot for P-TrkB on the right. **C:** Histogram on the left shows protein levels of phosphorylated Erk1/2 normalized to the respective total form in cortex homogenates from mice treated

as in A. Examples of immunoblot for P-Erk1/2 on the right. **D**: Histogram on the left shows protein levels of phosphorylated Akt normalized to the respective total form in cortex homogenates from mice treated as in A. Examples of immunoblot for P-Akt on the right. Data are expressed as a percentage of vehicle-treated wild-type (+/+) mice. Values are represented as means \pm SEM. * $p < 0.05$, ** $p < 0.01$, *** $p < 0.001$ (Fisher's LSD test after two-way ANOVA).

3.14 Treatment with luteolin ameliorates behavioral deficits in *Cdkl5* +/- mice

Finally, we investigated whether microglial overactivation contributed to behavioral impairment in *Cdkl5* +/- mice. To this purpose, we treated *Cdkl5* +/- mice with luteolin or vehicle for 20 days and assessed the effects of the treatment on impaired locomotor activity, stereotyped and autistic-like behaviors, and memory using a battery of behavioral tests. The behavioral evaluation started on the eighth day of treatment and lasted twelve days, during which treatment was not interrupted (Fig. 36A). We first evaluated the behavioral effect of luteolin by assessing motor stereotypies using the hind-limb clasp test. *Cdkl5* +/- mice spent more time in the clasp position during the test session in comparison with wild-type mice (Fig. 36B). Treatment with luteolin led to a significant reduction in clasp time in *Cdkl5* +/- mice (Fig. 36B), indicating a treatment-induced improvement of motor stereotypies. *Cdkl5* +/- mice also showed a hyperactive profile when exposed to a new environment, as demonstrated by the stereotyped behavior (repetitive vertical jumping) and the higher distance travelled and increased velocity, compared to wild-type mice, during the open field task (Fig. 36C,D). Interestingly, treatment with luteolin normalized the stereotyped behavior in *Cdkl5* +/- mice (Fig. 36C) and improved the hyperactive phenotype (Fig. 36D). Finally, we performed a passive avoidance (PA) test to evaluate the functional effect of luteolin treatment on the memory ability of *Cdkl5* +/- mice. While on the first day of the test, all groups showed similar step-through latencies (Fig. 36E), during the second-day trial, *Cdkl5* +/- mice were severely impaired at performing this task, showing a reduced latency to enter

the dark compartment compared to wild-type mice (Fig. 36E). Albeit not statistically significant, treatment with luteolin increased the latency with which *Cdkl5* +/- mice entered the dark compartment (Fig. 36E), indicating an improvement in memory performance.

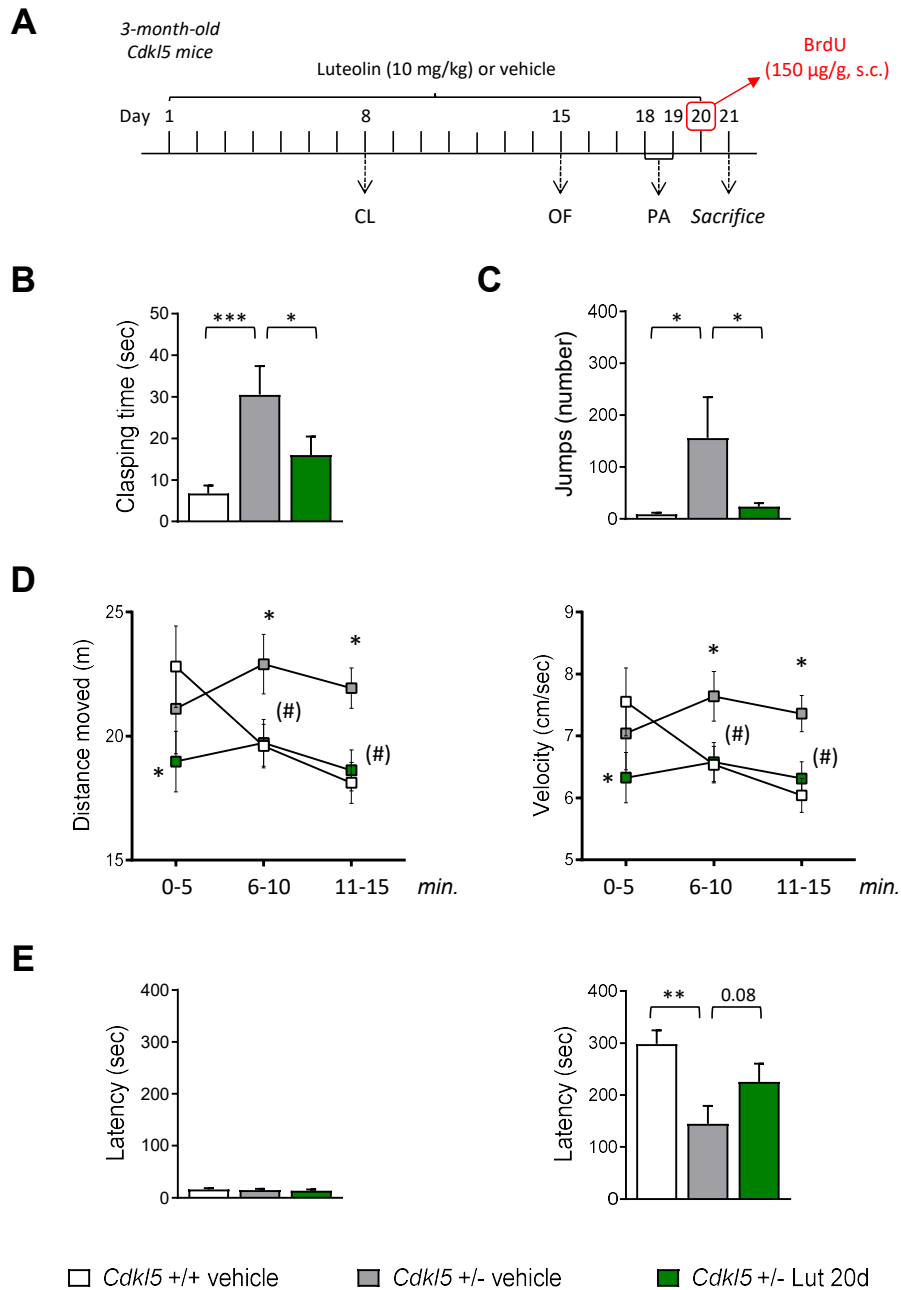


Figure 36. Effect of luteolin treatment on behavior in *Cdkl5* +/- mice. A: Experimental plan. 3-month-old *Cdkl5* mice were treated with vehicle or luteolin (10 mg/kg, i.p.) for 20 days. Behavioral tests were performed during the last two weeks of treatment. The day before sacrificed mice received a single subcutaneous injection of 5-Bromo-2'-deoxyuridine (BrdU; 150 µg/g). CL = Hind-limb Clapping, OF = Open Field, PA = Passive Avoidance. **B:** Total amount of time spent hind-limb clapping during a 2-min interval in vehicle-treated *Cdkl5* mice (+/+

n=21, +/- n=18) and 20-day luteolin-treated *Cdkl5* +/- mice (n=18). **C:** Number of stereotypic jumps (repetitive beam breaks < 1 s) in the corners of the open field arena during the 15-min trial in vehicle-treated *Cdkl5* mice (+/+ n=19, +/- n=18) and 20-day luteolin-treated *Cdkl5* +/- mice (n=17). **D:** Locomotor activity measured as average locomotion velocity (right graph) and total distance travelled (left graph) during a 15-min open field test in vehicle-treated *Cdkl5* mice (+/+ n=19, +/- n=18) and 20-day luteolin-treated *Cdkl5* +/- mice (n=17). **E:** Passive avoidance test on vehicle-treated *Cdkl5* mice (+/+ n=21, +/- n=18) and 20-day luteolin-treated *Cdkl5* +/- mice (n=17). Graphs show the latency to enter the dark compartment on the 1st day (on the left) and on the 2nd day (on the right) of the behavioral procedure. Values are represented as means \pm SEM. * p<0.05, ** p<0.01, *** p<0.001, as compared to the vehicle-treated wild-type (+/+) mice; (#) p<0.065, as compared to the vehicle-treated *Cdkl5* +/- mice (Fisher's LSD test after one-way ANOVA for data set in B,C,E and after two-way ANOVA for data set in D).

4. DISCUSSION

The lack of effective therapies for CDD stresses the urgency with which pathogenic mechanisms underlying the disorder need to be identified. Our results highlight, for the first time, the presence of a generalized status of microglia overactivation in the brain of a mouse model of CDD. We found alterations in microglia morphology and number, increased levels of AIF-1 and pro-inflammatory cytokines, and increased STAT3 signaling in the brain of *Cdkl5* KO mice. Remarkably, treatment with luteolin, a natural anti-inflammatory flavonoid, recovers impaired neuronal survival and maturation, and ameliorates behavioral performance in *Cdkl5* KO mice, suggesting that a hyperactive state of microglia plays a causative role in CDD phenotype.

Recently, a cytokine dysregulation, proportional to clinical severity and redox imbalance, has been found in children affected by CDD (Cortelazzo et al., 2017; Leoncini et al., 2015). Results included increased tumor necrosis factor (TNF)- α , interleukin (IL)-1 β , and IL-6 in the peripheral blood of children with CDD. These inflammatory cytokines could signal inflammatory changes in the brain that, in turn, could strongly impact neurodevelopment and neural function in CDD. Our finding of an overactivation of microglial cells with increased TNF- α , IL-1 β , and IL-6 levels in the brain of *Cdkl5* KO mice is in line with the results observed in CDD patients and suggests the involvement of neuroinflammatory processes in the pathophysiology of CDD. Microglia activation, associated with an increase in cell body size, as well as cytokine alterations in the peripheral blood, has been recently described in neurodevelopmental disorders such as autism spectrum disorders (ASD), Down syndrome, and Rett syndrome (Jin et al., 2017; Kahanovitch et al., 2019; Martini et al., 2020; Matta et al., 2019; Pinto et al., 2020). Similarly to Rett syndrome (Schafer et al., 2016), the mechanism by which the absence of *Cdkl5* induces microglia overactivation appeared to be non-cell autonomous. By using *Emx1*-

cKO mice, a conditional *Cdkl5* KO mouse model which does not carry *Cdkl5* deletion in microglial cells (Amendola et al., 2014; Lupori et al., 2019), we found that microglia overactivation is independent of microglia-specific loss of *Cdkl5* expression. This finding suggests that microglial activation in the *Cdkl5* KO brain may be attributable to neuronal loss of *Cdkl5*.

Among various substances capable of inhibiting microglia, a growing body of literature shows that luteolin, is a potent microglia inhibitor with antioxidant, anti-inflammatory, and neuroprotective effects both *in vitro* and *in vivo* (Ashaari et al., 2018; Aziz et al., 2018; Muruganathan et al., 2022). Although luteolin treatment had no effect on the number of microglial cells, we found that it restored microglial body size and shape, and, importantly, pro-inflammatory cytokines and P-STAT3 levels in *Cdkl5* +/- mice. The evidence that in microglial cells not only STAT3 phosphorylation levels but also total STAT3 levels are higher in *Cdkl5* +/- mice may depend on the increased STAT3 gene expression in response to pro-inflammatory cytokines (Yang et al., 2005). On the other hand, the evidence that luteolin promotes ubiquitin-dependent degradation of the Tyr705-phosphorylated STAT3 protein (Selvendiran et al., 2006; Yanagimichi et al., 2021) can underlie the drastically reduced STAT3 levels in luteolin-treated *Cdkl5* +/- mice. However, we currently have no indication why the effect on STAT3 degradation is evident in microglial cells and not in brain extracts of luteolin-treated *Cdkl5* +/- mice. We can hypothesize a different regulatory effect on STAT3 stability at the neuronal level.

Accumulating evidence indicates the presence of bidirectional microglia-neuron communication in the healthy and diseased brain (Szepesi et al., 2018). In the healthy brain, microglia exhibit an actively repressed “surveying” phenotype that is dependent on a dynamic crosstalk between microglia and neurons (Biber et al., 2007). It has been proposed that the removal of this neuronal-derived inhibitory control represents a type of danger signal for microglia, indicating that neuronal function is impaired and leads to alterations in microglia morphology and function. The chronic activation of microglia may, in

turn, cause reduced neuronal survival through the release of potentially cytotoxic molecules such as pro-inflammatory cytokines (Lull and Block, 2010; Wang et al., 2015). Our finding that inhibition of microglia overactivation by luteolin restores survival of mature neurons (NeuN-positive cells) in the CA1 field of the hippocampus of 3-month-old *Cdkl5* +/- mice is in line with this hypothesis. In addition, we found that luteolin treatment is able to restore the age-dependent decreased hippocampal neuron survival in middle-aged (11-month-old) *Cdkl5* +/- mice. This is in agreement with recent studies that suggest the important role of luteolin in counteracting age-induced microglia activation in aged mice (Burton et al., 2016; Jang et al., 2010). However, the evidence that other compounds (APAP and Stattic) are able to inhibit microglia overactivation by different mechanisms to those of luteolin (Kim et al., 2015; Lu et al., 2014; Millot et al., 2020; Zhao et al., 2017), positively affecting neuronal survival, further supports the detrimental role of microglia overactivation in *Cdkl5* +/- mice.

As previously reported in male *Cdkl5* KO mice (Fuchs et al., 2019; Loi et al., 2020), we found that hippocampal neurons of heterozygous female *Cdkl5* mice showed an increased vulnerability to excitotoxicity. Inflammatory processes, including activation of microglia and production of pro-inflammatory cytokines, such as TNF- α , IL-1 β , and IL-6, are associated with excitotoxic stimuli (Kim et al., 2010; Zhang et al., 2010). Similarly, we observed an increased microglial overactivation in response to NMDA treatment. Importantly, microglia activation was higher in *Cdkl5* +/- mice than in wild-type mice. Luteolin pre-treatment recovered the increased NMDA-induced cell death in hippocampal neurons of *Cdkl5* +/- mice. Since the increased cell death of hippocampal neurons observed in response to NMDA treatment correlates with increased microglial overactivation, the beneficial effect of luteolin on neuronal survival can be, at least in part, attributed to the inhibition of microglia activation. Luteolin was observed to exert a similar neuroprotective activity against kainic acid-induced brain damage in mice (Lin et al., 2016). In a study conducted by Fuchs and

colleagues, no differences were reported between male *Cdkl5* ^{-/Y} and wild-type (+/Y) mice in seizure intensity following NMDA administration (Fuchs et al., 2019). Our finding that NMDA-treated heterozygous female *Cdkl5* mice show increased seizure persistence, but no difference in seizure severity, compared to their wild-type counterparts, highlights a difference between hemizygous male and heterozygous female *Cdkl5* mice in response to epileptic stimulus. This is in line with recent findings showing that only heterozygous female *Cdkl5* mice are prone to developing spontaneous seizure activity (Mulcahey et al., 2020; Terzic et al., 2021b). Interestingly, pre-treatment with luteolin partially restores NMDA-induced tonic-clonic seizure persistence. This effect may be ascribed to the increased release of pro-inflammatory cytokines by activated microglial cells which may lead to neuronal hyperexcitability (Devinsky et al., 2013; Nikbakht et al., 2020; Vezzani et al., 2011). It has been shown that epileptic seizures are induced in rats after intraventricular injection with an activated microglia-conditioned medium, suggesting that activation of microglia may also be an important process for the onset of epilepsy (Zhao et al., 2018). Accordingly, several studies have shown that pre-treatment with luteolin significantly reduces the frequency of pentylenetetrazol (PTZ)-induced seizures in animal models of epilepsy (Birman et al., 2012; Tambe et al., 2017; Zhen et al., 2016).

Recent studies have demonstrated the direct involvement of microglia in the survival of neuronal precursors, showing that microglial cells residing in the subgranular zone (SGZ) and subventricular zone (SVZ) – the two neurogenic niches of the rodent adult brain – play a crucial role in neuroblast survival (Kreisel et al., 2019; Marshall et al., 2014; Ribeiro Xavier et al., 2015), while pro-inflammatory cytokines released by activated microglial cells impair progenitor survival and differentiation (Chesnokova et al., 2016; Kim et al., 2016). Our finding that inhibition of microglia overactivation by luteolin restores survival and maturation of newborn granule cells (DCX-positive cells) in the hippocampal dentate gyrus of *Cdkl5* +/- mice supports this evidence. Importantly, we found that a 20-day luteolin treatment is able to

increase the rate of cell proliferation in the subgranular zone of the hippocampal dentate gyrus of *Cdkl5* +/- mice. Similarly, recent findings have demonstrated an increase in hippocampal neurogenesis in the Ts65Dn mouse, a mouse model of Down syndrome, following a long-term (4 weeks) luteolin treatment (Zhou et al., 2019) and in a rat model of Alzheimer's Disease treated with quercetin (Karimipour et al., 2019), another anti-inflammatory flavonoid. However, our finding that a 7-day luteolin treatment, albeit sufficient to restore microglial activation to control levels, did not induce an increase in cell proliferation suggests that luteolin is effective at increasing the proliferation rate of granule cell precursors only after prolonged administration.

Dendrites and spines are the main neuronal structures that receive input from other neurons, and dendritic and spine number size and morphology are some of the crucial factors for the proper functioning of the nervous system and cognitive processes. Neurodevelopmental disorders are characterized by altered neuronal maturation and increased number of spines with immature morphology (Martínez-Cerdeño, 2017). In *Cdkl5* +/- mice, severe defects in the cortical and hippocampal region, in terms of dendritic arborization, spine maturation, and synapse development, have been repeatedly described (Amendola et al., 2014; Della Sala et al., 2016; Fuchs et al., 2018; Fuchs et al., 2014; Gennaccaro et al., 2021a; Pizzo et al., 2016; Ren et al., 2019). Our evidence that inhibition of microglia overactivation by 20-day luteolin treatment in *Cdkl5* +/- mice strongly improved dendritic length not only of newly formed neurons (DCX-positive cells) – born during the treatment period – but also of older neurons, suggests that a proper microglial function is important both during development and maturation of neuronal cells. Interestingly, while luteolin treatment restored the total dendritic length of DCX-positive cells in *Cdkl5* +/- mice by enhancing dendritic elongation without incrementing the number of branches, in hippocampal and cortical pyramidal neurons the same improvement in dendritic length was achieved, mainly through a restoration of the number of branches. Recent studies have shown that microglia positively regulate

developmental neurite growth through two mechanisms, direct microglia-neuron interaction and the release of soluble factors, such as IGF-1 and BDNF, known to promote neurite growth (Araki et al., 2021; Guo et al., 2018; Rodríguez-Iglesias et al., 2019). Moreover, several studies using mouse models, in which microglial cells are dysfunctional/overactive, have suggested the involvement of microglia in dendritic tree sprouting of newborn granule cells (Rodríguez-Iglesias et al., 2019). Although we currently have no explanation as to why treatment with luteolin differently affects elongation or number of branches in newborn and mature neurons, our results confirm the role of microglia in the modulation of neurite growth and maintenance. Interestingly, Wang and colleagues (Wang et al., 2017) found that treatment with the flavonoid 7,8-dihydroxyflavone (DHF), a small-molecule BDNF receptor agonist, enhances dendritic elongation without affecting branching of newborn granule cells in aged mice, suggesting that the effect of luteolin on dendritic arborization of DCX-positive cells in *Cdkl5* +/- mice may be driven by the boost in BDNF/TrkB signaling.

Along with the restoration of dendritic arbor complexity, we found that treatment with luteolin promoted the restoration of the balance between mature and immature spines in the hippocampus and cortex of *Cdkl5* +/- mice. Furthermore, in the hippocampus of luteolin-treated *Cdkl5* +/- mice, spine maturation correlated with an increase in the number of immunoreactive puncta for PSD-95, a key excitatory postsynaptic scaffold protein required for synaptic stabilization (Berry and Nedivi, 2017; Cane et al., 2014). The contribution of microglia to the synaptic circuit remodeling and maturation through the release of soluble factors that induce changes in the molecular composition of pre- and postsynaptic compartments is well characterized (Parkhurst et al., 2013; Rodríguez-Iglesias et al., 2019; Salter and Beggs, 2014). On the other hand, when overactivated, microglial release of molecules, such as cytokines, chemokines, and reactive oxygen species, leads to synaptic plasticity and learning and memory deficits (Cornell et al., 2022; Wang et al., 2015).

BDNF is one of the master regulators of dendritic development and spine density production/maturation (Libersat and Duch, 2004; Zagrebelsky et al., 2020). It has been shown that luteolin treatment promotes the increase in BDNF expression in the cerebral cortex and hippocampus of mice (Liu et al., 2009; Zhou et al., 2019). We found that a 7-day luteolin treatment increased BDNF expression in the cerebral cortex of *Cdk15* KO mice. Furthermore, we showed that luteolin-induced increased BDNF levels induce an increase in TrkB phosphorylation and activation of downstream pathways (Akt and Erk), important players in neuronal survival, neurogenesis, neurite outgrowth, and synaptic plasticity (Cunha et al., 2010; Kowiański et al., 2018). Indeed, it has been shown that persistent dual phosphorylation of Erk1/2 is important for local cytoskeletal effects and transcriptional changes that lead to dendritic remodeling in hippocampal pyramidal neurons (Wu et al., 2001). Similarly, the Akt/mTOR signaling pathway promotes dendritic growth and branching through the upregulation of protein and lipid synthesis (Jaworski et al., 2005; Kumar et al., 2005). Therefore, the mechanism underlying the amelioration of dendritic pathology by luteolin may be associated with the increase in BDNF. However, it is not clear why the effect of luteolin on BDNF levels, and consequently on the downstream pathways, is not retained after prolonged (20 days) luteolin administration. Accumulating data indicate that there is a regulatory negative feedback loop between BDNF and miRNAs in the brain. Indeed, BDNF stimulates expression of neuronal miRNAs, which, in turn, act by inhibiting BDNF expression (Keifer et al., 2015). This negative feedback loop could account for the lower BDNF levels present in the cortex of 20-day luteolin-treated *Cdk15* +/- mice in comparison to 7-day treated mice. However, we believe that, despite the activation of BDNF-dependent pathways is no longer present in 20-day-treated *Cdk15* +/- mice, the molecular changes induced by the early activation of the BDNF signaling cascade are able to induce a long-lasting effect that, along with the inhibition of neuroinflammation through an attenuation of microglial activation and associated pro-inflammatory cytokine release, concur

in promoting the recovery of brain function in *Cdkl5* +/- mice. This hypothesis is supported by observations showing that BDNF can induce long-lasting strengthening of synapses and neuronal survival *in vivo*, and this effect is dependent on transcription (Kang and Schuman, 1995; Vink et al., 2021; Ying et al., 2002). However, considering the different actions of luteolin as an antioxidant, anticancer, and anti-inflammatory agent (Ashaari et al., 2018; Aziz et al., 2018; Muruganathan et al., 2022), we cannot exclude the possibility that other luteolin-activated signaling pathways contribute to the positive effect of the 20-day luteolin treatment in *Cdkl5* +/- mice. Finally, we found that neuroanatomical changes induced by the 20-day luteolin treatment correlated with improved behavioral performance of *Cdkl5* +/- mice in open field and passive avoidance tests. Recent findings have shown that luteolin improves hippocampal-dependent learning and memory performance in a mouse model of Down syndrome (Zhou et al., 2019). Our finding that a long-term luteolin treatment ameliorated hippocampal-dependent memory in *Cdkl5* +/- mice supports the efficacy of luteolin in the improvement of hippocampal function in neurodevelopmental disorders. Moreover, in line with evidence that treatment with luteolin ameliorated social behaviors in a murine model of autism (Bertolino et al., 2017), we showed a marked improvement in motor stereotypies and hyperactivity phenotype (abnormalities that are linked to autistic-like behaviors) in *Cdkl5* +/- mice treated with luteolin, suggesting the therapeutic efficacy of luteolin in other brain regions besides the hippocampus. Since it has been well documented that chronic treatment with luteolin does not affect behavior in wild-type mice (Ahmad et al., 2021; Gadotti and Zamponi, 2019; Jang et al., 2010; Zhou et al., 2019) the effect of luteolin on the *Cdkl5* +/- mouse could be explained by the selective recovery of microglia overactivation exerted by luteolin in the *Cdkl5* KO condition. This is in line with recent evidence suggesting that microglial activation contributes to cognitive and motor impairments in mouse models of brain disorders (Giridharan et al., 2020; Gyengesi et al., 2019; Zhang et al., 2021b).

5. CONCLUSION

The function of microglia remains controversial, especially in the context of disease pathology, as they play both beneficial and detrimental roles within the CNS. The present data provide a clear picture of how deeply neuroinflammatory processes contribute to the brain alterations in *Cdk15* KO mice and how effective an anti-inflammatory treatment with luteolin is in recovering the brain dysfunctions. Luteolin, a natural flavonoid that can freely penetrate the blood-brain barrier due to its lipophilicity (Sawmiller et al., 2014), is safe and has beneficial effects in several mouse models of brain disorders (Ashaari et al., 2018). Moreover, in clinical trials with dietary supplements that contain luteolin, treatment has been found to be safe and, more importantly, effective in promoting an improvement in behavioral symptoms of ASD in autistic children (Bertolino et al., 2017; Taliou et al., 2013; Theoharides et al., 2012; Tsilioni et al., 2015). Therefore, the suppression of microglia-mediated inflammation induced by luteolin could represent a valid and beneficial adjuvant therapeutic strategy to ameliorate brain functionality in patients affected by CDD.

Current treatment modalities for monogenic diseases have largely focused on complementation of the affected cells, organs, or entire organisms with a functional gene copy (gene therapy, GT) or protein (enzyme replacement therapy, ERT). However, limitations associated with each of these therapeutic approaches reduce the effectiveness of treatment of CNS diseases. The major hurdle is associated with the efficient delivery of the therapeutic gene/protein to the CNS, which hampers a complete restoration of the pathological phenotype. Recently, it has been demonstrated that both an ERT (Trazzi et al., 2018) and a GT (Medici et al., 2022) approach provide neurodevelopmental and behavioral improvements in a mouse model of CDD. However, although these approaches were very promising, they allowed only a partial recovery of the pathological phenotype in *Cdk15* KO mice. Based on the present results, it will be interesting to

evaluate, in future studies, whether an adjuvant therapy with dietary luteolin supplementation, in combination with an approach based on the delivery of a functional CDKL5 protein to the brain, may allow a synergistic curative efficacy on CDKL5-related neurological defects.

6. BIBLIOGRAPHY

- Ahmad, S., et al., 2021. Deciphering the Potential Neuroprotective Effects of Luteolin against A β . *Int J Mol Sci.* 22.
- Allou, L., et al., 2017. Rett-like phenotypes: expanding the genetic heterogeneity to the KCNA2 gene and first familial case of CDKL5-related disease. *Clin Genet.* 91, 431-440.
- Amendola, E., et al., 2014. Mapping pathological phenotypes in a mouse model of CDKL5 disorder. *PLoS One.* 9, e91613.
- Amin, S., et al., 2017. Caregiver's perception of epilepsy treatment, quality of life and comorbidities in an international cohort of CDKL5 patients. *Hippokratia.* 21, 130-135.
- Amir, R. E., et al., 1999. Rett syndrome is caused by mutations in X-linked MECP2, encoding methyl-CpG-binding protein 2. *Nat Genet.* 23, 185-8.
- Araki, T., et al., 2021. The effects of microglia- and astrocyte-derived factors on neurogenesis in health and disease. *Eur J Neurosci.* 54, 5880-5901.
- Arcuri, C., et al., 2017. The Pathophysiological Role of Microglia in Dynamic Surveillance, Phagocytosis and Structural Remodeling of the Developing CNS. *Front Mol Neurosci.* 10, 191.
- Ariani, F., et al., 2008. FOXP1 is responsible for the congenital variant of Rett syndrome. *Am J Hum Genet.* 83, 89-93.
- Aronica, E., et al., 2017. Neuroinflammatory targets and treatments for epilepsy validated in experimental models. *Epilepsia.* 58 27–38.
- Artuso, R., et al., 2010. Early-onset seizure variant of Rett syndrome: definition of the clinical diagnostic criteria. *Brain Dev.* 32, 17-24.
- Ashaari, Z., et al., 2018. The Flavone Luteolin Improves Central Nervous System Disorders by Different Mechanisms: A Review. *J Mol Neurosci.* 65, 491-506.
- Aziz, N., et al., 2018. Anti-inflammatory effects of luteolin: A review of in vitro, in vivo, and in silico studies. *J Ethnopharmacol.* 225, 342-358.
- Aznar-Laín, G., et al., 2023. CDKL5 Deficiency Disorder Without Epilepsy. *Pediatr Neurol.* 144, 84-89.
- Bahi-Buisson, N., Bienvenu, T., 2012. CDKL5-Related Disorders: From Clinical Description to Molecular Genetics. *Mol Syndromol.* 2, 137-152.
- Bahi-Buisson, N., et al., 2010. Epileptic encephalopathy in a girl with an interstitial deletion of Xp22 comprising promoter and exon 1 of the CDKL5 gene. *Am J Med Genet B Neuropsychiatr Genet.* 153B, 202-7.
- Bahi-Buisson, N., et al., 2008a. The three stages of epilepsy in patients with CDKL5 mutations. *Epilepsia.* 49, 1027-37.

- Bahi-Buisson, N., et al., 2008b. Key clinical features to identify girls with CDKL5 mutations. *Brain*. 131, 2647-61.
- Bahi-Buisson, N., et al., 2012. Recurrent mutations in the CDKL5 gene: genotype-phenotype relationships. *Am J Med Genet A*. 158A, 1612-9.
- Baltussen, L. L., et al., 2018. Chemical genetic identification of CDKL5 substrates reveals its role in neuronal microtubule dynamics. *The EMBO journal*. 37, e99763.
- Barbiero, I., et al., 2017a. The neurosteroid pregnenolone reverts microtubule derangement induced by the loss of a functional CDKL5-IQGAP1 complex. *Hum Mol Genet*. 26, 3520-3530.
- Barbiero, I., et al., 2017b. CDKL5 localizes at the centrosome and midbody and is required for faithful cell division. *Sci Rep*. 7, 6228.
- Bartnik, M., et al., 2011. Early-onset seizures due to mosaic exonic deletions of CDKL5 in a male and two females. *Genet Med*. 13, 447-52.
- Bergo, A., et al., 2015. Methyl-CpG binding protein 2 (MeCP2) localizes at the centrosome and is required for proper mitotic spindle organization. *J Biol Chem*. 290, 3223-37.
- Berry, K. P., Nedivi, E., 2017. Spine Dynamics: Are They All the Same? *Neuron*. 96, 43-55.
- Bertani, I., et al., 2006. Functional consequences of mutations in CDKL5, an X-linked gene involved in infantile spasms and mental retardation. *J Biol Chem*. 281, 32048-56.
- Bertolino, B., et al., 2017. Beneficial Effects of Co-Ultramicronized Palmitoylethanolamide/Luteolin in a Mouse Model of Autism and in a Case Report of Autism. *CNS Neurosci Ther*. 23, 87-98.
- Biber, K., et al., 2007. Neuronal 'On' and 'Off' signals control microglia. *Trends Neurosci*. 30, 596-602.
- Birman, H., et al., 2012. Effects of Luteolin on Liver, Kidney and Brain in Pentylentetrazol-Induced Seizures: Involvement of Metalloproteinases and NOS Activities. *Balkan medical journal*. 29, 188–196.
- Boksa, P., 2012. Abnormal synaptic pruning in schizophrenia: Urban myth or reality? *J Psychiatry Neurosci*. 37, 75-7.
- Bradford, M. M., 1976. A rapid and sensitive method for the quantitation of microgram quantities of protein utilizing the principle of protein-dye binding. *Anal Biochem*. 72, 248-54.
- Brock, D., et al., 2021. Cerebral Visual Impairment in CDKL5 Deficiency Disorder Correlates With Developmental Achievement. *J Child Neurol*. 36, 974-980.
- Brown, G. C., Neher, J. J., 2014. Microglial phagocytosis of live neurons. *Nat Rev Neurosci*. 15, 209-16.
- Burton, M. D., et al., 2016. Dietary Luteolin Reduces Proinflammatory Microglia in the Brain of Senescent Mice. *Rejuvenation Res*. 19, 286–292.
- Cane, M., et al., 2014. The relationship between PSD-95 clustering and spine stability in vivo. *J Neurosci*. 34, 2075-86.

- Canning, P., et al., 2018. CDKL Family Kinases Have Evolved Distinct Structural Features and Ciliary Function. *Cell reports*. 22, 885–894.
- Carli, S., et al., 2021. In vivo magnetic resonance spectroscopy in the brain of *Cdkl5* null mice reveals a metabolic profile indicative of mitochondrial dysfunctions. *J Neurochem*. 157, 1253-1269.
- Chahrour, M., Zoghbi, H. Y., 2007. The story of Rett syndrome: from clinic to neurobiology. *Neuron*. 56, 422-37.
- Chapleau, C. A., et al., 2012. Hippocampal CA1 pyramidal neurons of *Mecp2* mutant mice show a dendritic spine phenotype only in the presymptomatic stage. *Neural Plast*. 2012, 976164.
- Chen, Q., et al., 2010. CDKL5, a protein associated with rett syndrome, regulates neuronal morphogenesis via Rac1 signaling. *J Neurosci*. 30, 12777-86.
- Cherry, J. D., et al., 2014. Neuroinflammation and M2 microglia: the good, the bad, and the inflamed. *Journal of neuroinflammation*. 11, 98.
- Chesnokova, V., et al., 2016. Chronic peripheral inflammation, hippocampal neurogenesis, and behavior. *Brain Behav Immun*. 58, 1-8.
- Cornell, J., et al., 2022. Microglia regulation of synaptic plasticity and learning and memory. *Neural Regen Res*. 17, 705-716.
- Cortelazzo, A., et al., 2017. Inflammatory protein response in CDKL5-Rett syndrome: evidence of a subclinical smouldering inflammation. *Inflamm Res*. 66, 269-280.
- Cunha, C., et al., 2010. A simple role for BDNF in learning and memory? *Front Mol Neurosci*. 3, 1.
- Davis, B. M., et al., 2017. Characterizing microglia activation: a spatial statistics approach to maximize information extraction. *Scientific reports*. 7, 1576.
- Della Sala, G., et al., 2016. Dendritic Spine Instability in a Mouse Model of CDKL5 Disorder Is Rescued by Insulin-like Growth Factor 1. *Biol Psychiatry*. 80, 302-311.
- Demarest, S. T., et al., 2019. CDKL5 deficiency disorder: Relationship between genotype, epilepsy, cortical visual impairment, and development. *Epilepsia*. 60, 1733-1742.
- Derecki, N. C., et al., 2012. Wild-type microglia arrest pathology in a mouse model of Rett syndrome. *Nature*. 484, 105-9.
- Devinsky, O., et al., 2013. Glia and epilepsy: excitability and inflammation. *Trends Neurosci*. 36, 174-84.
- Di Marco, B., et al., 2016. Neuro-Inflammatory Mechanisms in Developmental Disorders Associated with Intellectual Disability and Autism Spectrum Disorder: A Neuro- Immune Perspective. *CNS Neurol Disord Drug Targets*. 15, 448-63.
- Di Nardo, A., et al., 2022. Phenotypic characterization of *Cdkl5*-knockdown neurons establishes elongated cilia as a functional assay for CDKL5 Deficiency Disorder. *Neurosci Res*. 176, 73-78.

- Dong, X. X., et al., 2009. Molecular mechanisms of excitotoxicity and their relevance to pathogenesis of neurodegenerative diseases. *Acta Pharmacol Sin.* 30, 379-87.
- Du, L., et al., 2017. Role of Microglia in Neurological Disorders and Their Potentials as a Therapeutic Target. *Mol Neurobiol.* 54, 7567-7584.
- Essa, M. M., et al., 2013. Excitotoxicity in the pathogenesis of autism. *Neurotox Res.* 23, 393-400.
- Fehr, S., et al., 2016b. Functional abilities in children and adults with the CDKL5 disorder. *Am J Med Genet A.* 170, 2860-2869.
- Fehr, S., et al., 2013. The CDKL5 disorder is an independent clinical entity associated with early-onset encephalopathy. *Eur J Hum Genet.* 21, 266-73.
- Fehr, S., et al., 2016a. Seizure variables and their relationship to genotype and functional abilities in the CDKL5 disorder. *Neurology.* 87, 2206-2213.
- Fuchs, C., et al., 2020. Pharmacotherapy with sertraline rescues brain development and behavior in a mouse model of CDKL5 deficiency disorder. *Neuropharmacology.* 167, 107746.
- Fuchs, C., et al., 2018. Heterozygous CDKL5 Knockout Female Mice Are a Valuable Animal Model for CDKL5 Disorder. *Neural Plast.* 2018, 9726950.
- Fuchs, C., et al., 2019. CDKL5 deficiency predisposes neurons to cell death through the deregulation of SMAD3 signaling. *Brain Pathol.* 29, 658-674.
- Fuchs, C., et al., 2015. Inhibition of GSK3 β rescues hippocampal development and learning in a mouse model of CDKL5 disorder. *Neurobiol Dis.* 82, 298-310.
- Fuchs, C., et al., 2014. Loss of CDKL5 impairs survival and dendritic growth of newborn neurons by altering AKT/GSK-3 β signaling. *Neurobiol Dis.* 70, 53-68.
- Fuks, F., et al., 2003. The methyl-CpG-binding protein MeCP2 links DNA methylation to histone methylation. *J Biol Chem.* 278, 4035-40.
- Gadotti, V. M., Zamponi, G. W., 2019. Anxiolytic effects of the flavonoid luteolin in a mouse model of acute colitis. *Mol Brain.* 12, 114.
- Gao, Y., et al., 2020. Gene replacement ameliorates deficits in mouse and human models of cyclin-dependent kinase-like 5 disorder. *Brain.* 143, 811–832.
- Gennaccaro, L., et al., 2021a. Age-Related Cognitive and Motor Decline in a Mouse Model of CDKL5 Deficiency Disorder is Associated with Increased Neuronal Senescence and Death. *Aging Dis.* 12, 764-785.
- Gennaccaro, L., et al., 2021b. A GABA_B receptor antagonist rescues functional and structural impairments in the perirhinal cortex of a mouse model of CDKL5 deficiency disorder. *Neurobiol Dis.* 153, 105304.
- Gilbert, W., 1978. Why genes in pieces? *Nature.* 271, 501.

- Ginhoux, F., et al., 2010. Fate mapping analysis reveals that adult microglia derive from primitive macrophages. *Science*. 330, 841-5.
- Giridharan, V. V., et al., 2020. Neuroinflammation trajectories precede cognitive impairment after experimental meningitis-evidence from an in vivo PET study. *J Neuroinflammation*. 17, 5.
- Gomez Perdiguero, E., et al., 2015. Tissue-resident macrophages originate from yolk-sac-derived erythro-myeloid progenitors. *Nature*. 518, 547-51.
- Graser, S., et al., 2007. Cep164, a novel centriole appendage protein required for primary cilium formation. *J Cell Biol*. 179, 321-30.
- Greco, A., et al., 2003. Paracetamol effectively reduces prostaglandin E2 synthesis in brain macrophages by inhibiting enzymatic activity of cyclooxygenase but not phospholipase and prostaglandin E synthase. *J Neurosci Res*. 71, 844-52.
- Guo, W., et al., 2018. Differential effects of transient and sustained activation of BDNF-TrkB signaling. *Dev. Neurobiol*. 78, 647-659.
- Gupta, S., et al., 2014. Transcriptome analysis reveals dysregulation of innate immune response genes and neuronal activity-dependent genes in autism. *Nat Commun*. 5, 5748.
- Gurgone, A., et al., 2023. mGluR5 PAMs rescue cortical and behavioural defects in a mouse model of CDKL5 deficiency disorder. *Neuropsychopharmacology*. 48, 877-886.
- Gyengesi, E., et al., 2019. Chronic Microglial Activation in the GFAP-IL6 Mouse Contributes to Age-Dependent Cerebellar Volume Loss and Impairment in Motor Function. *Front Neurosci*. 13, 303.
- Hadzsiev, K., et al., 2011. Analysis of Hungarian patients with Rett syndrome phenotype for MECP2, CDKL5 and FOXP1 gene mutations. *J Hum Genet*. 56, 183-7.
- Hagberg, B., 2002. Clinical manifestations and stages of Rett syndrome. *Ment Retard Dev Disabil Res Rev*. 8, 61-5.
- Harden, C., et al., 2017. Practice guideline summary: Sudden unexpected death in epilepsy incidence rates and risk factors: Report of the Guideline Development, Dissemination, and Implementation Subcommittee of the American Academy of Neurology and the American Epilepsy Society. *Neurology*. 88, 1674-1680.
- Hector, R. D., et al., 2016. Characterisation of CDKL5 Transcript Isoforms in Human and Mouse. *PLoS One*. 11, e0157758.
- Hector, R. D., et al., 2017. *CDKL5* variants: Improving our understanding of a rare neurologic disorder. *Neurology. Genetics*. 3, e200.
- Hickman, S., et al., 2018. Microglia in neurodegeneration. *Nature neuroscience*. 21, 1359-1369.
- Hong, W., et al., 2022. CDKL5 Deficiency Disorder-Related Epilepsy: A Review of Current and Emerging Treatment. *CNS Drugs*. 36, 591-604.
- Hutsler, J. J., Zhang, H., 2010. Increased dendritic spine densities on cortical projection neurons in autism spectrum disorders. *Brain Res*. 1309, 83-94.

- Illes, P., et al., 2021. Surveilling microglia dampens neuronal activity: operation of a purinergically mediated negative feedback mechanism. *Signal Transduct Target Ther.* 6, 160.
- Ito, D., et al., 1998. Microglia-specific localisation of a novel calcium binding protein, Iba1. *Brain Res Mol Brain Res.* 57, 1-9.
- Jakimiec, M., et al., 2020. CDKL5 Deficiency Disorder-A Complex Epileptic Encephalopathy. *Brain Sci.* 10.
- Jang, S., et al., 2010. Luteolin inhibits microglia and alters hippocampal-dependent spatial working memory in aged mice. *J Nutr.* 140, 1892-8.
- Javanmehr, N., et al., 2022. Microglia dynamics in aging-related neurobehavioral and neuroinflammatory diseases. *J Neuroinflammation.* 19, 273.
- Jaworski, J., et al., 2005. Control of dendritic arborization by the phosphoinositide-3'-kinase-Akt-mammalian target of rapamycin pathway. *J Neurosci.* 25, 11300-12.
- Jhang, C. L., et al., 2017. Mice lacking cyclin-dependent kinase-like 5 manifest autistic and ADHD-like behaviors. *Hum Mol Genet.* 26, 3922-3934.
- Jin, X., et al., 2019. Natural products as a potential modulator of microglial polarization in neurodegenerative diseases. *Pharmacol Res.* 145, 104253.
- Jin, X. R., et al., 2017. MeCP2 Deficiency in Neuroglia: New Progress in the Pathogenesis of Rett Syndrome. *Front Mol Neurosci.* 10, 316.
- Joo, E., Olson, M. F., 2021. Regulation and functions of the RhoA regulatory guanine nucleotide exchange factor GEF-H1. *Small GTPases.* 12, 358-371.
- Kahanovitch, U., et al., 2019. Glial Dysfunction in MeCP2 Deficiency Models: Implications for Rett Syndrome. *Int J Mol Sci.* 20.
- Kalscheuer, V. M., et al., 2003. Disruption of the serine/threonine kinase 9 gene causes severe X-linked infantile spasms and mental retardation. *Am J Hum Genet.* 72, 1401-11.
- Kameshita, I., et al., 2008. Cyclin-dependent kinase-like 5 binds and phosphorylates DNA methyltransferase 1. *Biochem Biophys Res Commun.* 377, 1162-7.
- Kang, H., Schuman, E. M., 1995. Long-lasting neurotrophin-induced enhancement of synaptic transmission in the adult hippocampus. *Science.* 267, 1658-62.
- Karimipour, M., et al., 2019. Quercetin promotes learning and memory performance concomitantly with neural stem/progenitor cell proliferation and neurogenesis in the adult rat dentate gyrus. *Int J Dev Neurosci.* 74, 18-26.
- Katayama, S., et al., 2020. Cyclin-Dependent Kinase-Like 5 (CDKL5): Possible Cellular Signalling Targets and Involvement in CDKL5 Deficiency Disorder. *Neural Plast.* 2020, 6970190.

- Kaur, N., et al., 2020. Neuroinflammation Mechanisms and Phytotherapeutic Intervention: A Systematic Review. *ACS chemical neuroscience*. 11, 3707–3731.
- Keifer, J., et al., 2015. A MicroRNA-BDNF Negative Feedback Signaling Loop in Brain: Implications for Alzheimer's Disease. *Microna*. 4, 101-8.
- Khanam, T., et al., 2021. CDKL5 kinase controls transcription-coupled responses to DNA damage. *EMBO J*. 40, e108271.
- Kierdorf, K., et al., 2013. Microglia emerge from erythromyeloid precursors via Pu.1- and Irf8-dependent pathways. *Nat Neurosci*. 16, 273-80.
- Kiljan, S., et al., 2019. Enhanced GABAergic Immunoreactivity in Hippocampal Neurons and Astroglia of Multiple Sclerosis Patients. *J Neuropathol Exp Neurol*. 78, 480-491.
- Kilstrup-Nielsen, C., et al., 2012. What we know and would like to know about CDKL5 and its involvement in epileptic encephalopathy. *Neural Plast*. 2012, 728267.
- Kim, D. H., et al., 2010. Synaptic acid attenuates kainic acid-induced hippocampal neuronal damage in mice. *Neuropharmacology*. 59, 20-30.
- Kim, H., et al., 2015. A combinational effect of acetaminophen and oriental herbs on the regulation of inflammatory mediators in microglia cell line, BV2. *Anat Cell Biol*. 48, 244-50.
- Kim, H. J., et al., 2017. Deficient autophagy in microglia impairs synaptic pruning and causes social behavioral defects. *Molecular psychiatry*. 22, 1576–1584.
- Kim, J. Y., et al., 2020. A kinome-wide screen identifies a CDKL5-SOX9 regulatory axis in epithelial cell death and kidney injury. *Nature communications*. 11, 1924.
- Kim, Y. K., et al., 2016. The role of pro-inflammatory cytokines in neuroinflammation, neurogenesis and the neuroendocrine system in major depression. *Prog Neuropsychopharmacol Biol Psychiatry*. 64, 277-84.
- Kobayashi, Y., et al., 2021. Clinical manifestations and epilepsy treatment in Japanese patients with pathogenic CDKL5 variants. *Brain Dev*. 43, 505-514.
- Kofler, J., Wiley, C. A., 2011. Microglia: key innate immune cells of the brain. *Toxicol Pathol*. 39, 103-14.
- Kowiański, P., et al., 2018. BDNF: A Key Factor with Multipotent Impact on Brain Signaling and Synaptic Plasticity. *Cell Mol Neurobiol*. 38, 579-593.
- Kozłowski, C., Weimer, R. M., 2012. An automated method to quantify microglia morphology and application to monitor activation state longitudinally in vivo. *PLoS One*. 7, e31814.
- Kreisel, T., et al., 2019. Unique role for dentate gyrus microglia in neuroblast survival and in VEGF-induced activation. *Glia*. 67, 594-618.

- Kumar, V., et al., 2005. Regulation of dendritic morphogenesis by Ras-PI3K-Akt-mTOR and Ras-MAPK signaling pathways. *J Neurosci.* 25, 11288-99.
- Kwan, J., et al., 2016. DLG5 connects cell polarity and Hippo signaling protein networks by linking PAR-1 with MST1/2. *Genes Dev.* 30, 2696-2709.
- Kwon, H. S., Koh, S. H., 2020. Neuroinflammation in neurodegenerative disorders: the roles of microglia and astrocytes. *Translational neurodegeneration.* 9, 42.
- La Montanara, P., et al., 2020. Cyclin-dependent-like kinase 5 is required for pain signaling in human sensory neurons and mouse models. *Science translational medicine.* 12, eaax4846.
- Leonard, H., et al., 2022. CDKL5 deficiency disorder: clinical features, diagnosis, and management. *Lancet Neurol.* 21, 563-576.
- Leoncini, S., et al., 2015. Cytokine Dysregulation in MECP2- and CDKL5-Related Rett Syndrome: Relationships with Aberrant Redox Homeostasis, Inflammation, and ω -3 PUFAs. *Oxid Med Cell Longev.* 2015, 421624.
- Libersat, F., Duch, C., 2004. Mechanisms of dendritic maturation. *Mol Neurobiol.* 29, 303-20.
- Lin, C., et al., 2005. CDKL5/Stk9 kinase inactivation is associated with neuronal developmental disorders. *Hum Mol Genet.* 14, 3775-86.
- Lin, T. Y., et al., 2016. Luteolin protects the hippocampus against neuron impairments induced by kainic acid in rats. *Neurotoxicology.* 55, 48-57.
- Lipton, J. O., Sahin, M., 2014. The neurology of mTOR. *Neuron.* 84, 275-91.
- Liu, C. Y., et al., 2019. Pharmacological Targeting of Microglial Activation: New Therapeutic Approach. *Front Cell Neurosci.* 13, 514.
- Liu, R., et al., 2009. The anti-amnesic effects of luteolin against amyloid beta(25-35) peptide-induced toxicity in mice involve the protection of neurovascular unit. *Neuroscience.* 162, 1232-43.
- Lo Martire, V., et al., 2017. CDKL5 deficiency entails sleep apneas in mice. *J Sleep Res.* 26, 495-497.
- Loi, M., et al., 2023. Cardiac Functional and Structural Abnormalities in a Mouse Model of CDKL5 Deficiency Disorder. *Int J Mol Sci.* 24.
- Loi, M., et al., 2020. Increased DNA Damage and Apoptosis in CDKL5-Deficient Neurons. *Mol Neurobiol.* 57, 2244-2262.
- Lu, Y., et al., 2014. Differential pro-inflammatory responses of astrocytes and microglia involve STAT3 activation in response to 1800 MHz radiofrequency fields. *PLoS One.* 9, e108318.
- Lull, M. E., Block, M. L., 2010. Microglial activation and chronic neurodegeneration. *Neurotherapeutics.* 7, 354-65.
- Luo, J., 2012. The role of GSK3beta in the development of the central nervous system. *Frontiers in biology.* 7, 212-220.

- Luo, X. G., Chen, S. D., 2012. The changing phenotype of microglia from homeostasis to disease. *Translational neurodegeneration*. 1, 9.
- Lupori, L., et al., 2019. Site-specific abnormalities in the visual system of a mouse model of CDKL5 deficiency disorder. *Hum Mol Genet*. 28, 2851-2861.
- Lyon, M. F., 1961. Gene action in the X-chromosome of the mouse (*Mus musculus* L.). *Nature*. 190, 372-3.
- López-Rivera, J. A., et al., 2020. A catalogue of new incidence estimates of monogenic neurodevelopmental disorders caused by de novo variants. *Brain*. 143, 1099-1105.
- MacKay, C. I., et al., 2021. Exploring genotype-phenotype relationships in the CDKL5 deficiency disorder using an international dataset. *Clin Genet*. 99, 157-165.
- Maetzawa, I., Jin, L. W., 2010. Rett syndrome microglia damage dendrites and synapses by the elevated release of glutamate. *J Neurosci*. 30, 5346-56.
- Mangatt, M., et al., 2016. Prevalence and onset of comorbidities in the CDKL5 disorder differ from Rett syndrome. *Orphanet journal of rare diseases*. 11, 39.
- Mari, F., et al., 2005. CDKL5 belongs to the same molecular pathway of MeCP2 and it is responsible for the early-onset seizure variant of Rett syndrome. *Hum Mol Genet*. 14, 1935-46.
- Marshall, G. P., et al., 2014. Microglia from neurogenic and non-neurogenic regions display differential proliferative potential and neuroblast support. *Front Cell Neurosci*. 8, 180.
- Martini, A. C., et al., 2020. Distribution of microglial phenotypes as a function of age and Alzheimer's disease neuropathology in the brains of people with Down syndrome. *Alzheimers Dement (Amst)*. 12, e12113.
- Martini, F. H., et al., 2012. *Anatomia umana*. Napoli, Italia.
- Martínez-Cerdeño, V., 2017. Dendrite and spine modifications in autism and related neurodevelopmental disorders in patients and animal models. *Dev Neurobiol*. 77, 393-404.
- Marín-Teva, J. L., et al., 2011. Microglia and neuronal cell death. *Neuron Glia Biol*. 7, 25-40.
- Matta, S. M., et al., 2019. The influence of neuroinflammation in autism spectrum disorder. *Brain Behav Immun*. 79, 75–90.
- Mazziotti, R., et al., 2017. Searching for biomarkers of CDKL5 disorder: early-onset visual impairment in CDKL5 mutant mice. *Hum Mol Genet*. 26, 2290-2298.
- Medici, G., et al., 2022. Expression of a Secretable, Cell-Penetrating CDKL5 Protein Enhances the Efficacy of Gene Therapy for CDKL5 Deficiency Disorder. *Neurotherapeutics*. 19, 1886-1904.
- Miller, K. R., Streit, W. J., 2007. The effects of aging, injury and disease on microglial function: a case for cellular senescence. *Neuron Glia Biol*. 3, 245-53.

- Millot, P., et al., 2020. STAT3 inhibition protects against neuroinflammation and BACE1 upregulation induced by systemic inflammation. *Immunol Lett.* 228, 129-134.
- Mittelbronn, M., et al., 2001. Local distribution of microglia in the normal adult human central nervous system differs by up to one order of magnitude. *Acta Neuropathol.* 101, 249-55.
- Montini, E., et al., 1998. Identification and characterization of a novel serine-threonine kinase gene from the Xp22 region. *Genomics.* 51, 427-33.
- Morgan, J. T., et al., 2010. Microglial activation and increased microglial density observed in the dorsolateral prefrontal cortex in autism. *Biol Psychiatry.* 68, 368-76.
- Mulcahey, P. J., et al., 2020. Aged heterozygous Cdkl5 mutant mice exhibit spontaneous epileptic spasms. *Exp Neurol.* 332, 113388.
- Muruganathan, N., et al., 2022. Recent Updates on Source, Biosynthesis, and Therapeutic Potential of Natural Flavonoid Luteolin: A Review. *Metabolites.* 12, 1145.
- Muzio, L., et al., 2021. Microglia in Neuroinflammation and Neurodegeneration: From Understanding to Therapy. *Front Neurosci.* 15, 742065.
- Muñoz, I. M., et al., 2018. Phosphoproteomic screening identifies physiological substrates of the CDKL5 kinase. *EMBO J.* 37.
- Nabavi, S. F., et al., 2015. Luteolin as an anti-inflammatory and neuroprotective agent: A brief review. *Brain Res Bull.* 119, 1-11.
- Nan, X., et al., 1998. Gene silencing by methyl-CpG-binding proteins. *Novartis Found Symp.* 214, 6-16; discussion 16-21, 46-50.
- Nawaz, M. S., et al., 2016. CDKL5 and Shootin1 Interact and Concur in Regulating Neuronal Polarization. *PLoS One.* 11, e0148634.
- Neul, J. L., et al., 2010. Rett syndrome: revised diagnostic criteria and nomenclature. *Ann Neurol.* 68, 944-50.
- Nikbakht, F., et al., 2020. How does the COVID-19 cause seizure and epilepsy in patients? The potential mechanisms. *Mult Scler Relat Disord.* 46, 102535.
- Njie, E. G., et al., 2012. Ex vivo cultures of microglia from young and aged rodent brain reveal age-related changes in microglial function. *Neurobiol Aging.* 33, 195.e1-12.
- Ochocka, N., Kaminska, B., 2021. Microglia Diversity in Healthy and Diseased Brain: Insights from Single-Cell Omics. *Int J Mol Sci.* 22.
- Okuda, K., et al., 2017. CDKL5 controls postsynaptic localization of GluN2B-containing NMDA receptors in the hippocampus and regulates seizure susceptibility. *Neurobiol Dis.* 106, 158-170.
- Okuda, K., et al., 2018. Comprehensive behavioral analysis of the Cdkl5 knockout mice revealed significant enhancement in anxiety- and fear-related behaviors and impairment in both acquisition and long-term retention of spatial reference memory. *PLoS One.* 13, e0196587.

- Olson, H. E., et al., 2021b. Cerebral visual impairment in CDKL5 deficiency disorder: vision as an outcome measure. *Dev Med Child Neurol.* 63, 1308-1315.
- Olson, H. E., et al., 2021a. Current neurologic treatment and emerging therapies in CDKL5 deficiency disorder. *J Neurodev Disord.* 13, 40.
- Olson, H. E., et al., 2019. Cyclin-Dependent Kinase-Like 5 Deficiency Disorder: Clinical Review. *Pediatr Neurol.* 97, 18-25.
- Orihuela, R., et al., 2016. Microglial M1/M2 polarization and metabolic states. *Br J Pharmacol.* 173, 649-65.
- Pandey, K. B., Rizvi, S. I., 2009. Plant polyphenols as dietary antioxidants in human health and disease. *Oxid Med Cell Longev.* 2, 270-8.
- Paolicelli, R. C., et al., 2011. Synaptic pruning by microglia is necessary for normal brain development. *Science.* 333, 1456-8.
- Park, S. M., et al., 2019. Roles of Primary Cilia in the Developing Brain. *Front Cell Neurosci.* 13, 218.
- Parkhurst, C. N., et al., 2013. Microglia promote learning-dependent synapse formation through brain-derived neurotrophic factor. *Cell.* 155, 1596-609.
- Pinto, B., et al., 2020. Rescuing Over-activated Microglia Restores Cognitive Performance in Juvenile Animals of the Dp(16) Mouse Model of Down Syndrome. *Neuron.* 108, 887-904.e12.
- Pizzo, R., et al., 2016. Lack of Cdkl5 Disrupts the Organization of Excitatory and Inhibitory Synapses and Parvalbumin Interneurons in the Primary Visual Cortex. *Front Cell Neurosci.* 10, 261.
- Pizzo, R., et al., 2020. Structural Bases of Atypical Whisker Responses in a Mouse Model of CDKL5 Deficiency Disorder. *Neuroscience.* 445, 130-143.
- Przanowski, P., et al., 2014. The signal transducers Stat1 and Stat3 and their novel target Jmjd3 drive the expression of inflammatory genes in microglia. *J Mol Med (Berl).* 92, 239-54.
- Rana, A., Musto, A. E., 2018. The role of inflammation in the development of epilepsy. *J Neuroinflammation.* 15, 144.
- Ren, E., et al., 2019. Functional and Structural Impairments in the Perirhinal Cortex of a Mouse Model of CDKL5 Deficiency Disorder Are Rescued by a TrkB Agonist. *Front Cell Neurosci.* 13, 169.
- Ribeiro Xavier, A. L., et al., 2015. A Distinct Population of Microglia Supports Adult Neurogenesis in the Subventricular Zone. *J Neurosci.* 35, 11848-61.
- Ricciardi, S., et al., 2012. CDKL5 ensures excitatory synapse stability by reinforcing NGL-1-PSD95 interaction in the postsynaptic compartment and is impaired in patient iPSC-derived neurons. *Nat Cell Biol.* 14, 911-23.
- Rodríguez-Iglesias, N., et al., 2019. Rewiring of Memory Circuits: Connecting Adult Newborn Neurons With the Help of Microglia. *Front Cell Dev Biol.* 7, 24.

- Rusconi, L., et al., 2008. CDKL5 expression is modulated during neuronal development and its subcellular distribution is tightly regulated by the C-terminal tail. *J Biol Chem.* 283, 30101-11.
- Russo, S., et al., 2009. Novel mutations in the CDKL5 gene, predicted effects and associated phenotypes. *Neurogenetics.* 10, 241-50.
- Salter, M. W., Beggs, S., 2014. Sublime microglia: expanding roles for the guardians of the CNS. *Cell.* 158, 15–24.
- Salter, M. W., Stevens, B., 2017. Microglia emerge as central players in brain disease. *Nature medicine.* 23, 1018–1027.
- Savino, R., et al., 2023. The Emerging Role of Flavonoids in Autism Spectrum Disorder: A Systematic Review. *J Clin Med.* 12.
- Sawmiller, D., et al., 2014. Luteolin reduces Alzheimer's disease pathologies induced by traumatic brain injury. *Int J Mol Sci.* 15, 895-904.
- Scala, E., et al., 2005. CDKL5/STK9 is mutated in Rett syndrome variant with infantile spasms. *J Med Genet.* 42, 103-7.
- Schafer, D. P., et al., 2016. Microglia contribute to circuit defects in *Mecp2* null mice independent of microglia-specific loss of *Mecp2* expression. *Elife.* 5.
- Schafer, D. P., et al., 2012. Microglia sculpt postnatal neural circuits in an activity and complement-dependent manner. *Neuron.* 74, 691-705.
- Schroeder, E., et al., 2019. Neuron-Type Specific Loss of CDKL5 Leads to Alterations in mTOR Signaling and Synaptic Markers. *Mol Neurobiol.* 56, 4151-4162.
- Sekiguchi, M., et al., 2013. Identification of amphiphysin 1 as an endogenous substrate for CDKL5, a protein kinase associated with X-linked neurodevelopmental disorder. *Arch Biochem Biophys.* 535, 257-67.
- Selvendiran, K., et al., 2006. Luteolin promotes degradation in signal transducer and activator of transcription 3 in human hepatoma cells: an implication for the antitumor potential of flavonoids. *Cancer Res.* 66, 4826-34.
- Shaikh, M. F., et al., 2013. Anticonvulsant screening of luteolin in four mouse seizure models. *Neurosci Lett.* 550, 195-9.
- Sheng, J. G., et al., 1998. Enlarged and phagocytic, but not primed, interleukin-1 alpha-immunoreactive microglia increase with age in normal human brain. *Acta Neuropathologica.* 95, 229 –234.
- Slepko, N., Levi, G., 1996. Progressive activation of adult microglial cells in vitro. *Glia.* 16, 241-246.
- Sominsky, L., et al., 2018. Microglia: Key players in neurodevelopment and neuronal plasticity. *Int J Biochem Cell Biol.* 94, 56-60.
- Spittau, B., 2017. Aging Microglia-Phenotypes, Functions and Implications for Age-Related Neurodegenerative Diseases. *Front Aging Neurosci.* 9, 194.
- Stence, N., et al., 2001. Dynamics of microglial activation: a confocal time-lapse analysis in hippocampal slices. *Glia.* 33, 256-66.

- Streit, W. J., 2000. Microglial response to brain injury: a brief synopsis. *Toxicol Pathol.* 28, 28-30.
- Subramaniam, S. R., Federoff, H. J., 2017. Targeting Microglial Activation States as a Therapeutic Avenue in Parkinson's Disease. *Front Aging Neurosci.* 9, 176.
- Sucksdorff, M., et al., 2019. Natalizumab treatment reduces microglial activation in the white matter of the MS brain. *Neurol Neuroimmunol Neuroinflamm.* 6, e574.
- Sun, X., Wang, T., 2023. Research progress on the pathogenesis of CDKL5 pathogenic variants and related encephalopathy. *Eur J Pediatr.*
- Suzuki, K., et al., 2013. Microglial activation in young adults with autism spectrum disorder. *JAMA psychiatry.* 70, 49–58.
- Symonds, J. D., et al., 2019. Incidence and phenotypes of childhood-onset genetic epilepsies: a prospective population-based national cohort. *Brain.* 142, 2303-2318.
- Szepesi, Z., et al., 2018. Bidirectional Microglia-Neuron Communication in Health and Disease. *Front Cell Neurosci.* 12, 323.
- Taheri, Y., et al., 2021. Paving Luteolin Therapeutic Potentialities and Agro-Food-Pharma Applications: Emphasis on. *Oxid Med Cell Longev.* 2021, 1987588.
- Takeuchi, H., Neurotoxicity by microglia: Mechanisms and potential therapeutic strategy., Vol. 1. *Clinical and Experimental Neuroimmunology*, 2010, pp. 12–21.
- Taliou, A., et al., 2013. An open-label pilot study of a formulation containing the anti-inflammatory flavonoid luteolin and its effects on behavior in children with autism spectrum disorders. *Clinical therapeutics.* 35, 592–602.
- Tambe, R., et al., 2017. Assessment of luteolin isolated from *Eclipta alba* leaves in animal models of epilepsy. *Pharmaceutical biology.* 55, 264–268.
- Tang, S., et al., 2019. Altered NMDAR signaling underlies autistic-like features in mouse models of CDKL5 deficiency disorder. *Nat Commun.* 10, 2655.
- Tang, S., et al., 2017. Loss of CDKL5 in Glutamatergic Neurons Disrupts Hippocampal Microcircuitry and Leads to Memory Impairment in Mice. *J Neurosci.* 37, 7420-7437.
- Tao, J., et al., 2004. Mutations in the X-linked cyclin-dependent kinase-like 5 (CDKL5/STK9) gene are associated with severe neurodevelopmental retardation. *Am J Hum Genet.* 75, 1149-54.
- Tassinari, M., et al., 2023. Early-onset brain alterations during postnatal development in a mouse model of CDKL5 deficiency disorder. *Neurobiol Dis.* 182, 106146.
- Terzic, B., et al., 2021b. X-linked cellular mosaicism underlies age-dependent occurrence of seizure-like events in mouse models of CDKL5 deficiency disorder. *Neurobiol Dis.* 148, 105176.

- Terzic, B., et al., 2021a. Temporal manipulation of Cdkl5 reveals essential postdevelopmental functions and reversible CDKL5 deficiency disorder-related deficits. *J Clin Invest.* 131.
- Tetreault, N. A., et al., 2012. Microglia in the cerebral cortex in autism. *J Autism Dev Disord.* 42, 2569-84.
- Theoharides, T. C., et al., 2012. A case series of a luteolin formulation (NeuroProtek®) in children with autism spectrum disorders. *Int J Immunopathol Pharmacol.* 25, 317-23.
- Toriyama, M., et al., 2006. Shootin1: A protein involved in the organization of an asymmetric signal for neuronal polarization. *J Cell Biol.* 175, 147-57.
- Torres-Platas, S. G., et al., 2014. Morphometric characterization of microglial phenotypes in human cerebral cortex. *J Neuroinflammation.* 11, 12.
- Trazzi, S., et al., 2018. CDKL5 protein substitution therapy rescues neurological phenotypes of a mouse model of CDKL5 disorder. *Hum Mol Genet.* 27, 1572-1592.
- Trazzi, S., et al., 2016. HDAC4: a key factor underlying brain developmental alterations in CDKL5 disorder. *Hum Mol Genet.* 25, 3887-3907.
- Tremblay, M., et al., 2011. The role of microglia in the healthy brain. *J Neurosci.* 31, 16064-9.
- Tsilioni, I., et al., 2015. Children with autism spectrum disorders, who improved with a luteolin-containing dietary formulation, show reduced serum levels of TNF and IL-6. *Transl Psychiatry.* 5, e647.
- Valli, E., et al., 2012. CDKL5, a novel MYCN-repressed gene, blocks cell cycle and promotes differentiation of neuronal cells. *Biochim Biophys Acta.* 1819, 1173-85.
- Van Bergen, N. J., et al., 2022. CDKL5 deficiency disorder: molecular insights and mechanisms of pathogenicity to fast-track therapeutic development. *Biochem Soc Trans.* 50, 1207-1224.
- Vargas, D. L., et al., 2005. Neuroglial activation and neuroinflammation in the brain of patients with autism. *Ann Neurol.* 57, 67-81.
- Vezzani, A., 2014. Epilepsy and inflammation in the brain: overview and pathophysiology. *Epilepsy Curr.* 14, 3-7.
- Vezzani, A., et al., 2023. Neuroimmunology of status epilepticus. *Epilepsy Behav.* 140, 109095.
- Vezzani, A., et al., 2011. The role of inflammation in epilepsy. *Nat Rev Neurol.* 7, 31-40.
- Vidal, S., et al., 2019. The most recurrent monogenic disorders that overlap with the phenotype of Rett syndrome. *Eur J Paediatr Neurol.* 23, 609-620.
- Viglione, A., et al., 2022. Behavioral impulsivity is associated with pupillary alterations and hyperactivity in CDKL5 mutant mice. *Hum Mol Genet.* 31, 4107-4120.

- Villasana-Salazar, B., Vezzani, A., 2023. Neuroinflammation microenvironment sharpens seizure circuit. *Neurobiol Dis.* 178, 106027.
- Villumsen, B. H., et al., 2013. A new cellular stress response that triggers centriolar satellite reorganization and ciliogenesis. *EMBO J.* 32, 3029-40.
- Vink, H. A., et al., 2021. BDNF-mediated preservation of spiral ganglion cell peripheral processes and axons in comparison to that of their cell bodies. *Hear. Res.* 400, 108-114.
- Viviani, B., et al., 2014. Perspectives on neuroinflammation and excitotoxicity: a neurotoxic conspiracy? *Neurotoxicology.* 43, 10-20.
- Voineagu, I., et al., 2011. Transcriptomic analysis of autistic brain reveals convergent molecular pathology. *Nature.* 474, 380-4.
- von Bernhardi, R., et al., 2015. Microglial cell dysregulation in brain aging and neurodegeneration. *Front Aging Neurosci.* 7, 124.
- von Bernhardi, R., et al., 2010. Aging-dependent changes of microglial cells and their relevance for neurodegenerative disorders. *J Neurochem.* 112, 1099-114.
- Wake, H., et al., 2013. Microglia: actively surveying and shaping neuronal circuit structure and function. *Trends Neurosci.* 36, 209-17.
- Wang, H. T., et al., 2021. CDKL5 deficiency in forebrain glutamatergic neurons results in recurrent spontaneous seizures. *Epilepsia.* 62, 517-528.
- Wang, I. T., et al., 2012. Loss of CDKL5 disrupts kinome profile and event-related potentials leading to autistic-like phenotypes in mice. *Proc Natl Acad Sci U S A.* 109, 21516-21.
- Wang, W. Y., et al., 2015. Role of pro-inflammatory cytokines released from microglia in Alzheimer's disease. *Ann Transl Med.* 3, 136.
- Wang, X., et al., 2017. Aging impairs dendrite morphogenesis of newborn neurons and is rescued by 7, 8-dihydroxyflavone. *Aging Cell.* 16, 304-311.
- Weaving, L. S., et al., 2004. Mutations of CDKL5 cause a severe neurodevelopmental disorder with infantile spasms and mental retardation. *Am J Hum Genet.* 75, 1079-93.
- Wendimu, M. Y., Hooks, S. B., 2022. Microglia Phenotypes in Aging and Neurodegenerative Diseases. *Cells.* 11.
- Wes, P. D., et al., 2016. Targeting microglia for the treatment of Alzheimer's Disease. *Glia.* 64, 1710-32.
- Williamson, S. L., et al., 2012. A novel transcript of cyclin-dependent kinase-like 5 (CDKL5) has an alternative C-terminus and is the predominant transcript in brain. *Hum Genet.* 131, 187-200.
- Witcher, K. G., et al., 2021. Traumatic Brain Injury Causes Chronic Cortical Inflammation and Neuronal Dysfunction Mediated by Microglia. *J Neurosci.* 41, 1597-1616.
- Wong, W. T., 2013. Microglial aging in the healthy CNS: phenotypes, drivers, and rejuvenation. *Frontiers in cellular neuroscience.* 7, 22.

- Wu, G., et al., 2005. Enhanced susceptibility to kainate-induced seizures, neuronal apoptosis, and death in mice lacking ganglioside GM1: protection with LIGA 20, a membrane-permeant analog of GM1. *J Neurosci.* 25, 11014-22.
- Wu, G. Y., et al., 2001. Spaced stimuli stabilize MAPK pathway activation and its effects on dendritic morphology. *Nat Neurosci.* 4, 151-8.
- Yanagimichi, M., et al., 2021. Analyses of putative anti-cancer potential of three STAT3 signaling inhibitory compounds derived from. *Biochem Biophys Rep.* 25, 100882.
- Yang, J., et al., 2005. Novel roles of unphosphorylated STAT3 in oncogenesis and transcriptional regulation. *Cancer Res.* 65, 939-47.
- Yennawar, M., et al., 2019. AMPA Receptor Dysregulation and Therapeutic Interventions in a Mouse Model of CDKL5 Deficiency Disorder. *J Neurosci.* 39, 4814-4828.
- Ying, S. W., et al., 2002. Brain-derived neurotrophic factor induces long-term potentiation in intact adult hippocampus: requirement for ERK activation coupled to CREB and upregulation of Arc synthesis. *J Neurosci.* 22, 1532-40.
- Yokota, T., et al., 2018. STAT3 inhibition attenuates the progressive phenotypes of Alport syndrome mouse model. *Nephrol Dial Transplant.* 33, 214-223.
- Yoo, D. Y., et al., 2013. Effects of luteolin on spatial memory, cell proliferation, and neuroblast differentiation in the hippocampal dentate gyrus in a scopolamine-induced amnesia model. *Neurol Res.* 35, 813-20.
- Yousefizadeh, A., et al., 2022. Pharmacological targeting of microglia dynamics in Alzheimer's disease: Preclinical and clinical evidence. *Pharmacol Res.* 184, 106404.
- Yu, C. Y., et al., 2014. Neuronal and astroglial TGF β -Smad3 signaling pathways differentially regulate dendrite growth and synaptogenesis. *Neuromolecular Med.* 16, 457-72.
- Zagrebelsky, M., et al., 2020. BDNF signaling during the lifetime of dendritic spines. *Cell Tissue Res.* 382, 185-199.
- Zhang, D., et al., 2021b. Microglial activation contributes to cognitive impairments in rotenone-induced mouse Parkinson's disease model. *J. Neuroinflamm.* 18.
- Zhang, G., et al., 2021a. Microglia in Alzheimer's Disease: A Target for Therapeutic Intervention. *Front Cell Neurosci.* 15, 749587.
- Zhang, X. M., et al., 2010. Kainic acid-induced microglial activation is attenuated in aged interleukin-18 deficient mice. *J Neuroinflammation.* 7, 26.
- Zhao, H., et al., 2018. Microglial activation: an important process in the onset of epilepsy. *Am J Transl Res.* 10, 2877-2889.
- Zhao, W. X., et al., 2017. Acetaminophen attenuates lipopolysaccharide-induced cognitive impairment through antioxidant activity. *J Neuroinflammation.* 14, 17.

- Zhen, J. L., et al., 2016. Luteolin rescues pentylenetetrazole-induced cognitive impairment in epileptic rats by reducing oxidative stress and activating PKA/CREB/BDNF signaling. *Epilepsy Behav.* 57, 177-184.
- Zhou, W. B., et al., 2019. Luteolin induces hippocampal neurogenesis in the Ts65Dn mouse model of Down syndrome. *Neural Regen Res.* 14, 613-620.
- Zhou, Y., Danbolt, N. C., 2014. Glutamate as a neurotransmitter in the healthy brain. *J Neural Transm (Vienna)*. 121, 799-817.
- Zhu, Y. C., et al., 2013. Palmitoylation-dependent CDKL5-PSD-95 interaction regulates synaptic targeting of CDKL5 and dendritic spine development. *Proc Natl Acad Sci U S A.* 110, 9118-23.
- Zhu, Y. C., Xiong, Z. Q., 2019. Molecular and Synaptic Bases of CDKL5 Disorder. *Dev Neurobiol.* 79, 8-19.